

2

THE SINGLE-AXIS D. C. MACHINE AS A
CONTROL SYSTEM ELEMENT.

ROBERT CYRIL JOHNSON

UNIVERSITY OF ASTON IN BIRMINGHAM
DEPARTMENT OF ELECTRICAL ENGINEERING

Ph. D. Thesis

April, 1969.

-2FEB71 135172

SUMMARY

The interaction between the direct-axis flux and quadrature-axis flux, which is brought about by magnetic saturation, makes the prediction of machine transient performance a difficult proposition. This factor was treated as having prime importance, but other non-linearities were considered as well, in developing the mathematical model of the machine.

The model was treated as a multi-variable non-linear control system for analysis by numerical methods. Results from the analysis indicate that a reasonably accurate prediction of performance was obtained over a wide range of initial conditions.

A method was then evolved, using a hill climbing technique, which enabled prediction of the control strategy required to optimise to a desired transient performance.

ACKNOWLEDGEMENTS

I wish to thank Professor W. K. Roots for his guidance and encouragement during the latter stages of the project.

I should also like to thank Mrs. M. Palser for typing the manuscript and Mr. L. Radford for workshop assistance.

CONTENTS

	Page
Summary	II
Acknowledgements	III
List of principal symbols	VII
 <u>Chapter 1 - INTRODUCTION.</u>	
1. 1. General Introduction	1
1. 2. Background to present research	2
1. 3. Conclusion	7
 <u>Chapter 2 - SYSTEM REPRESENTATION</u>	
2. 1. Introduction	9
2. 2. Single-axis d. c. motor	9
2. 2. 1. Direct-axis equations	11
2. 2. 2. Quadrature-axis equations	13
2. 2. 3. Electromechanical relationships	16
2. 2. 4. Overall block diagram	18
2. 3. Summary	19
 <u>Chapter 3 - EVALUATION OF SYSTEM PARAMETERS</u>	
3. 1. Introduction	20
3. 2. Description of Apparatus	21
3. 3. Evaluation of Machine Characteristics	25
3. 3. 1. Steady-state tests	26
3. 3. 2. Transient tests.	41
3. 4. Summary	66

Chapter 4 - ANALYSIS OF RESULTS

4.1. Introduction	68
4.2. The average direct-axis flux linkages	68
4.3. Estimation of the armature flux linkages	72
4.4. Effect of Commutation	78
4.5. Time delay introduced by eddy currents	79
4.6. Summary	81

Chapter 5 - SYSTEM SIMULATION

5.1. Introduction	82
5.2. Non linear functions	82
5.3. Method of integration	91
5.4. Formulation of computer program	94
5.5. Results from simulation	95
5.6. Summary	105

Chapter 6 - CONTROL STRATEGY TO PRODUCE A GIVEN
PERFORMANCE.

6.1. Introduction	106
6.2. Review of steepest descent method	107
6.3. Computer program to realise steepest descent calculations	108
6.4. Application of steepest descent to the system	111
6.5. Interaction between stages	113
6.6. Computer program to realise control strategy	115
6.7. Choice of desired trajectory	115
6.8. Results	117
6.9. Errors encountered in the prediction process	118
6.10. Summary	118.

Chapter 7 - SUMMARY OF RESEARCH & GENERAL CONCLUSIONS

7.1. Object of research	126
7.2. Discussion on the method adopted to deal with cross-axis interference	127
7.3. Discussion on the treatment of eddy currents	128
7.4. Method of simulation of machine performance	129
7.5. Discussion on prediction of control strategy	130
7.6. General Comments	132
7.7. Suggestions for further work	133
7.8. Conclusions	133a

APPENDICES

8.1. Average flux calculations	134
8.2. Single valued functions of a single variable	136
8.3. Single valued functions of two variables	137
8.4. Simulation of model	138
8.5. Extremum search	143
9.0. References.	153

LIST OF PRINCIPAL SYMBOLS.

- a - $2a$ = number of parallel paths.
 AT - ampere turns.
 b - constant.
 B_z - Flux density.
 c - constant.
 C_z - Number of ordinates or fractional value between ordinates, depending upon suffix.
 d - direction vector.
 e - generated e. m. f.
 h_z - number of ordinates.
 h - fractional value between ordinates.
 i - current.
 $I(N)$ - output of integrator N . (State variable).
 J - inertia.
 k_z - leakage ratio.
 K_z - constant.
 m - $2m$ = number of poles.
 n - integer.
 N_z - number of turns.
 N - number of integrators.
 p \equiv d/dt .
 q - constant.
 r - integer.
 r_z - resistance
 R_z - number of ordinates or fractional value between ordinates, depending upon suffix.
 t_z - torque.

List of principal symbols (continued).

t	-	time.
T_z	-	time constant.
T	-	sampling interval.
u	-	constant.
v	-	voltage.
x	-	distance.
x_z	-	past, present or future values of x .
y	-	control vector.
z	-	suffix.
α	-	slope.
Δ	-	increment.
δ	-	small increment.
θ	-	angle.
ρ	-	performance index.
ϕ	-	flux.
ψ	-	flux-linkages.
Ω	-	ohms.
ω	-	speed.
τ	-	Integrator time constant.
∇	-	gradient.

CHAPTER 1.

INTRODUCTION.

1.1 General Introduction.

1.2 Background to present research.

1.2.1 Choice of machine for a given application.

1.2.2 Evaluation of factors likely to effect transient
performance.

1.2.2.1 Saturation.

1.2.2.2 Hysteresis.

1.2.2.3 Eddy Currents.

1.2.2.4 Leakage flux.

1.2.2.5 Harmonics.

1.2.2.6 Armature resistance.

1.2.2.7 Commutation and brush effects.

1.2.2.8 Non-Linear load torque.

1.3 Conclusion.

CHAPTER 1 - INTRODUCTION

1.1 GENERAL INTRODUCTION.

The simple single-axis d. c. machine and multi-stage machines derived from it received a great deal of development and research during the period 1940-1952.

The interest arose from the increasing use of automatic control systems for industrial and military applications. With the result that it became essential to know the characteristics of system elements, such as machines, fairly accurately under transient conditions.

The subject has been covered by many authors who have considered that the only reasonable method of analysis has to be based on linear theory. Then non-linear effects, which are recognised as important, are allowed for by practical adjustment based on experience.

These methods are of course quite adequate when dealing with small signal or idealised conditions and they usually fall into (a) The General Theory approach ^{e. g. (1, 2, 3)} or (b) The Transfer Function approach ^{e. g. (4, 5)}. Both methods consist of setting up the fundamental relationships between the system variables and solving the resulting linear differential equations by well established manipulations.

1.2 BACKGROUND TO PRESENT RESEARCH.

Practical tests carried out on systems, which incorporated machine elements, had shown that under the influence of large signal variations the simple linear theory no longer adequately described the transient performance.

The need for operating systems with large signal variations results from the desire to produce rapid changes in speed of motors or changes of voltage in generators.

Methods of achieving the desired changes may include the addition of non-inductive resistance to reduce field time constants, or field forcing and appropriate use of feedback. ⁽⁶⁾ Sometimes field forcing may be accompanied by a saturating element to limit the maximum voltage available.

Armature current forcing may be required to enable a particular rate of change of speed to be obtained. The magnitude of this current and its period of application will usually be limited by the armature design and method of cooling.

Factors such as these are involved in choosing a system component for a particular control application. The purpose, therefore, of this work is to evaluate the parameters that affect the machine performance when it is subjected to the above type of large signal variations.

1.2.1 CHOICE OF MACHINE FOR A GIVEN APPLICATION.

It is well known that considerable improvement in the performance of a control system may be obtained by using machines which have been specially designed for a given application. Such machines should in general be constructed with their magnetic circuits laminated, otherwise eddy currents set up when the flux in the machine frame is changing will produce a phase

lag between excitation ampere turns and airgap flux.

Machines specifically designed for such work usually have the necessary degree of lamination and their proportions⁽⁷⁾ are invariably based on the (Power gain to time constant) ratio for generators and (Torque to Inertia) ratio for motors.

But even these machines are not usually assessed for their ability to withstand, say, many times full load armature current for short periods with a weak field.

In the operation of motors with high acceleration and deceleration rates the peak armature current is of course limited by a satisfactory commutating performance. But again observation had shown that it was possible to operate with considerable armature current forcing without producing noticeable deterioration in commutating ability.

1.2.2 EVALUATION OF FACTORS LIKELY TO EFFECT TRANSIENT PERFORMANCE.

It has been suggested that the performance of a machine may be assessed with satisfactory accuracy, in many cases, by treating it as an idealised model. The properties of this model are then listed, e. g. (4, p. 155) and after derivation of the appropriate characteristics the assumptions are re-examined.

The most common causes of discrepancy listed by most authors e. g. ((1, p. 122), (5, p. 114)), include the effect of saturation, hysteresis, eddy currents, leakage flux, harmonics, varying armature circuit resistance, commutation, brush size and position and non-linear load torque.

1. 2. 2. 1 SATURATION.

For small signal operation it is possible to neglect the interaction between armature flux and field flux as well as the effect of saturation in the armature axis. (3, p. 433).

However, with the mode of forcing conditions usually experienced in control systems, both these conditions will be accentuated.

1. 2. 2. 2 HYSTERESIS.

The hysteresis effect that occurs in any iron core will of course be present in the machine frame and pole structures. Inevitably, therefore, when rapid cyclic changes are likely to occur the effect of hysteresis will play some part in producing a given transient characteristic.

1. 2. 2. 3 EDDY CURRENTS.

When a changing magnetic flux permeates any part of the iron core of a machine, eddy currents are induced. These eddy currents are restricted, in some parts of the core, by laminations. For example the armature core and the main poles are subjected to changing magnetisation even under steady load conditions.

Under transient conditions, where the magnetic flux is changing in all parts of the core, the presence of eddy currents is likely to affect performance particularly if non-laminated sections, such as the main frame or interpoles, exist.

1. 2. 2. 4 LEAKAGE FLUX.

Consideration of the magnetic circuit of a machine will show that flux set up by main poles and the interpoles will not all cross the airgap of the machine. Further, if the field circuit or armature circuit is being subjected to forcing such that saturation is considerable, then leakage will be a variable function of the total m. m. f. on the combined field and armature circuits.

1. 2. 2. 5 HARMONICS.

When an armature rotates in a non-uniform magnetic field the production of harmonic voltages is inevitable. These harmonics produce parasitic torques which have some effect on the machine performance. The policy of the machine designer appears to be that reduction of harmonics can only help performance, although the actual degree of improvement, apart from better output waveforms, is a little obscure.

1. 2. 2. 6 ARMATURE RESISTANCE.

The armature resistance is usually taken to be that of the armature windings and the brush contact resistance. However the brush contact resistance is not only influenced by the brush grading but it is also a function of brush current.

In addition the armature winding resistance is a function of speed due to the eddy currents induced by rotation.

1.2.2.7 COMMUTATION & BRUSH EFFECTS.

Commutation is regarded as one of the main factors which limit the operating range of a d. c. motor, ⁽⁸⁾ but it is not the purpose of this work to examine in detail the process of commutation. The subject has received attention from many authors e. g. (9, 10) who have adequately described the reasons for requiring good commutation and attaining the necessary degree of adjustment. It is, however, recognised that satisfactory commutation is required to prevent excessive commutator wear or damage during severe forcing conditions and therefore the concern here is basically to evaluate the effect of commutation adjustment on the performance of the machine.

When a given armature coil passes under the brush the current reverses its direction, but the stored energy in the coil delays the process of reversal. This stored energy is a function of the flux linking the armature due to armature conductor current and will be influenced by the proximity of the main pole and the interpole, as well as by the effect of short circuit currents produced during commutation. This factor will be significant in limiting the rate of rise of total armature current during transient conditions particularly in the presence of magnetic saturation of the main and interpole circuits.

The performance of the machine is considered to be effected to a marked degree when operating under linear steady-state conditions ⁽¹¹⁾ and will certainly be effected under transient conditions.

The significant points appear to be the effect of the short-circuit currents and the non-uniformly distributed brush currents on the main pole flux distribution.

1.2.2.8 NON-LINEAR LOAD TORQUE.

When a motor is accelerating from rest its acceleration will be reduced by frictional torques. These torques are of considerable importance in certain control applications and steps are usually taken to minimise their effect.⁽¹²⁾

It would be expected, however, that when considering pure acceleration of a d.c. motor on no load that these torques would be comparatively insignificant compared with the normal accelerating torque.

1.3 CONCLUSION.

The works referred to in the foregoing sections have been quoted to give an overall picture of the problems likely to be encountered in predicting the transient performance of a d.c. machine operating under control system conditions.

Research was directed along lines which it was thought might help to resolve some of the problems posed. Some of these problems were originally examined in mid 1963, but papers which appeared after that date did not substantially alter the mode of attack. Tests were therefore carried out on a single-axis d.c. machine to measure the transient characteristics as accurately as possible under various initial conditions. The results were then analysed by an appropriate simulation technique to verify the theories postulated.

The machine tested was, manufactured by Laurence Scott Electromotors, fitted with two laminated poles, two solid commutating poles and rated at 2 HP, 240 V, 8.3 A, 1500 RPM. It was not specifically designed for control system use, but it was felt that results obtained would not invalidate the treatment when applied to a machine of similar configuration, designed for a particular application. The choice of this machine was based on the fact that, under normal operating conditions, performance was influenced considerably by magnetic saturation.

The overall object of this research, therefore, was to develop the mathematical model of the machine, taking into account some of the factors which are outlined by the discussion in Section 1.2.2. Then using the mathematical model, as a basis, to develop a suitable control strategy to obtain a desired performance.

Some of the works quoted have inevitably been consulted in later chapters and these have been referred to more fully as appropriate.

CHAPTER 2.

SYSTEM REPRESENTATION.

2.1 Introduction.

2.2 Single-axis d. c. motor.

2.2.1 Direct-axis Equations.

2.2.2 Quadrature-axis Equations.

2.2.2.1 Armature Resistance.

2.2.2.2 Voltages generated in the armature.

2.2.3 Electromechanical relationships.

2.2.3.1 Torque equation.

2.2.3.2 Accelerating torque.

2.2.3.3 Load torque.

2.2.4 Overall Block Diagram.

2.3 Summary.

CHAPTER 2.

SYSTEM REPRESENTATION

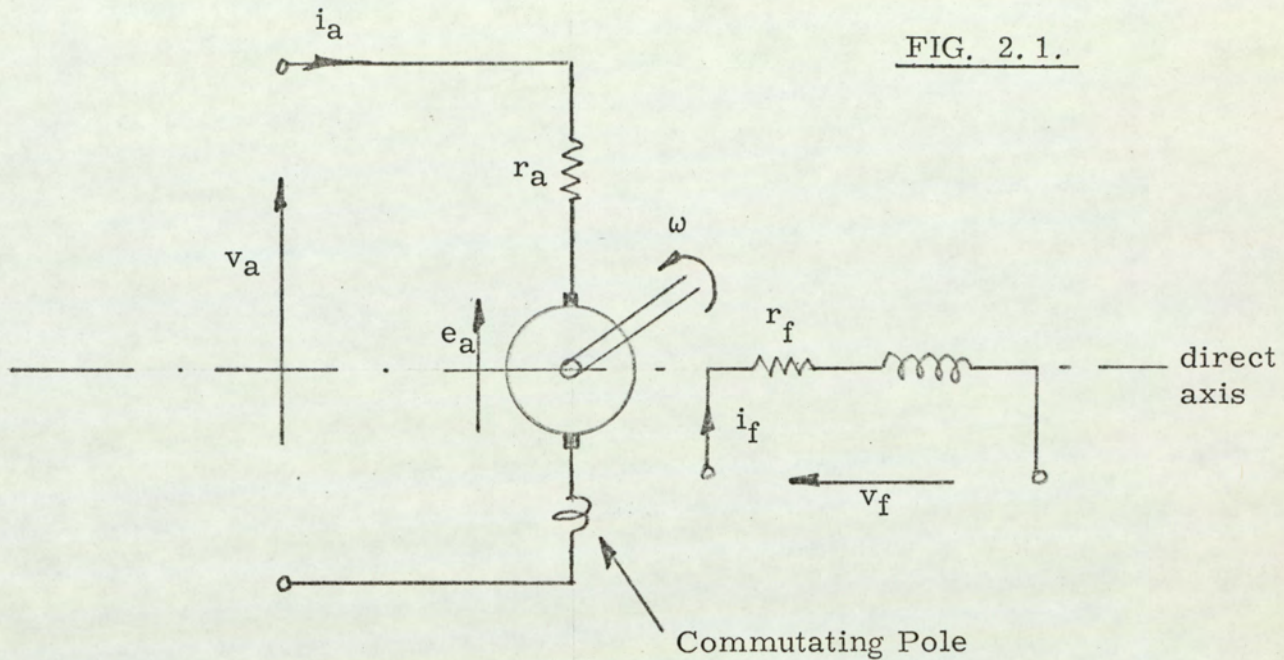
2.1 INTRODUCTION.

In this treatment the block diagram notation^(3, p. 428) was adopted for the presentation of the system equations and where representation differs from known practice the method has been explained in the text. Otherwise the conventions, which are adequately explained in the literature,⁽¹³⁾ have been adhered to.

The system has been illustrated by outlining the block diagram of one of the machines which was tested. This was a single-axis d. c. machine operating as a separately excited motor.

2.2 SINGLE-AXIS D. C. MOTOR.

The motor under consideration was a two pole machine with interpoles on the quadrature axis. (FIG. 2.1).



The arrows indicate the assumed positive directions of voltage and current.

If the following symbols refer to instantaneous or incremental values then let v_a and v_f represent the voltages applied to the armature (quadrature axis) and field (direct-axis) circuits respectively.

i_a & i_f represent the quadrature-axis and direct-axis currents respectively.

ψ_a, ψ_f represent the quadrature axis flux linkages and direct axis flux linkages respectively. (Wb - turns).

e_a be the brush voltage due to generated e. m. f. in the armature.

r_a be the armature resistance (Ω).

ω be the speed of the armature (rad/sec.).

t_a be the torque developed by the armature (N-m).

t_l be the load torque (N-m).

r_f be the direct-axis circuit resistance (Ω).

2.2.1 DIRECT-AXIS EQUATIONS.

$$v_f = i_f r_f + p \psi_f \quad \text{where } p = \frac{d}{dt} \quad - \quad (2.1)$$

$$\psi_f = 2m N_f \phi_f \quad \text{Wb turns} \quad - \quad (2.2)$$

where ϕ_f = flux/pole linking field turns N_f
& $2m$ = total number of poles.

$$\phi_f = \phi_g + \phi_l \quad \text{where } \phi_g = \text{airgap flux/pole}$$

$$\phi_l = \text{leakage flux/pole}$$

If $k_d = \frac{\text{Airgap flux/pole}}{\text{Total field winding flux/pole}}$ then

$$\phi_g = \frac{k_d \psi_f}{2m N_f} \quad \text{Wb} \quad \text{-----} \quad (2.3)$$

k_d was considered to vary since the leakage increases when the magnetic circuit saturates.

$$\therefore \phi_g = f(\psi_f)$$

The airgap flux will be influenced considerably by the presence of armature m.m.f. adjacent to the pole face if the magnetic circuit is saturated.

Therefore $\phi_g = g(i_f, i_a)$, which is a non-linear function of two variables. It is not usual to present functions of two variables using block diagram notation and so therefore the method used here will be as shown below (FIG. 2.2).

The diagram is intended to show that an input of two known variables are required to compute the dependent variable. Therefore if the airgap flux and armature current are known, the direct-axis m. m. f. can be calculated. The resultant equation becomes $i_f N_f = f(\phi_g, i_a)$ ----- (2.4)

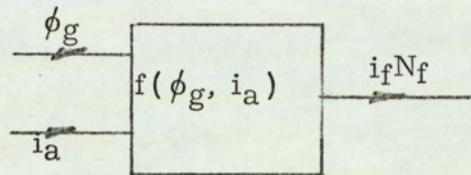


FIG. 2.2

The block diagram (FIG. 2.3) for the direct axis relationships was formulated by combining equations (2.1) to (2.4).

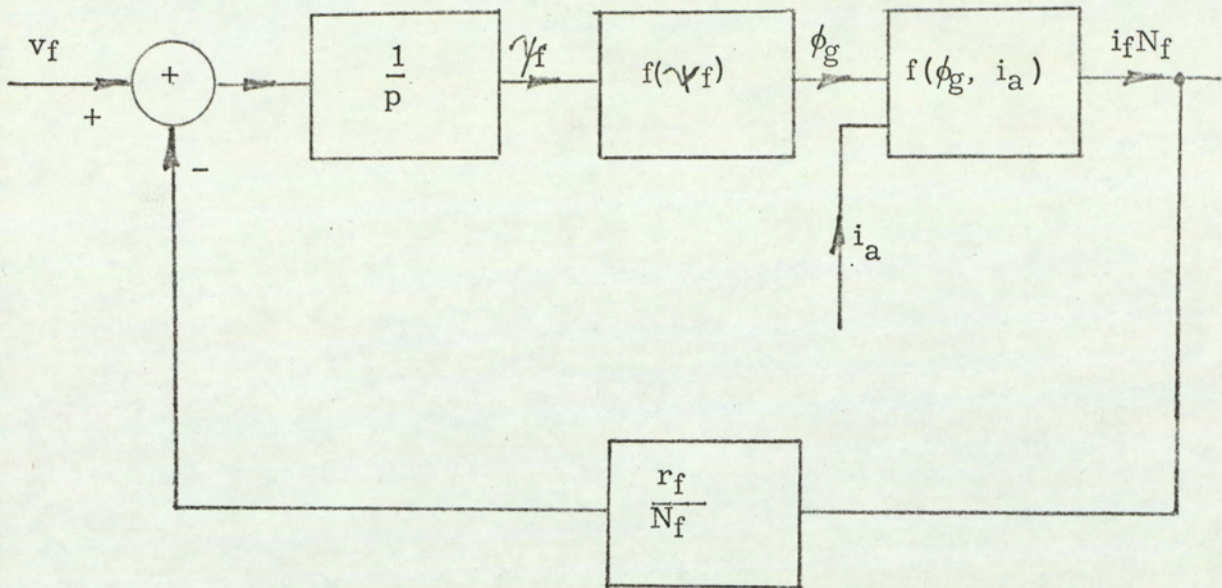


FIG. 2.3.

2.2.2 QUADRATURE-AXIS EQUATIONS.

$$v_a = e_a + i_a r_a + p \psi_a \quad \text{-----} \quad (2.5)$$

The armature flux linkages ψ_a will be dependent upon the total m. m. f. acting on the magnetic circuit and will therefore be expressed in a similar form to equation (2.4).

$$i_a N_a = f(\psi_a, i_f) \quad \text{-----} \quad (2.6)$$

where N_a = effective turns acting in the quadrature axis.

2. 2. 2. 1 ARMATURE RESISTANCE.

The total armature circuit resistance is made up of winding resistance, interpole resistance and brush resistance.

It was assumed that the interpole resistance remained virtually constant, but it is well known that the winding resistance is effected by rotation. The eddy currents in the conductors, produced by a current changing at a rate determined by the speed of rotation, produce an effective resistance that is somewhat greater than the measured d. c. value. (14, p. 178).

The brush contact resistance will depend upon the brush grading, brush pressure and current density. Of these factors brush manufacturers indicate the type of characteristics to be expected if the current density is uniform. Usually however the current density differs across the face of the brush depending upon the strength of the commutating field. (15).

It was therefore taken that the total armature circuit resistance $r_a = f(i_a, \omega)$ ----- (2. 7)

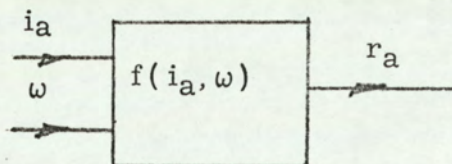


FIG. 2. 4.

2. 2. 2. 2 VOLTAGES GENERATED IN THE ARMATURE.

The e. m. f. generated in an armature coil of a d. c. machine is $e = - \left[\frac{\partial \psi}{\partial t} + \frac{\partial \psi}{\partial \Theta} \cdot \frac{d\Theta}{dt} \right]$

where ψ = flux linkages.

Θ = angular position of the coil with respect to the flux.

$\frac{d\Theta}{dt}$ = speed of the coil.

The first term in this expression represents the voltage produced due to the time variation of the flux linkages, which exists under transient conditions. The second term represents the voltage produced by rotation, and was the only term considered since brush shift was adjusted to be negligible.

It is well established^(14, p. 11) that the voltage measured at the brushes is proportional to the product of airgap flux/pole (ϕ_g) and the speed of rotation (ω), provided the brushes are diametrically opposite on the commutator and are coincident in space with the quadrature-axis. Further, this voltage is not dependent on the flux-density distribution since the area of the flux density-angular position curve is proportional to the airgap flux/pole.

$$\text{Therefore } e_a = K_1 \phi_g \omega \quad \text{-----} \quad (2.8)$$

where K_1 is a constant for a particular machine frame size and given windings.

2.2.3 ELECTROMECHANICAL RELATIONSHIPS.

2.2.3.1 TORQUE EQUATION.

The mechanical power developed by the armature, when equated to electrical power gives $\omega t_a = e_a i_a$ watts.

$$\therefore t_a = K_1 \phi_g i_a \text{ Nm.} \quad \text{-----} \quad (2.9)$$

by substitution from equation (2.8).

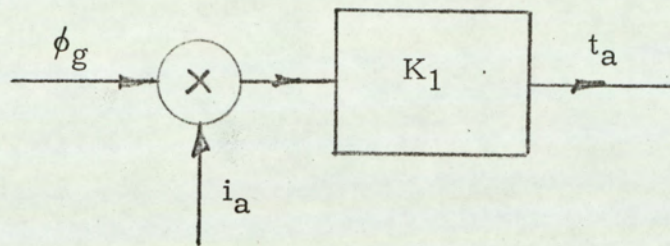


FIG. 2.5.

2.2.3.2 ACCELERATING TORQUE.

$$\text{The accelerating torque} = t_a - t_L = J p \omega \text{ Nm} \quad \text{---} \quad (2.10)$$

where t_L = load torque (Nm).

J = Inertia of motor + load, measured at the motor shaft
(kg-m^2).

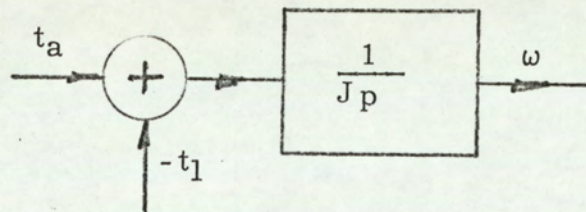


FIG. 2.6.

2. 2. 3. 3. LOAD TORQUE.

The single-axis d. c. machine under consideration was tested on no load and therefore the only load torque opposing acceleration was that due to the combined effects of stiction, coulomb friction, windage, hysteresis and eddy currents. Such effects are themselves dependent on such factors as brush pressure, degree of excitation, type of ventilation and speed.

It was felt that the dominant factor in this case was speed and therefore the load torque is defined as

$$t_l = f(\omega) Nm \quad \text{-----} \quad (2.11).$$

2. 2. 4 OVERALL BLOCK DIAGRAM.

The result of combining equations (2.1 - 2.11) produces the following block diagram (FIG. 2.7).

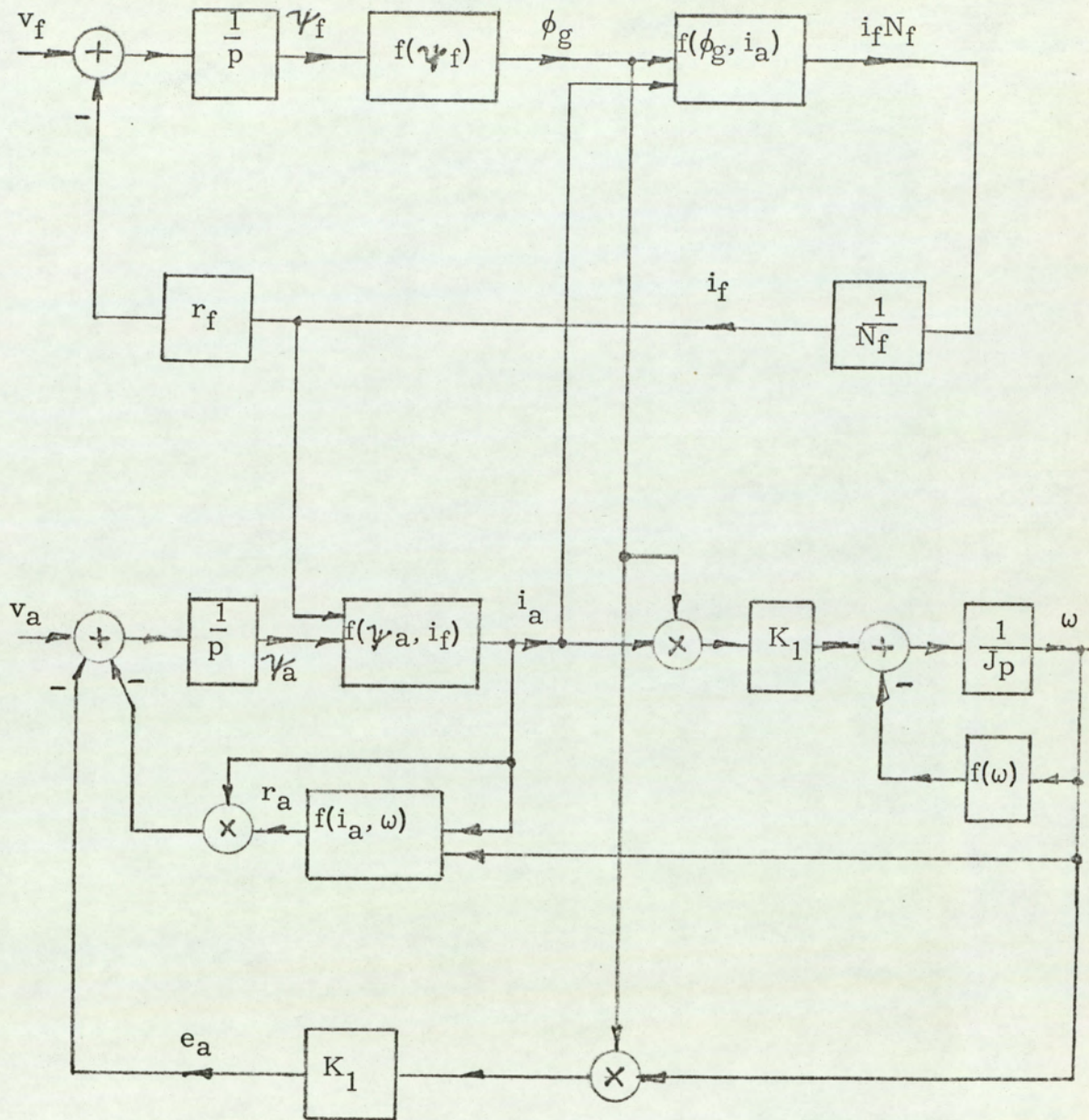


FIG. 2. 7.

2.3 SUMMARY.

The block diagram of the single axis d. c. machine was derived by considering the factors likely to effect the machine performance. It was not intended that this diagram should account for all points raised in Chapter 1. But the philosophy associated with the derivation was to set out the relationships which required determination before the equations could be solved. For example, clearly the equations are not soluble unless the non-linear functions, which have been defined, can be expressed adequately.

When dealing with d. c. machines having different circuit configurations the same method may be used to present the system equations, although some manipulation is required for each individual case.

The next chapter deals with the specific problems that have been posed by the introduction of the block diagram (FIG. 2. 7).

CHAPTER 3.

EVALUATION OF SYSTEM PARAMETERS.

3.1. Introduction.

3.2. Description of Apparatus.

3.3. Evaluation of Machine Characteristics.

3.3.1. Steady-state tests.

3.3.1.1. Open circuit characteristic.

3.3.1.2. Direct-axis flux ϕ_G /m. m. f. characteristic on no load.

3.3.1.3. Leakage flux.

3.3.1.3.1. Direct-axis leakage flux.

3.3.1.3.2. Quadrature-axis leakage flux.

3.3.1.4. Pole-face flux density.

3.3.1.5. Quadrature-axis circuit resistance.

3.3.1.6. Load torque characteristic.

3.3.2. Transient Tests.

3.3.2.1. Armature Inertia.

3.3.2.2. Dynamic relation between flux and m. m. f.

3.3.2.2.1. Direct-axis flux ϕ_G /m. m. f. relation with $i_a = 0$.

3.3.2.2.2. Quadrature-axis flux ϕ_J /m. m. f. relation with $i_f = 0$.

3.3.2.3. Machine accelerating from rest.

3.3.2.4. Relation between direct-axis flux ϕ_G /m. m. f. with the machine accelerating from rest.

3.3.2.5. Relation between quadrature-axis flux ϕ_J /m. m. f. with the machine accelerating from rest.

3.3.2.6. Direct-axis pole-face flux-density distribution with the machine accelerating from rest.

3.3.2.7. Commutation.

3.4. Summary.

CHAPTER 3.

EVALUATION OF SYSTEM PARAMETERS.

3. 1. INTRODUCTION.

To evaluate the effect of armature current forcing on a single-axis d. c. motor, the machine was accelerated from rest on no load with various initial direct-axis excitation conditions. No particular limit was placed on the peak armature current, or rate of change of current, except the desirability of retaining visual sparkless commutation.

It was also possible, with readily available supply voltages, to attain a peak armature current of six times the normal full load value.

At this stage it was desired to establish the behaviour of the direct-axis and quadrature-axis air-gap flux and therefore the machine was fitted with search coils to measure the flux-density distribution and the total flux/pole at the tips of the main pole and commutating pole (FIG. 3. 1.).

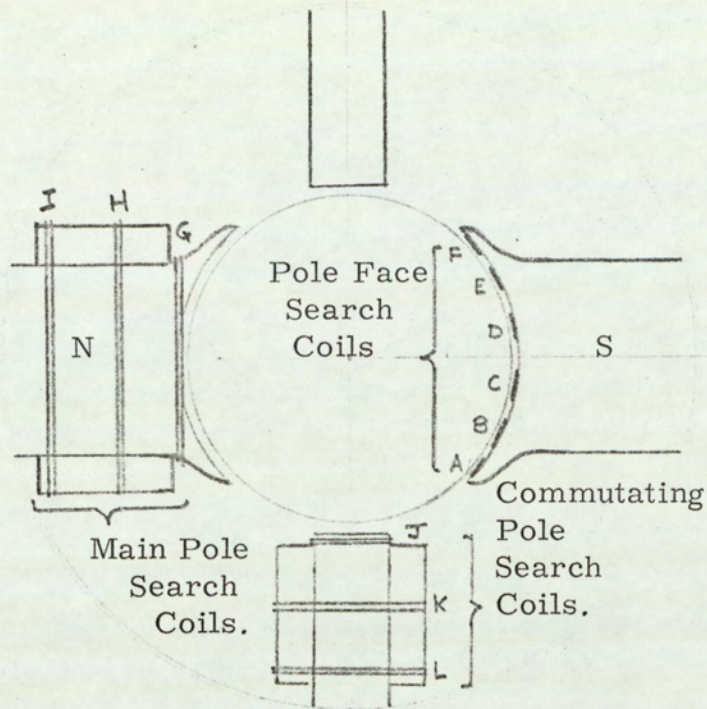


FIG. 3. 1a

In view of the type of information required, the only possible method was to obtain a large proportion of the data from traces obtained during transient tests.

3.2 DESCRIPTION OF APPARATUS.

The apparatus used for a particular test is shown by the typical layout in the diagram (FIG. 3. 2) and the photograph (FIG. 3. 3).

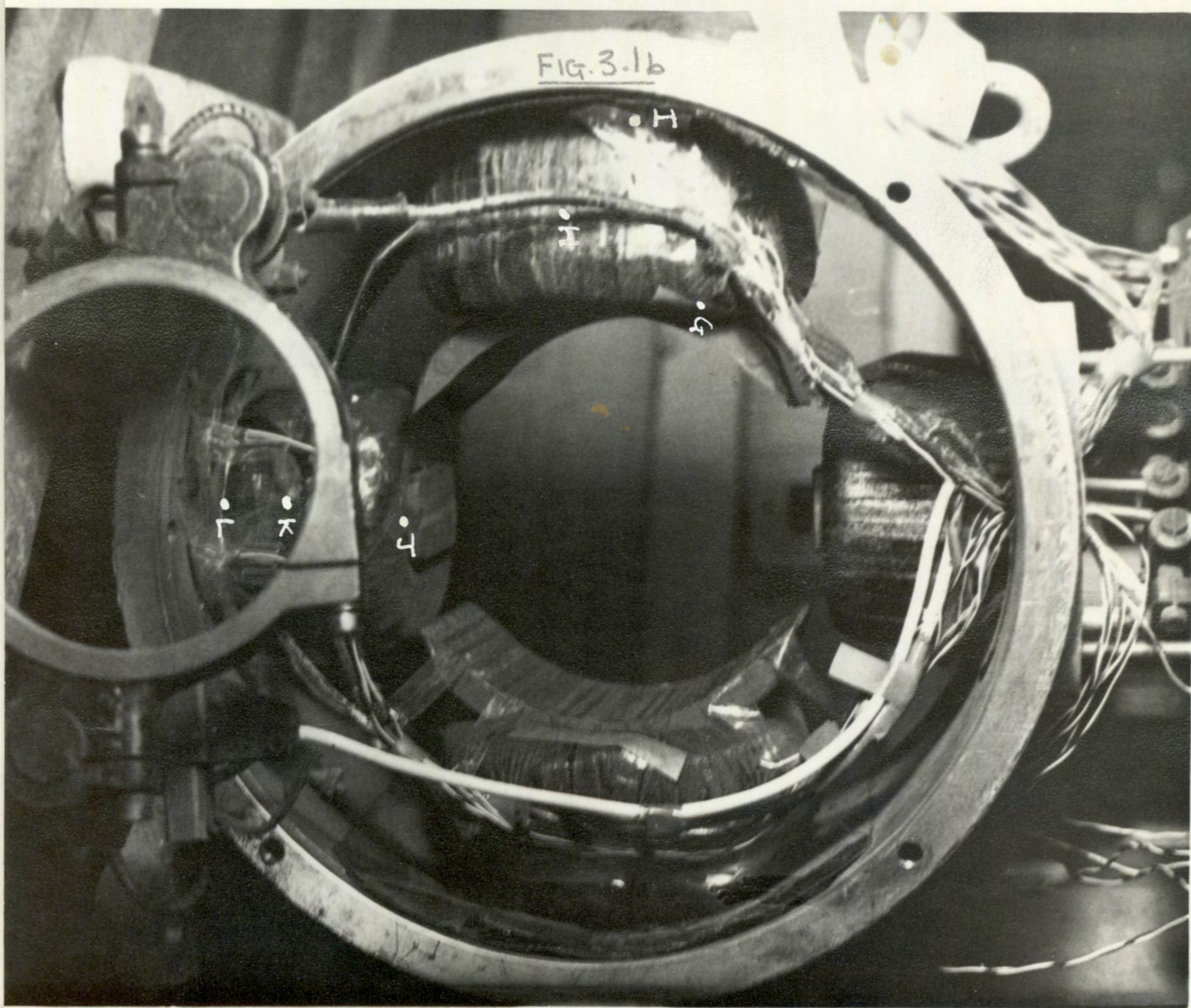
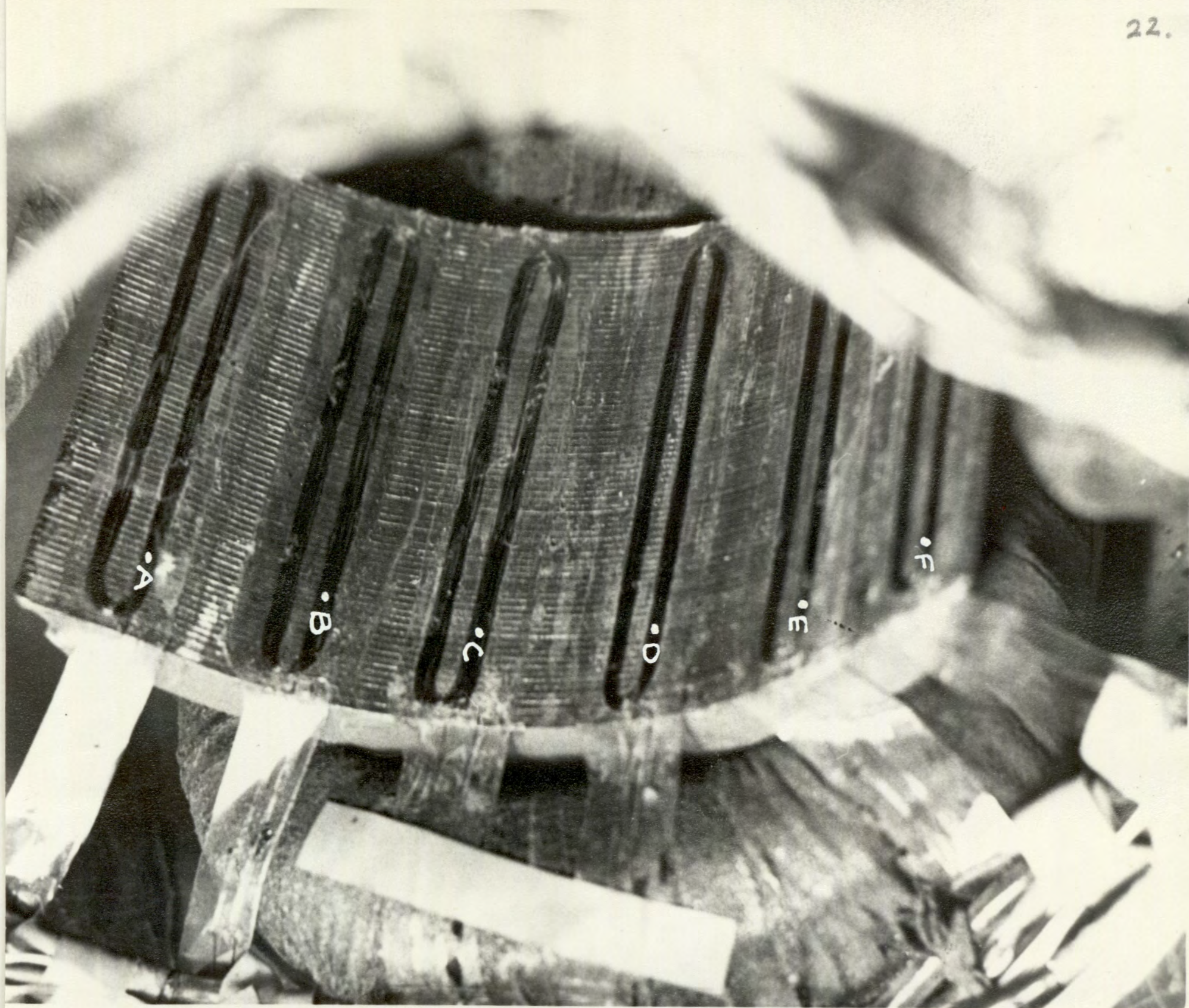




Fig. 3.3.

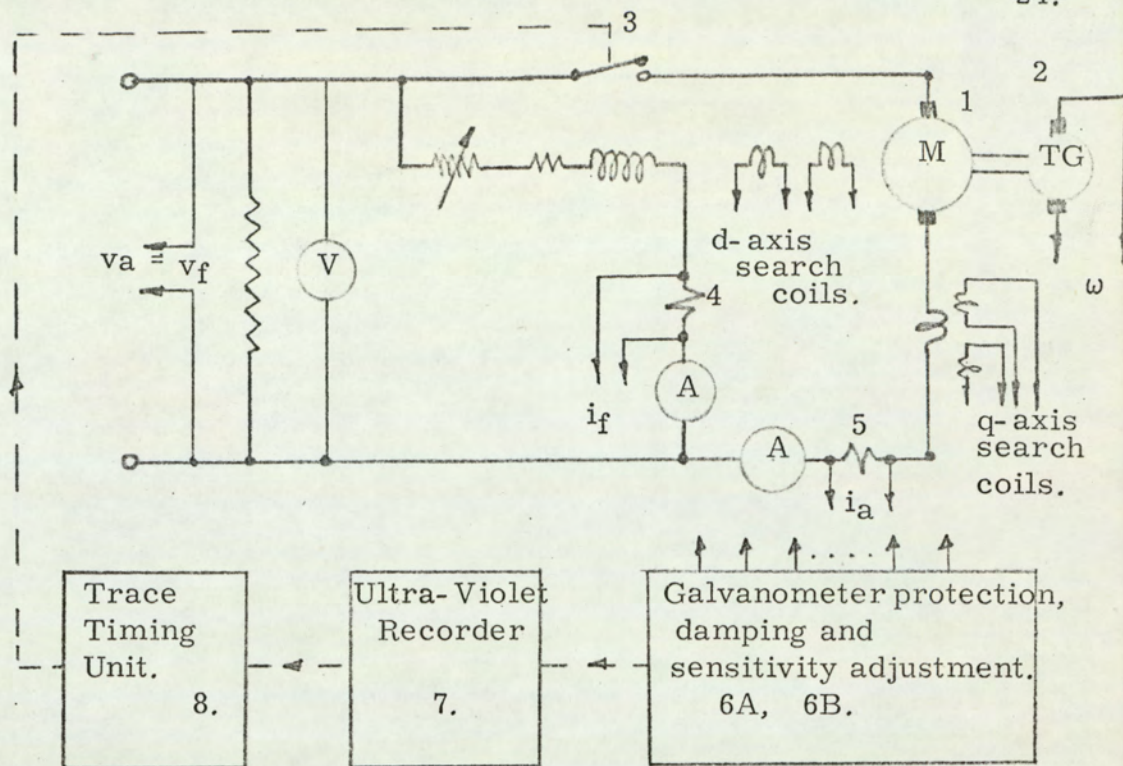


FIG. 3.2.

The following numerals refer to the items shown:-

1. Machine under test.
2. Tacho-generator to record speed.
3. Contactor for applying test condition.
4. Shunt to measure i_f .
5. Shunt to measure i_a .
- 6A. Galvanometer circuits for current measurement.
- 6B. Galvanometer circuits for voltage measurement.
7. Ultra-Violet Recorder.
8. Trace timing unit.
9. Fluxmeter for calibration.
10. Direct-coupled amplifiers.
11. Strobflash for calibration.

The trace timing unit (8) consisted of a delayed relay which started the recorder motor before initiating the main circuit contactor (3) and also timed the duration of the transient.

Search coil voltages were fed to direct-coupled integrators and amplifiers to record the changes in flux linking each coil, such that $\phi_S = k \int e_S dt$, where e_S = search coil voltage induced during a change.

The pole face search coils were calibrated separately against a standard coil for a number of different flux levels. For this purpose the coils were placed in the uniform field produced by a standard magnet having poles of 6" diameter.

From the results the average area of each coil was determined from the values obtained for each coil.

Traces were calibrated by checking the galvanometer deflection against a known current, voltage or speed.

3. 3. EVALUATION OF MACHINE CHARACTERISTICS.

In order to obtain the precise nature of some of the machine characteristics it was essential to carry out a large number of transient tests. This was partly brought about by the obvious difficulty of measuring variables which were being forced to many times their normal value, and partly by the desire to obtain consistent measurements. The very large number of results obtained renders a complete presentation both impractical and of no great value. Instead, where such

tests were necessary, typical results of the measurements are given.

3.3.1 STEADY-STATE TESTS

3.3.1.1 OPEN CIRCUIT CHARACTERISTIC

The machine was coupled to a driving motor and driven at a constant speed of 1500 r. p. m. Terminal voltage generated for increasing and decreasing direct-axis excitation was then measured (FIG. 3.4).

From design data, the relation given by equation (2.8) was evaluated to give $e_a = 275 \phi_g \omega$ volts. This gives an expression for the airgap flux, as a function of the open-circuit voltage, of

$$\phi_g = 2.32 \times 10^{-5} \times e_a \text{ Wb/pole at 1500 r. p. m. --- (3.1)}$$

3.3.1.2 DIRECT-AXIS FLUX ϕ_G / M. M. F.

CHARACTERISTIC ON NO-LOAD.

A measure of the main-pole flux was obtained, for varying levels of direct-axis ampere-turns, by noting the fluxmeter deflection for a given change in excitation. The main-pole search coil (G, FIG. 3.1) was employed for this purpose.

The results appear in FIG. 3.5 together with the values obtained from equation (3.1) which are, based on the average value of e_a , taken from FIG. 3.4 .

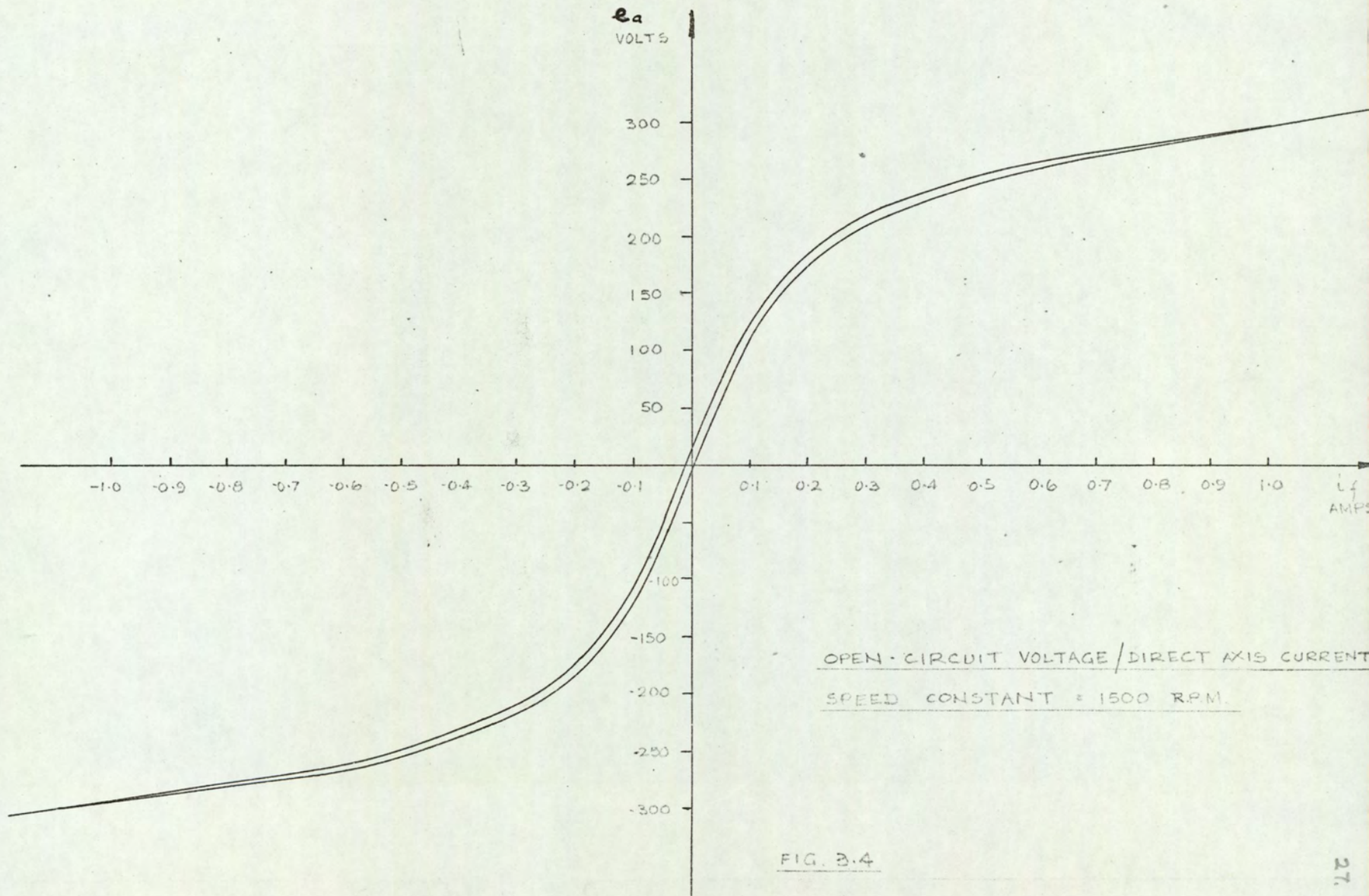


FIG. 3.4

FLUX/POLE
mwb

ESTIMATED AIR-GAP FLUX ϕ_g /DIRECT-AXIS MM.F (FROM FIG.3.4). MEASURED FLUX ϕ_a
(SEARCH COIL G)/DIRECT-AXIS MM.F (MACHINE STATIONARY)

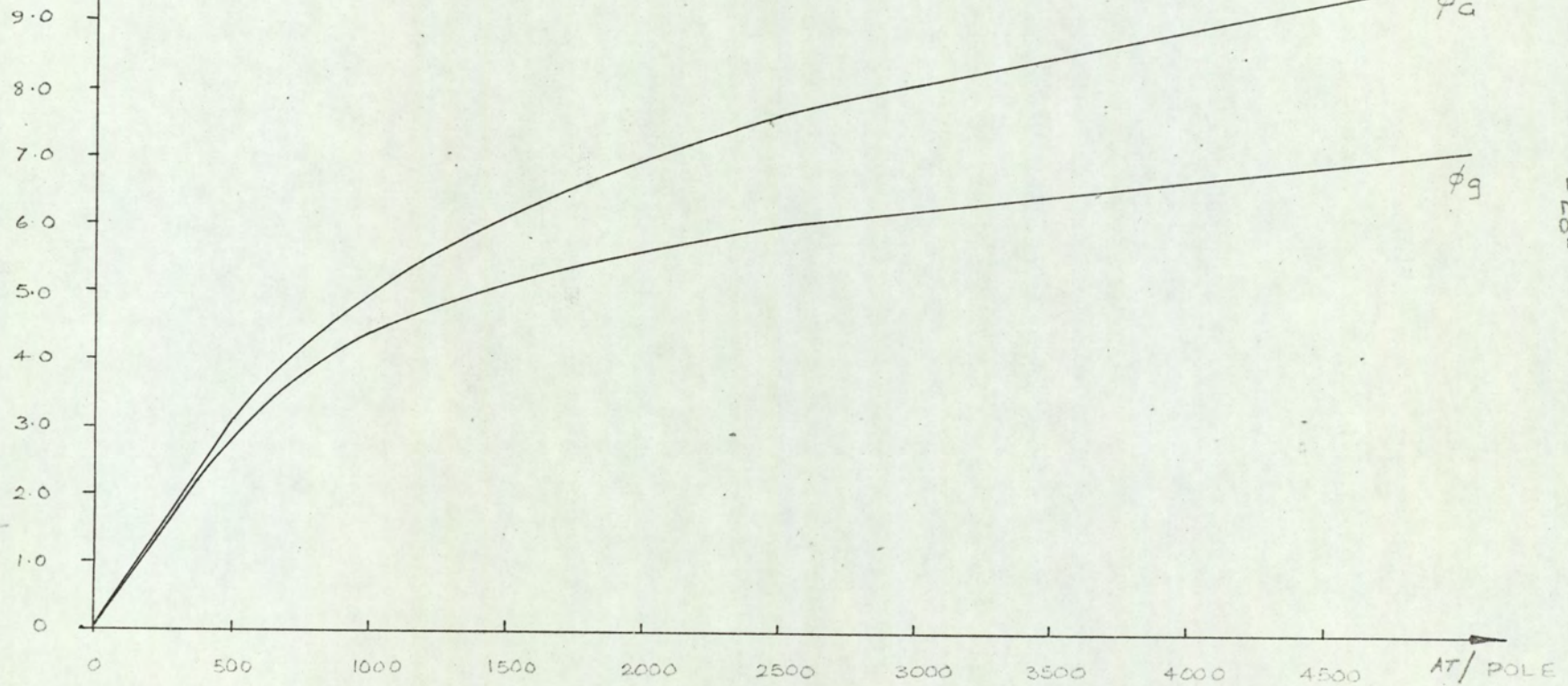


FIG. 3.5

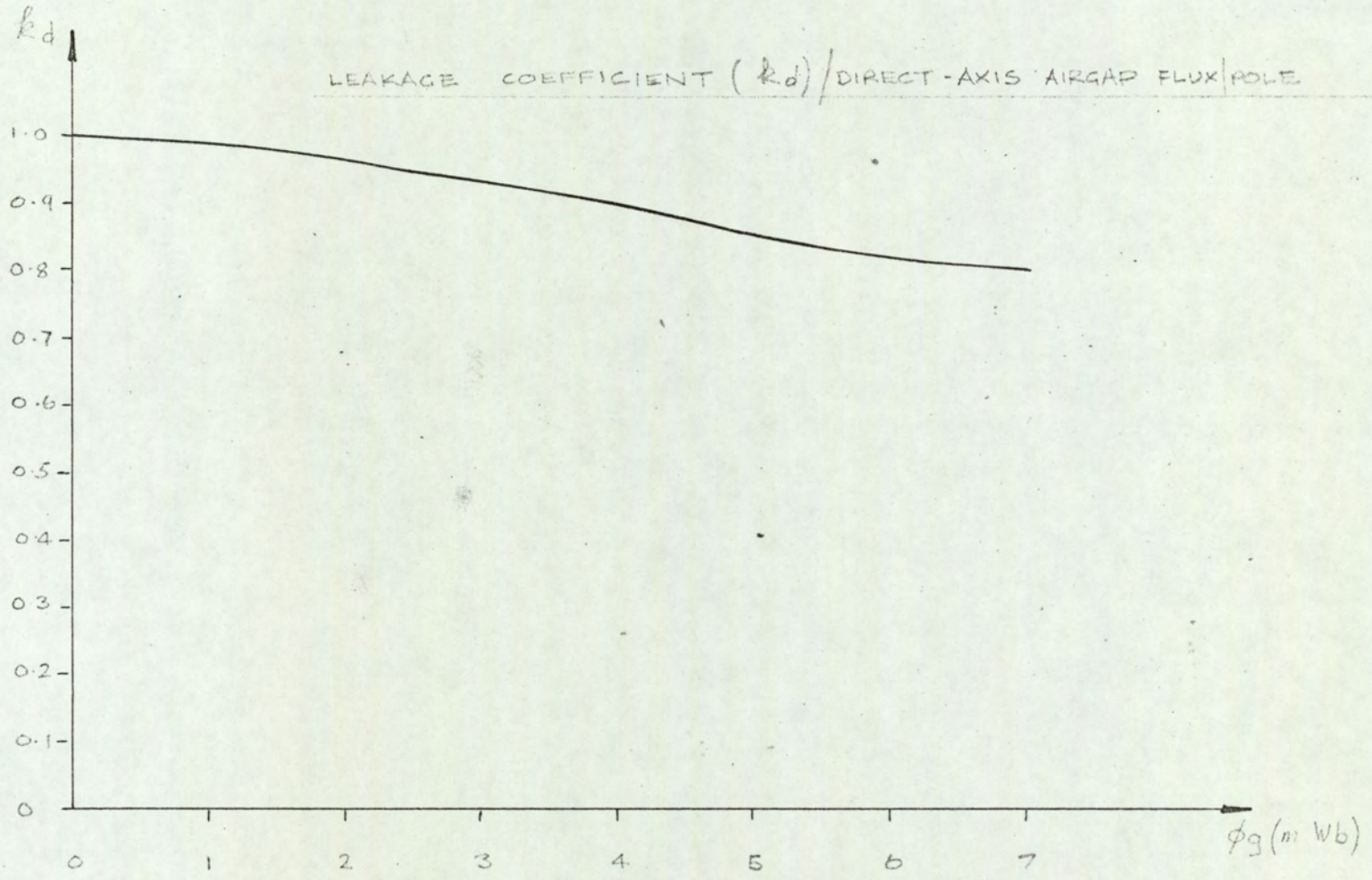


FIG. 3.5a

3.3.1.3.1 DIRECT-AXIS LEAKAGE FLUX.

The direct-axis leakage flux was estimated by comparing the flux linking search coils G, H and I with the estimated airgap flux ϕ_g . In fact the difference in flux linking search coils H and I compared with that linking search coil G proved to be insignificant. So that a measure of the leakage was taken directly from the results shown in FIG. 3.5.

The leakage coefficient k_d (equn. 2.3) plotted against airgap flux/pole (ϕ_g) is shown in FIG. 3.5a.

3.3.1.3.2 QUADRATURE-AXIS LEAKAGE FLUX.

The flux linking search coil J, which was wound close to the pole tip, was taken to represent the useful quadrature-axis flux under the pole. The results shown in FIG. 3.6 then gave $\phi_J \approx 0.7 \phi_L$ and $\phi_J \approx 0.77 \phi_K$.

3.3.1.4 POLE-FACE FLUX DENSITY

With the machine stationary the flux-density, at various positions (A-F) under the main pole, was measured for various values of direct-axis m. m. f. The quadrature axis being unexcited.

This measurement was then repeated for varying quadrature-axis m. m. f. with the direct-axis unexcited.

The results appear in FIGS. 3.7 and 3.8 respectively.

3.3.1.5 QUADRATURE-AXIS CIRCUIT RESISTANCE

Tests were conducted on the quadrature axis to estimate the change in resistance due to a) quadrature axis current and b) Speed of rotation.

FLUX/POLE
in Wb

SEARCH COIL FLUX/QUADRATURE-AXIS CURRENT i_q

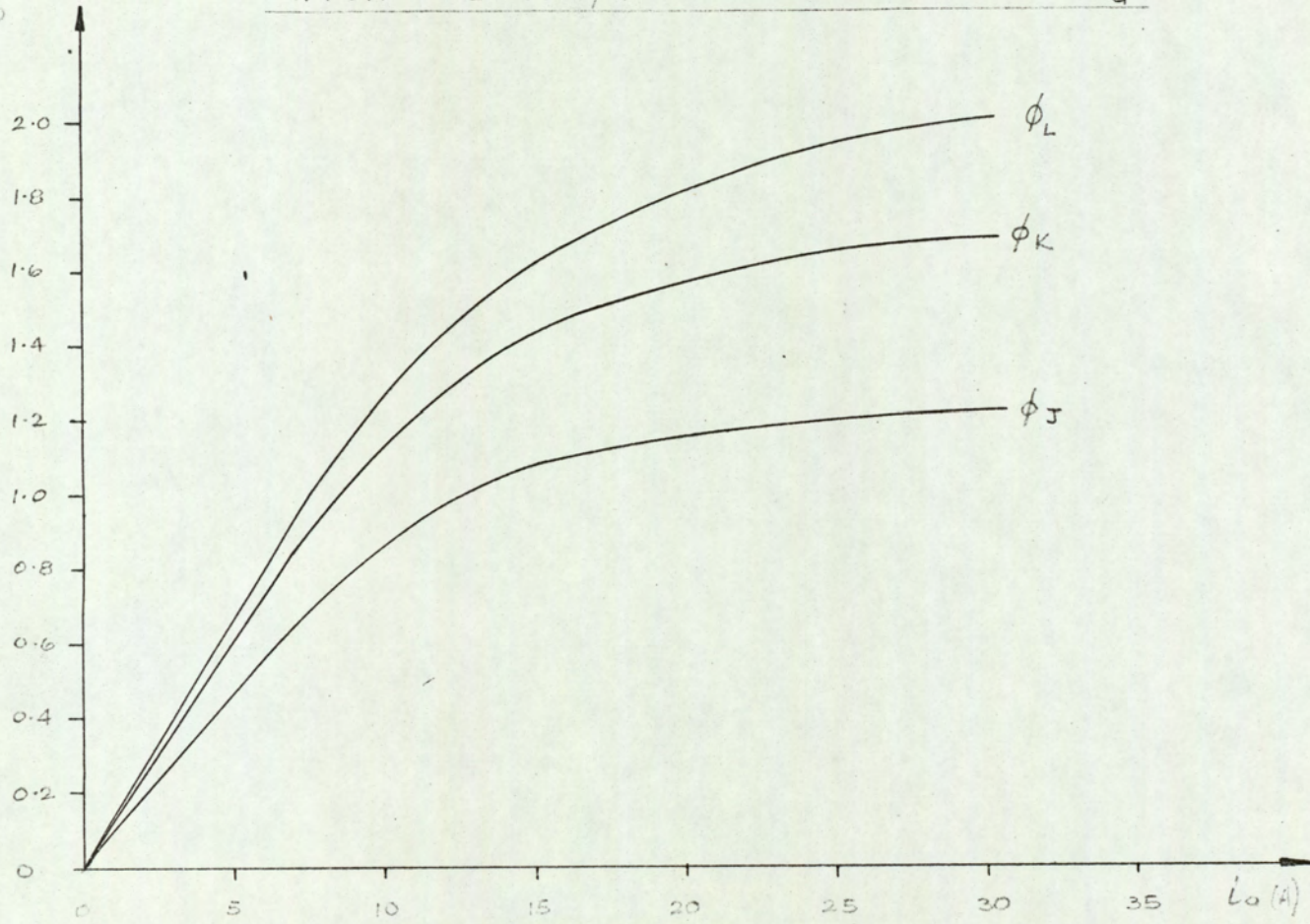


FIG. 3.6

B (Wb/M²)

DIRECT-AXIS POLE FACE FLUX-DENSITY /MMF
FOR VARIOUS SEARCH COIL POSITIONS

B_{av} - AVERAGE FLUX-DENSITY OBTAINED FROM
SEARCH COILS A-F

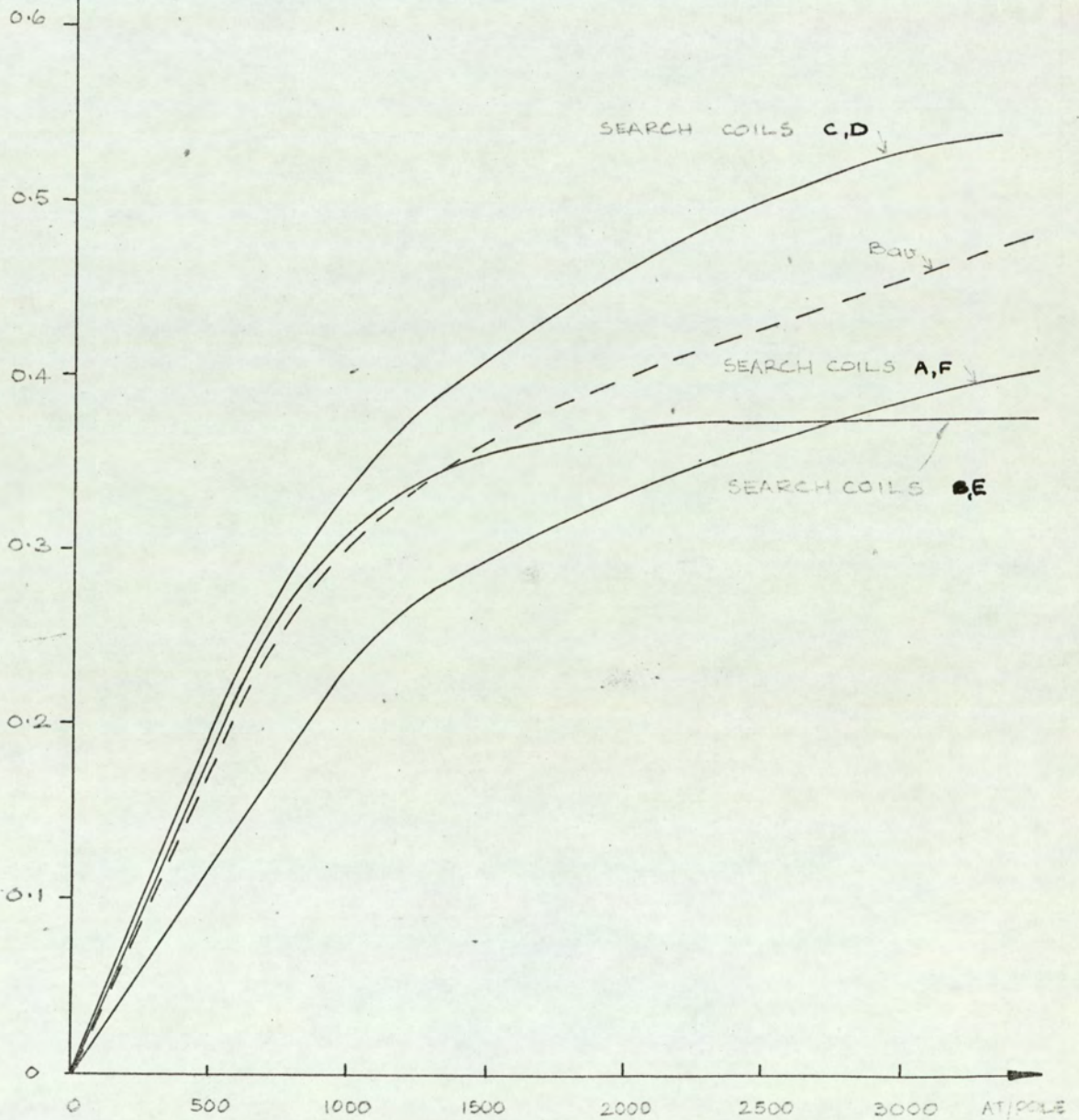
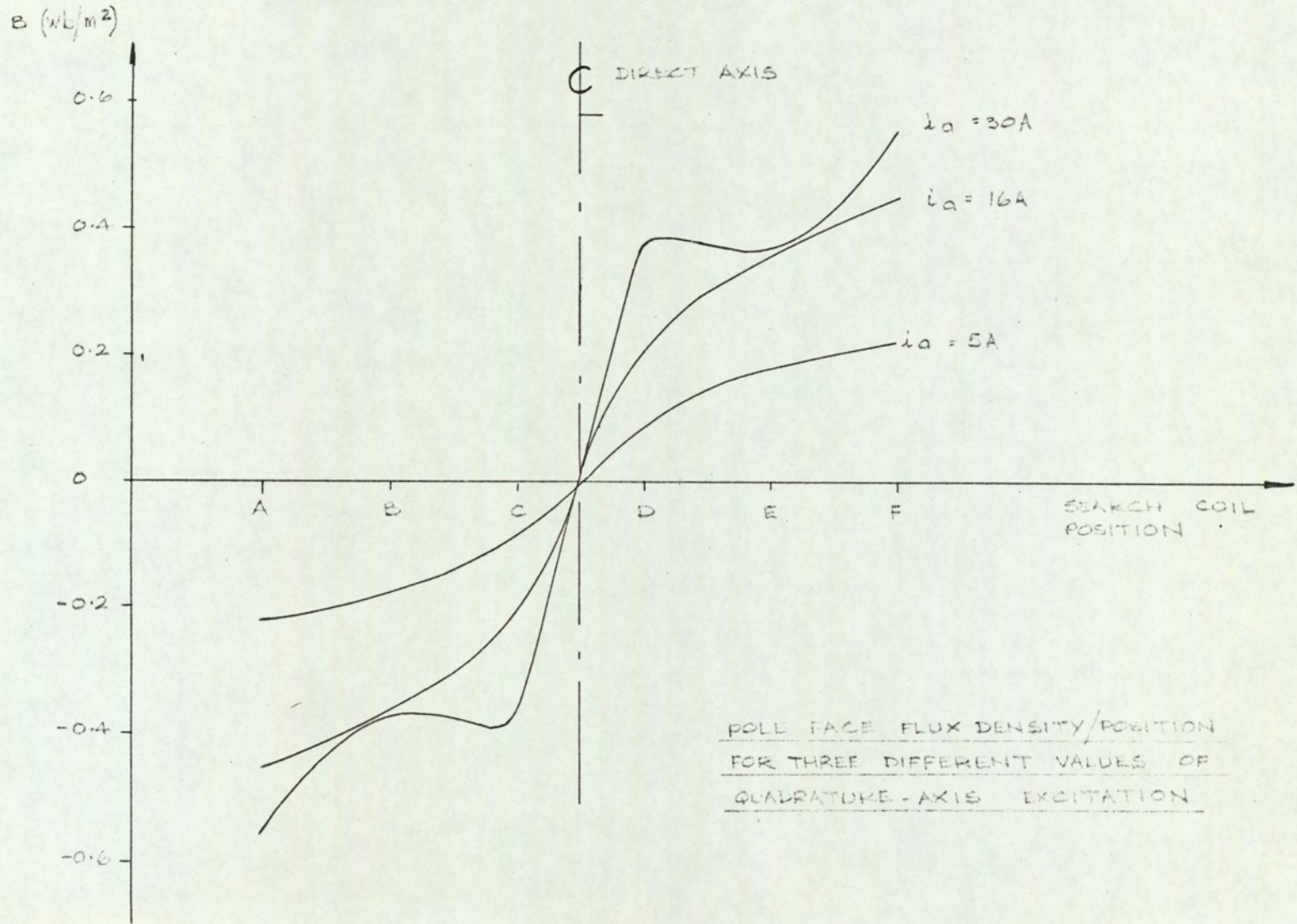


FIG. 3.7



POLE FACE FLUX DENSITY/POSITION
FOR THREE DIFFERENT VALUES OF
QUADRATURE-AXIS EXCITATION

FIG. 3.8

The machine was coupled to a driving motor in order that it could be driven without direct axis excitation, in both directions.

The brush voltage was then measured at different speeds, while maintaining a constant quadrature-axis current.

The results are shown in FIGS. 3.9 - 3.11, from which the curve (FIG. 3.12) was plotted to represent the change in slope of the curves (FIG. 3.11) as a function of current (i_a). The quadrature axis circuit resistance was then expressed in the form $r_a = \alpha \omega + 3.6$ ohms ----- (3.2)

$$\text{where } \alpha = b/i_a^c \text{ ----- (3.3)}$$

The constants b and c determined from a curve relating $\log(\alpha)$ and $\log(i_a)$ were $b = .042$ and $c = 0.69$.

In order to allow for the case when the current (i_a) fell to very small values the slope of the curve was fixed at $a = 0.09$ for values of $i_a < 0.5A$. This figure being based on the slope of the curve (FIG. 3.12) for low values of current. A similar procedure was adopted for the very high currents, where it was impractical to maintain heavy currents for more than a fraction of a second.

At zero speed there was a slight increase in resistance as the current level was reduced to less than 3A, but the change was assumed to be insignificant.

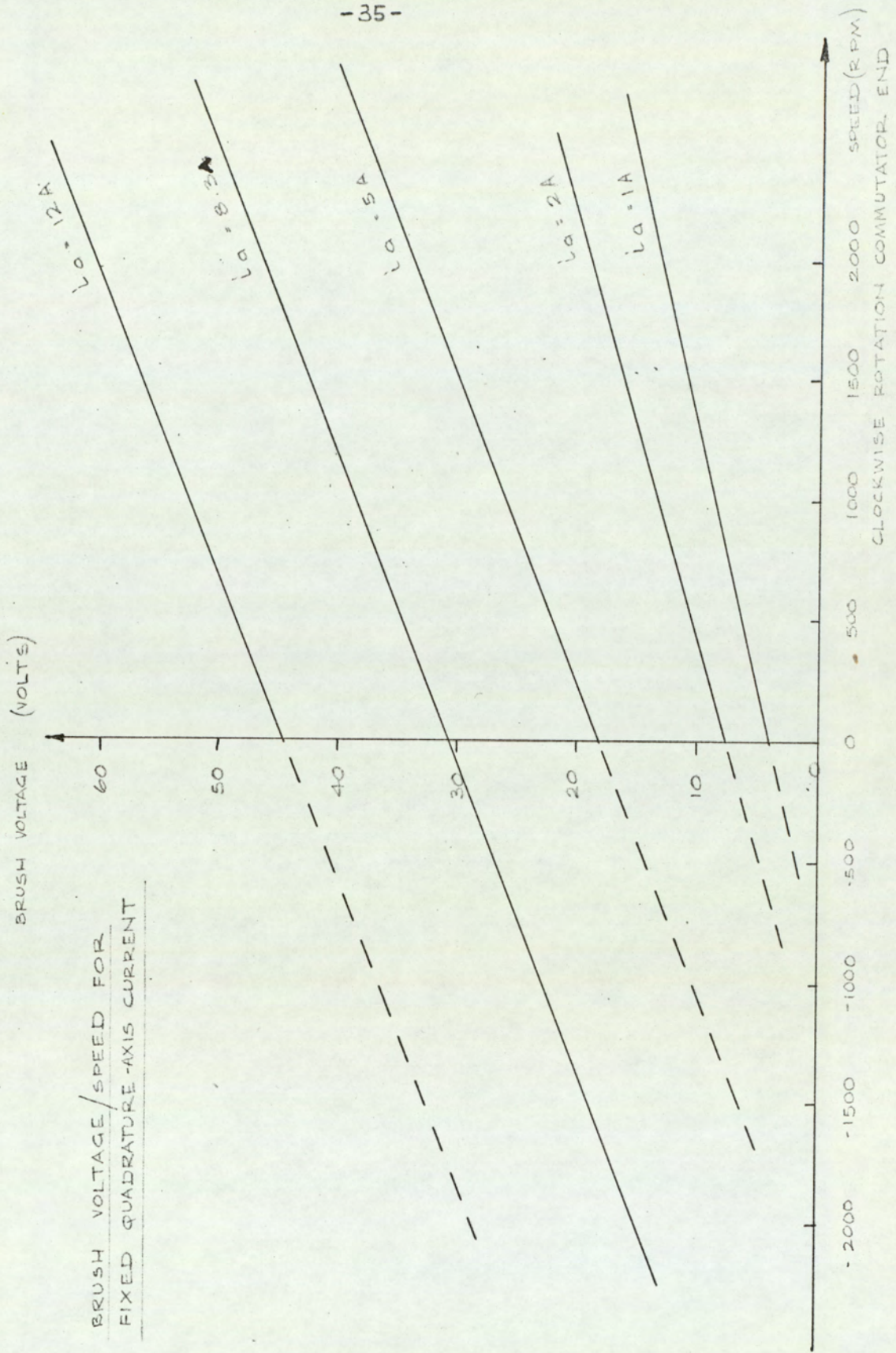


FIG. 3.9

$r_a (\Omega)$

QUADRATURE-AXIS CIRCUIT RESISTANCE/QUADRATURE-AXIS CURRENT

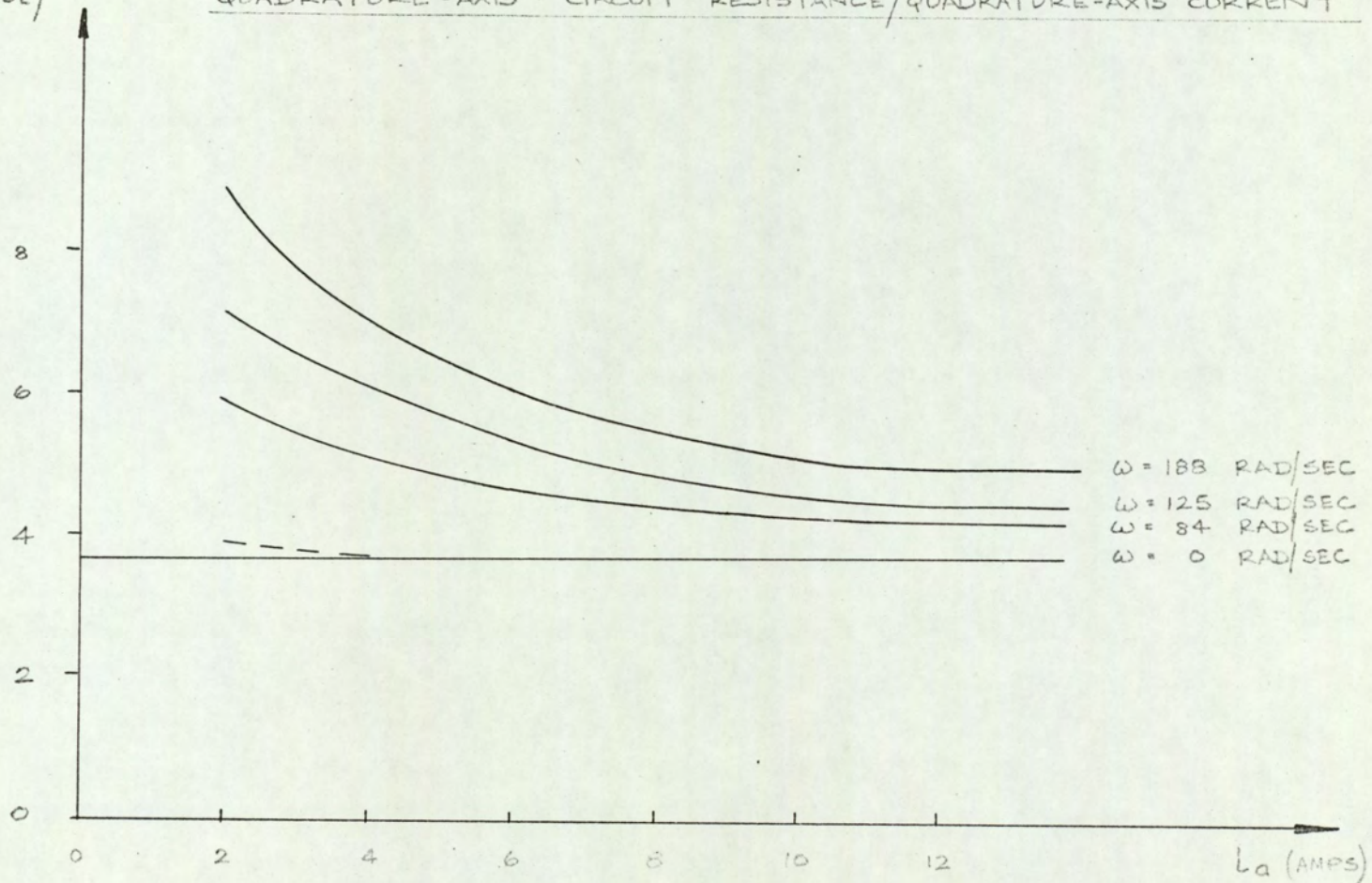


FIG. 3.10

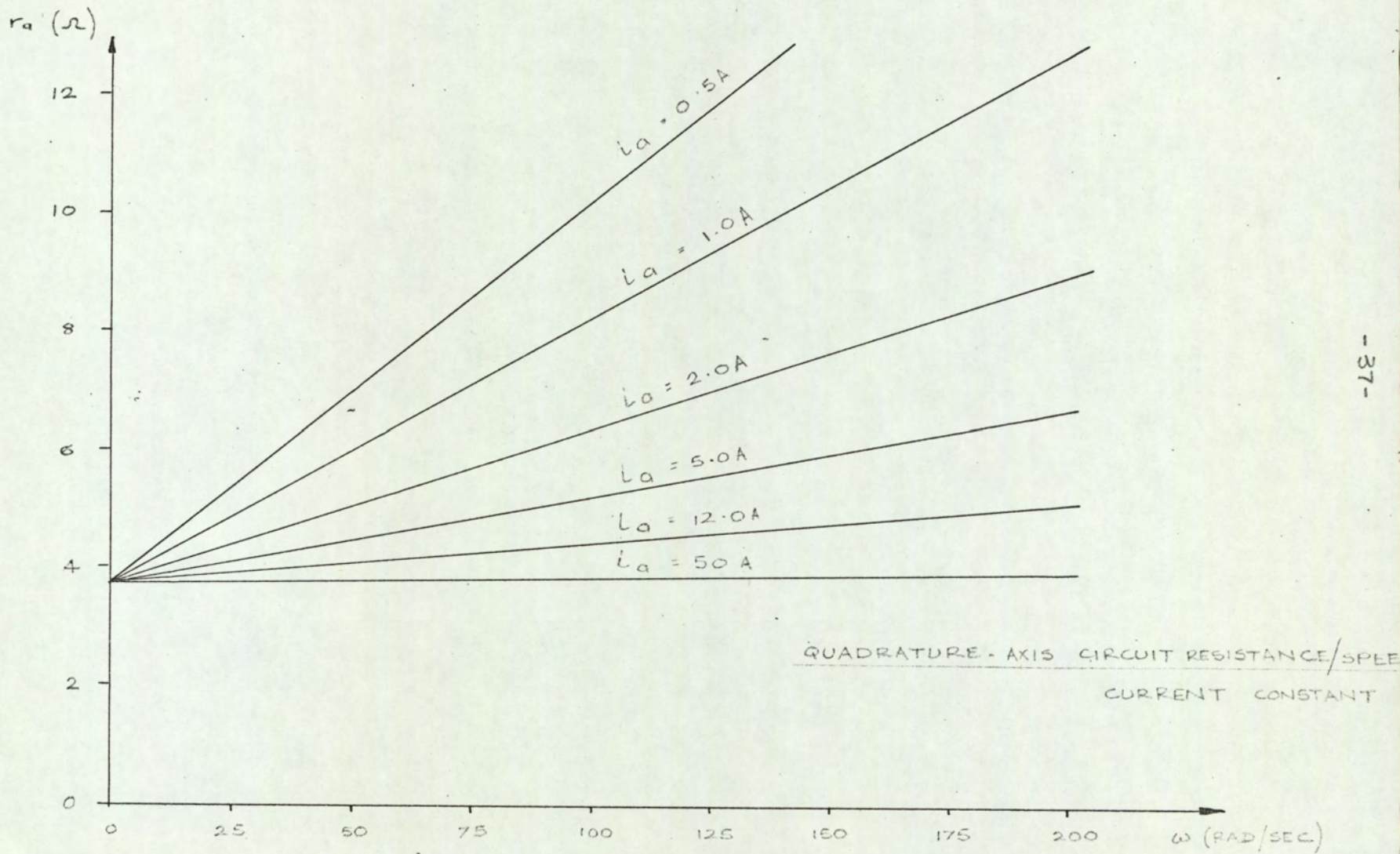


FIG. 3.11

α (RAD/SEC)

SLOPE (α) OF CURVES IN FIG. 3.11 / QUADRATURE-AXIS CURRENT

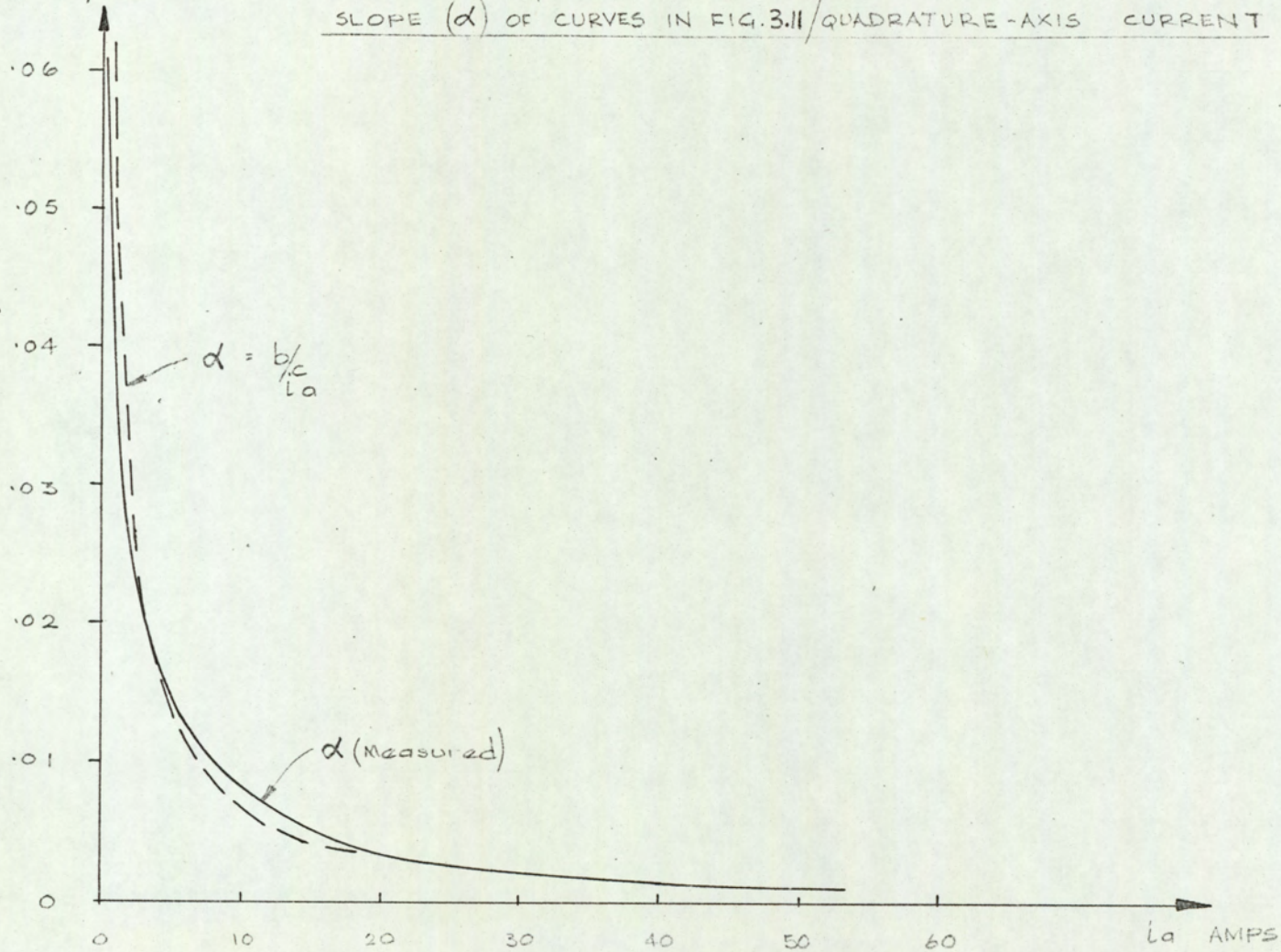


FIG. 3.12

3.3.1.6. LOAD TORQUE CHARACTERISTIC.

The machine was uncoupled and run on no load as a motor, with constant direct-axis excitation, and variable armature voltage. Then at different steady-state speeds, determined by the applied voltage, the quadrature axis current i_a was recorded.

From these results and a knowledge of r_a , from FIG. 3.11, the armature power output was determined as a function of speed. Hence enabling the no-load torque / speed characteristic to be obtained (FIG. 3.13).

One would expect this torque to be sufficient to overcome the opposing torques due to (a) friction and windage and (b) hysteresis and eddy currents. But although the tests were conducted at different fixed values of direct-axis current this produced no significant difference in the characteristic obtained over the speed range of interest.

As it was anticipated that the peak accelerating torques would be greatly in excess of the no-load torque it was decided to take the curve (FIG. 3.13) as a typical characteristic.

E_2 (Nm)

NO LOAD TORQUE/SPEED

2.0

1.5

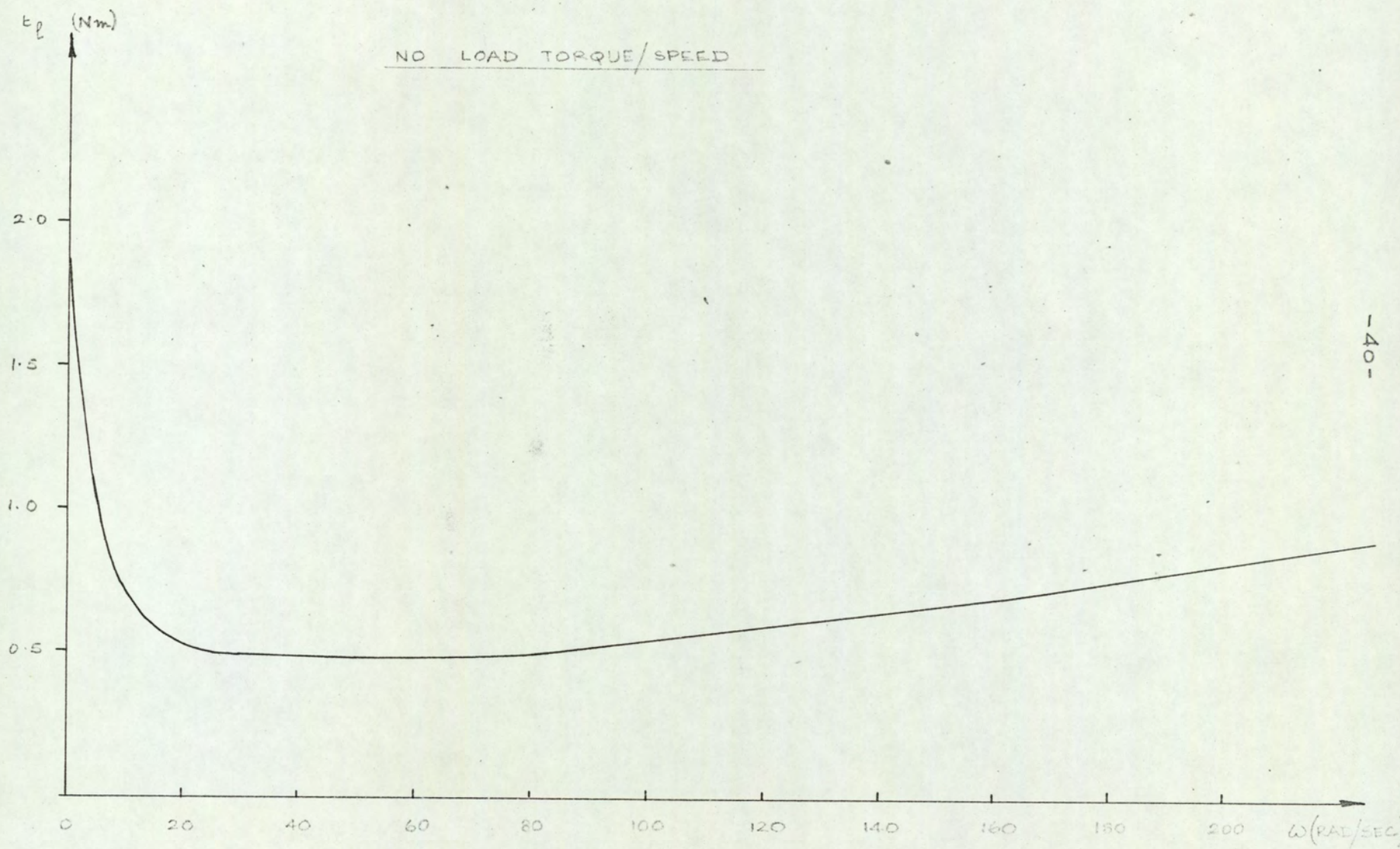
1.0

0.5

0 20 40 60 80 100 120 140 160 180 200 ω (RAD/SEC)

- 40 -

FIG. 3.13



3.3.2 TRANSIENT TESTS.

3.3.2.1 ARMATURE INERTIA

The armature inertia was deduced by employing the results of section (3.3.1.6). A deceleration test being performed using a suitable speed range chosen from the characteristic. (FIG. 3.13).

The time taken for the speed of the machine to fall from ω_1 to ω_2 was recorded, by open circuiting the quadrature-axis circuit and retaining constant direct-axis excitation. The decelerating torque, over the chosen speed range, is then defined by the expression $-(.305 + 2.38 \times 10^{-3} \omega) = J \frac{d\omega}{dt}$ Nm ----- (3.4) where J is the armature inertia in kg-m^2 .

The time taken for the speed to fall from $\omega_1 = 157$ rad/sec. to $\omega_2 = 83.8$ rad/sec. was recorded after a number of trials to be $t = 4.647$ sec.

$$\begin{aligned} \therefore \frac{0.305 t}{J} &= - \int_{\omega_1}^{\omega_2} \frac{d\omega}{(1 + 7.8 \times 10^{-3} \omega)} \\ &= \frac{1}{7.8 \times 10^{-3}} \left[\log_e (1 + 7.8 \times 10^{-3} \omega) \right]_{\omega_2}^{\omega_1} \end{aligned}$$

$$J = \frac{4.647 \times .305 \times 7.8 \times 10^{-3}}{.296} = 0.0373 \text{ kg-m}^2$$

3.3.2.2 DYNAMIC RELATION BETWEEN FLUX AND
EXCITING M. M. F.

3.3.2.2.1 DIRECT-AXIS FLUX ϕ_G /M. M. F. RELATION

WITH $i_a = 0$.

With the machine coupled to a driving motor, and driven at constant speed, the circuit was connected as shown in FIG. 3.14.

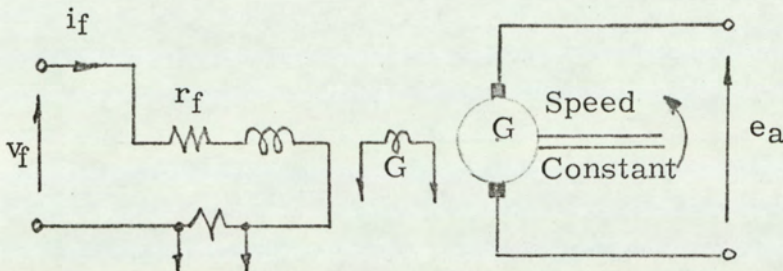


FIG. 3.14.

Measurements of i_f , e_a and ϕ_G were recorded as functions of time for a constant step change in voltage v_f , using the recording apparatus described in FIG. 3.2.

For a given value of i_f the value of the flux (ϕ_G) as given by the curve (FIG. 3.5) under steady-state conditions was plotted with the other results obtained. (FIG. 3.15). The discrepancy between the two curves ϕ_G and ϕ'_G was then taken to represent the phase lag which exists between the direct-axis flux and direct-axis m.m.f. during transient conditions.

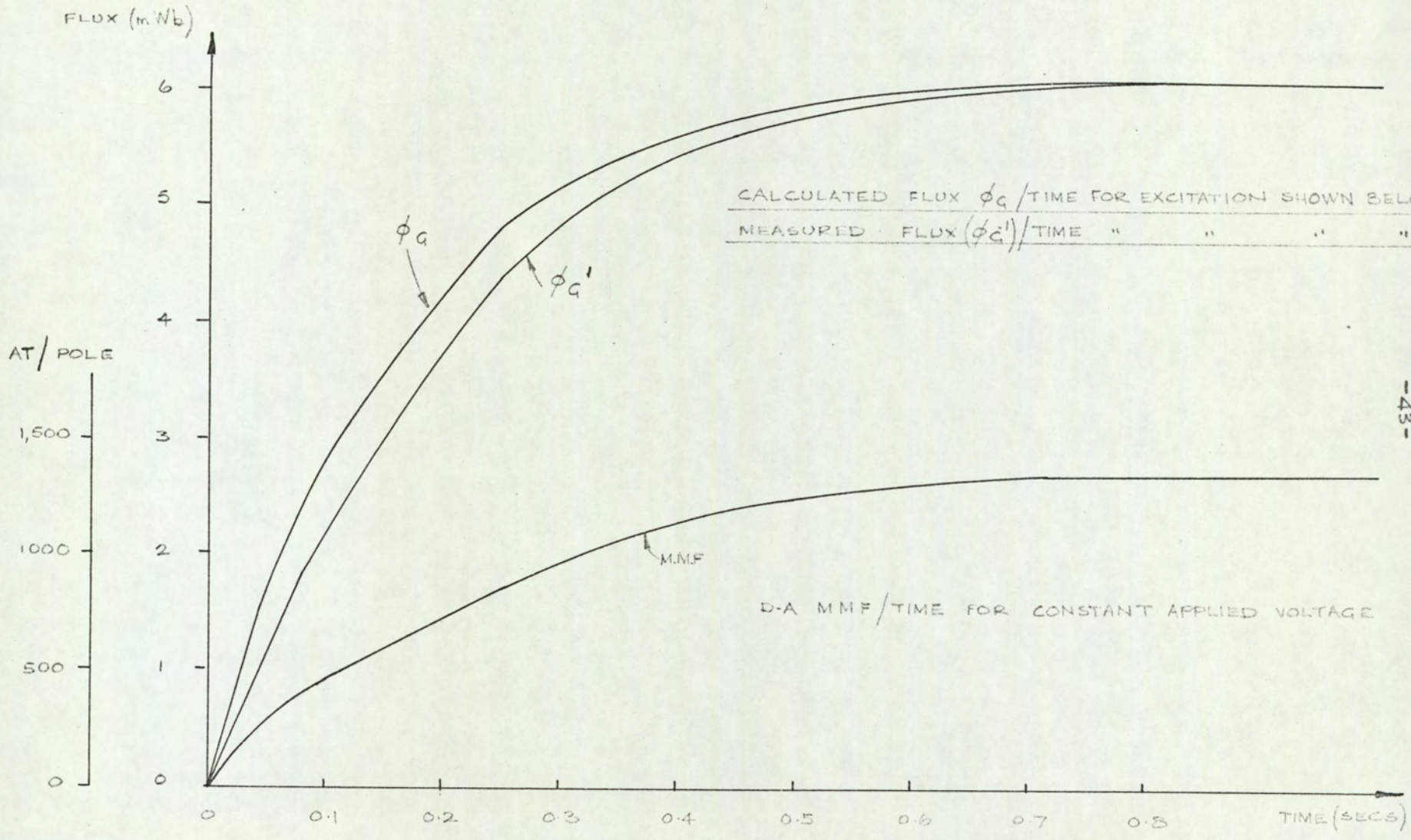


FIG. 3.15

EVALUATION OF $T\phi_d$

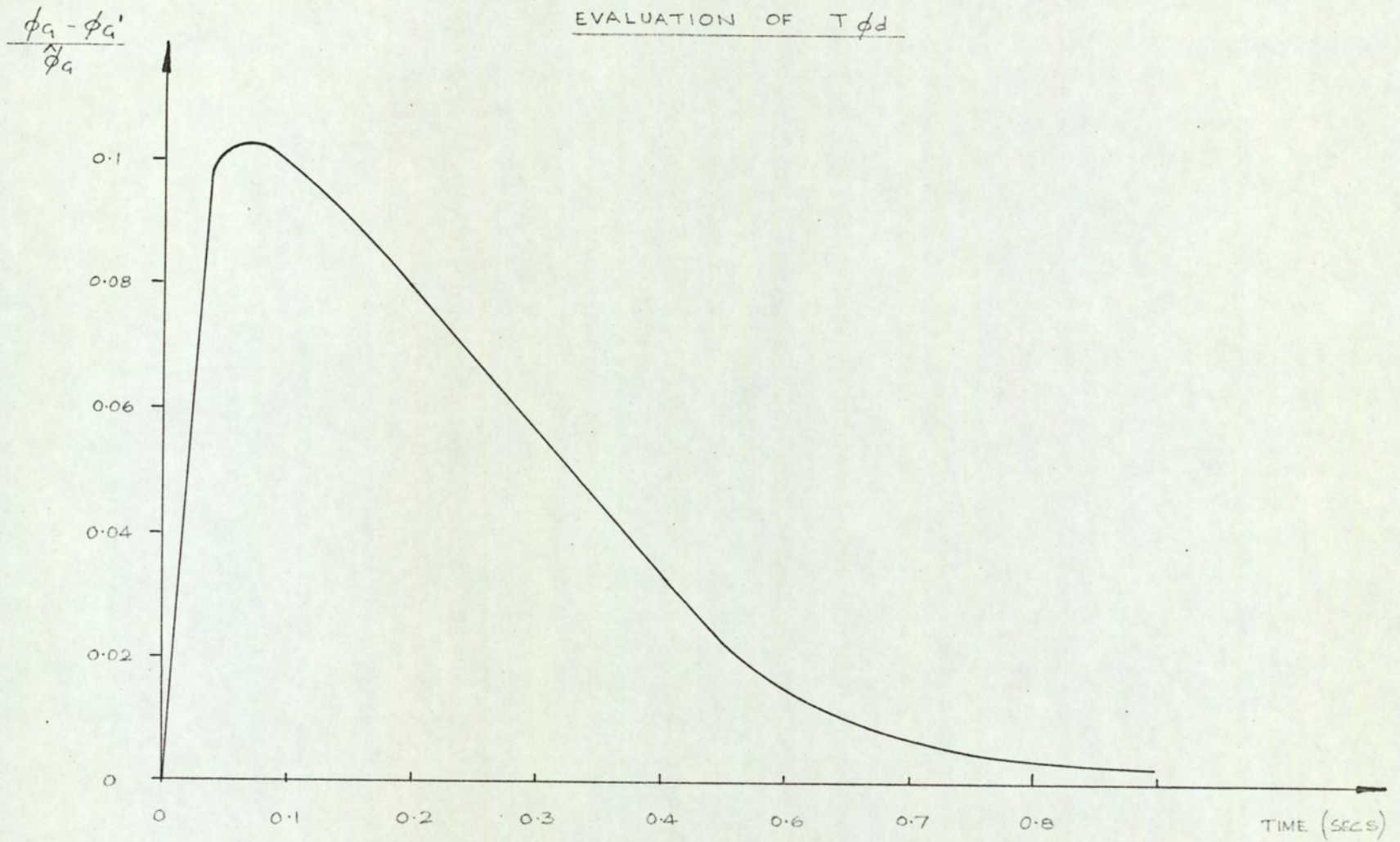


FIG. 3.16

$$\text{Then, if } \phi_G = \phi'_G + T\phi_d \frac{d\phi'_G}{dt} \text{ ----- (3.5)}$$

is taken to represent the relation between ϕ_G and ϕ'_G , the mean time-constant $T\phi_d$ may be evaluated.

Consideration of this relation will show that the non-linear nature of the magnetic circuit involves a changing value of $T\phi_d$. Also since the flux will probably be delayed by penetration time as well as eddy currents a more exact approximation could well involve a second order equation. However it was realised that the true nature of the relation could not be expressed more simply than the method chosen. Especially since the pattern of the flux distribution renders the two-dimensional approach an approximation.

It is, of course, possible to represent the time delay more closely than the mean value chosen by calculating the incremental value of $T\phi_d$ and treating it as a non-linear function.

However, the approximation given by equation (3.5) was taken, to give

$$T\phi_d = \int_0^t \frac{\phi_G - \phi'_G}{\phi_G} dt, \text{ which when evaluated from}$$

FIG. 3.16 gives $T\phi_d = 0.03$ sec.

It was found from the test that there was virtually no difference in the results obtained by measurement of e_a and hence ϕ_g , than those obtained by the use of search coil G. These results have therefore been omitted.

3.3.2.2.2 QUADRATURE-AXIS FLUX ϕ_J /M. M. F.

RELATION WITH $i_f = 0$.

With the machine stationary a suitable constant voltage v_a was suddenly applied to the quadrature axis and the resulting current i_a and flux ϕ_J was recorded on a C. R. O. against time.

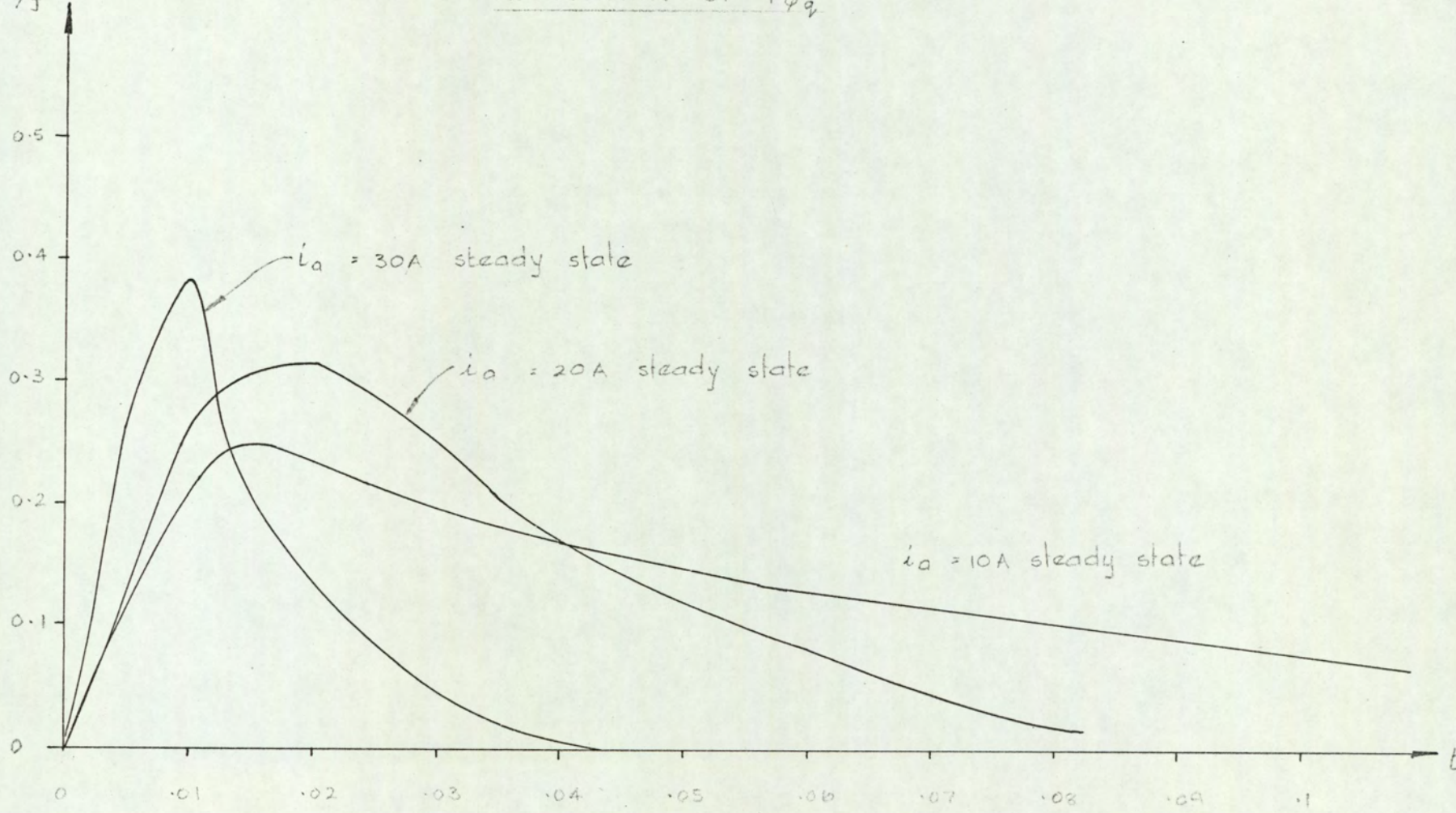
From the results obtained the equation

$$\phi_J = \phi'_J + T\phi_q \frac{d\phi'_J}{dt} \quad \text{----} \quad (3.6)$$

was evaluated in a similar manner to that described in section 3.3.2.2.1.

The resulting value of $T\phi_q$ was found to vary according to the magnitude of the steady state M. M. F., as the curves in FIG. 3.17. indicate.

$$\frac{\phi_J - \phi_J'}{\phi_J}$$



TIME (SECS)

FIG. 3.17

3.3.2.3. MACHINE ACCELERATING FROM REST.

With the machine connected as shown in FIG. 3.2 measurements of current (i_a), speed (ω), quadrature-axis flux (ϕ_J), direct-axis flux (ϕ_G) and current (i_f) were recorded as functions of time for a suddenly applied voltage ($v_a = v_f$).

Owing to the difficulty experienced in maintaining the applied voltage at a constant value, due to forcing the current (i_a), this was also recorded.

Measurements were repeated a number of times to obtain consistent results, which are tabulated in TABLES (3.1 - 3.6) with typical recordings shown in FIGS. (3.18, 3.19).

The tests were conducted under the following initial conditions, with $t = 0$:-

Test	Initial Applied Voltage $v_a = v_f$ (v)	Initial Direct-axis Current i_f (A)	Direct-axis circuit resistance r_f (Ω)	Average of Results Table No.	Typical Recording FIG. No.
1	222	0.0	1110	3.1	
2	225	0.0	790	3.2	3.18
3	222	0.0	556	3.3	
4	232	0.2	1160	3.4	
5	213	0.285	748	3.5	3.19
6	232	0.405	573	3.6	

TABLE 3.1

Current(i_a) amps.	Speed(ω) rad/sec.	Flux(ϕ_J) mWb.	Flux(ϕ_G) mWb.	Current(i_f) Amps.	Voltage $v_a=v_f$ Volts	Time(t) Secs.
0.0	0.0	0.0	0.0	0.0	222	0.0
40.0	3.5	1.04	0.302	0.059	202	0.025
56.0	8.65	1.04	0.505	0.0945	200	0.05
55.0	13.0	1.06	0.808	0.121	202	0.075
54.3	19.0	1.06	0.91	0.140	202	0.1
50.5	55.4	1.06	1.21	0.171	209	0.2
45.8	98.7	1.06	1.51	0.173	213	0.3
39.1	138.0	1.06	1.77	0.172	217	0.4
32.0	173.0	1.09	1.97	0.180	219	0.5
26.2	204.0	1.09	2.27	0.185	219	0.6
21.8	227.0	1.09	2.42	0.185	222	0.7
14.2	246.0	1.04	2.93	0.18	228	0.8
5.4	260.0	0.765	3.44	0.149	228	0.9
0.0	256.0	0.273	3.99	0.185	228	1.0
-2.2	246.0	0.082	4.05	0.19	228	1.1
0.5	215.0	0.205	4.6	0.20	228	1.5

ESTIMATED MEASUREMENT ACCURACY

Current (i_a)	\pm 2A in 50A
Speed (ω)	\pm 4 rad/sec. in \pm 250 rad/sec.
Flux (ϕ_J)	\pm 0.05 mWb. in \pm 3 mWb.
Flux (ϕ_G)	\pm 0.1 mWb. in \pm 6 mWb.
Current (i_f)	\pm 0.01 A. in 0.5A
Voltage (v_a, v_f)	\pm 4V. in 200V.

TABLE 3.2

Current(i_a) amps.	Speed(ω) rad/sec.	Flux(ϕ_J) mWb.	Flux(ϕ_G) mWb.	Current(i_f) Amps.	Voltage $v_a=v_f$ Volts	Time(t) Secs.
0.0	0.0	0.0	0.0	0.0	225	0.0
48.2	3.46	1.09	0.404	0.1425	204	0.025
56.5	8.65	1.09	0.505	0.187	204	0.05
57.4	19.0	1.09	0.807	0.197	204	0.075
57.0	24.2	1.12	1.06	0.212	204	0.1
52.1	71.0	1.09	1.52	0.246	208	0.2
43.2	117.5	1.09	1.87	0.246	214	0.3
32.5	161.0	1.09	2.17	0.256	219	0.4
23.6	201.0	1.09	2.67	0.256	223	0.5
13.3	225.0	1.04	3.38	0.212	225	0.6
1.78	235.0	0.545	4.34	0.231	232	0.7
-3.1	221.0	0.136	4.74	0.285	232	0.8
-2.2	204.0	0.136	5.05	0.29	227	0.9
0.0	187.0	0.218	5.21	0.29	225	1.0
0.7	171.0	0.314	5.73	0.29	225	1.5

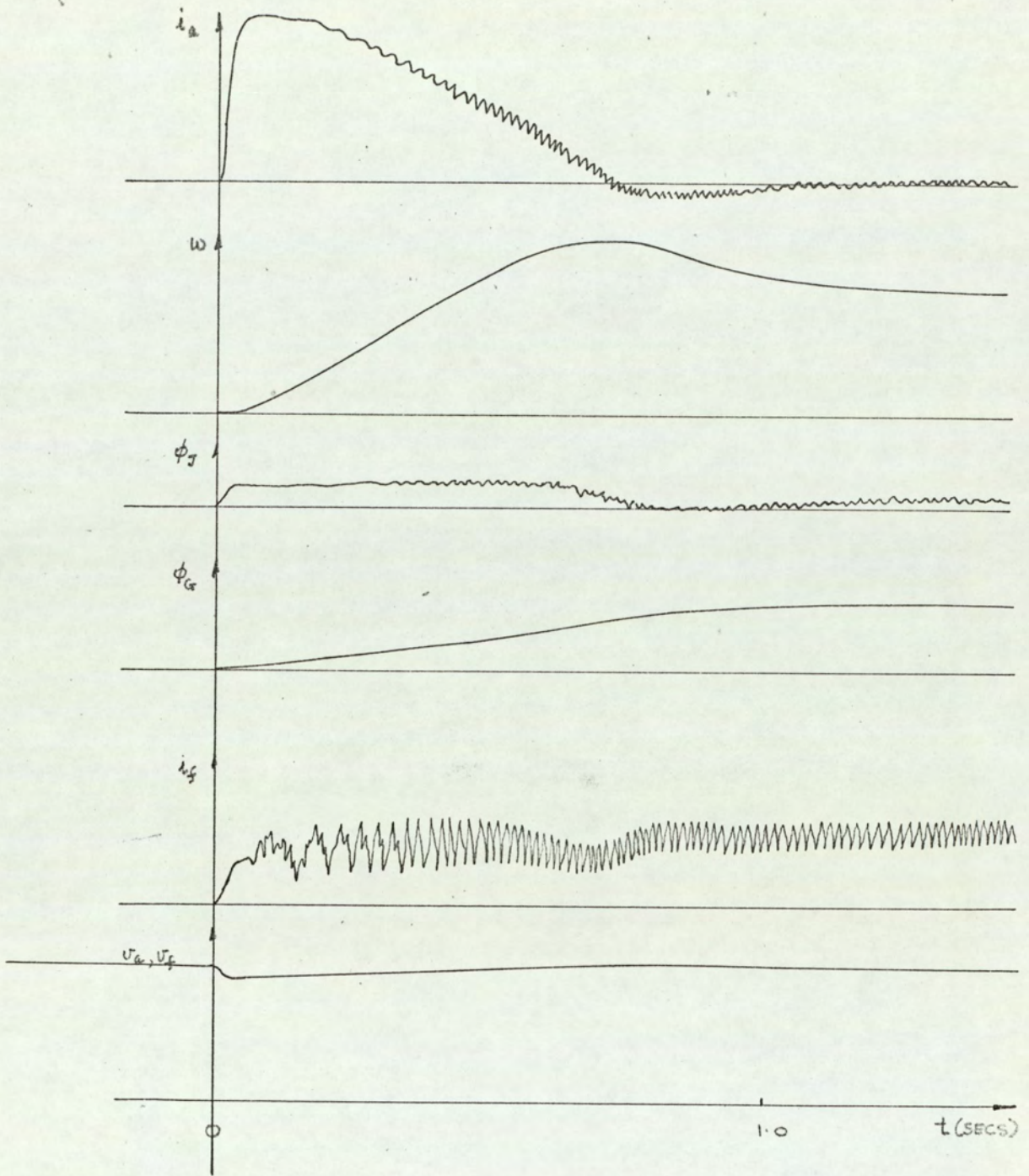


FIG. 3.18

TABLE 3.3

Current(i_a) Amps.	Speed(ω) rad/sec.	Flux(ϕ_J) mWb.	Flux(ϕ_G) mWb.	Current(i_f) Amps.	Voltage $v_a = v_f$ Volts	Time(t) Secs.
0.0	0.0	0.0	0.0	0.0	222	0.0
42.3	3.5	1.07	0.404	0.092	207	0.025
53.4	10.4	1.07	0.756	0.138	202	0.05
53.8	20.5	1.07	1.06	0.18	205	0.075
53.4	27.7	1.07	1.42	0.23	207	0.1
45.4	81.5	1.07	2.06	0.294	213	0.2
33.8	133.0	1.07	2.63	0.313	217	0.3
20.9	177.0	1.07	3.38	0.285	224	0.4
8.0	199.0	0.79	4.54	0.23	230	0.5
-4.5	195.0	0.11	5.46	0.317	233	0.6
-3.56	174.0	0.0	6.01	0.359	233	0.7
-0.9	158.0	0.19	6.27	0.368	230	0.8
0.5	150.0	0.3	6.46	0.391	228	0.9
0.8	145.0	0.38	6.46	0.395	228	1.0
0.8	143.0	0.38	6.52	0.395	228	1.1
0.5	142.0	0.425	6.6	0.4	228	1.5

TABLE 3.4

Current(i_a) amps.	Speed(ω) rad/sec.	Flux(ϕ'_J) mWb.	Flux(ϕ_G) mWb.	Current(i_f) Amps.	Voltage $v_a=v_f$ Volts	Time(t) Secs.
0.0	0.0	0.0	4.68	0.2	232	0.0
44.5	17.2	1.01	4.43	0.54	211	0.025
48.0	41.5	1.01	2.72	0.328	213	0.05
47.2	60.5	1.04	2.27	0.293	215	0.075
45.8	76.1	1.04	2.02	0.248	215	0.1
40.0	123.0	1.04	1.91	0.18	220	0.2
34.3	163.0	1.04	2.06	0.18	224	0.3
27.2	194.0	1.06	2.27	0.175	226	0.4
22.3	221.0	1.06	2.52	0.171	232	0.5
15.6	244.0	1.01	2.92	0.162	232	0.6
7.1	256.0	0.71	3.52	0.144	232	0.7
0	247.0	0.27	3.98	0.18	234	0.8
-2.2	240.0	0.08	4.13	0.193	234	0.9
-0.5	225.0	0.14	4.38	0.2	234	1.0
0	218.0	0.22	4.43	0.2	234	1.1
0.9	210.0	0.44	4.7	0.2	234	1.5

TABLE 3.5

Current(i_a) amps.	Speed(ω) rad/sec.	Flux(ϕ_J) mWb.	Flux(ϕ_G) mWb.	Current(i_f) Amps.	Voltage $v_a=v_f$ Volts	Time(t) Secs.
0.0	0.0	0.0	5.62	0.285	213	0.0
36.5	22.5	1.04	4.43	0.653	196	0.025
39.2	48.4	1.09	3.62	0.516	198	0.05
36.5	71.0	1.15	3.32	0.457	202	0.075
33.0	90.0	1.15	3.11	0.398	209	0.1
25.0	143.5	1.15	2.81	0.285	211	0.2
16.5	176.5	1.09	3.22	0.226	212	0.3
7.5	200.0	0.71	4.13	0.196	213	0.4
-0.8	199.0	0.545	4.63	0.246	213	0.5
-2.2	183.5	0.272	5.13	0.275	213	0.6
-0.5	173.0	0.109	5.44	0.285	213	0.7
0.7	161.0	0.30	5.47	0.285	213	1.0
0.7	159.0	0.30	5.59	0.285	213	1.5

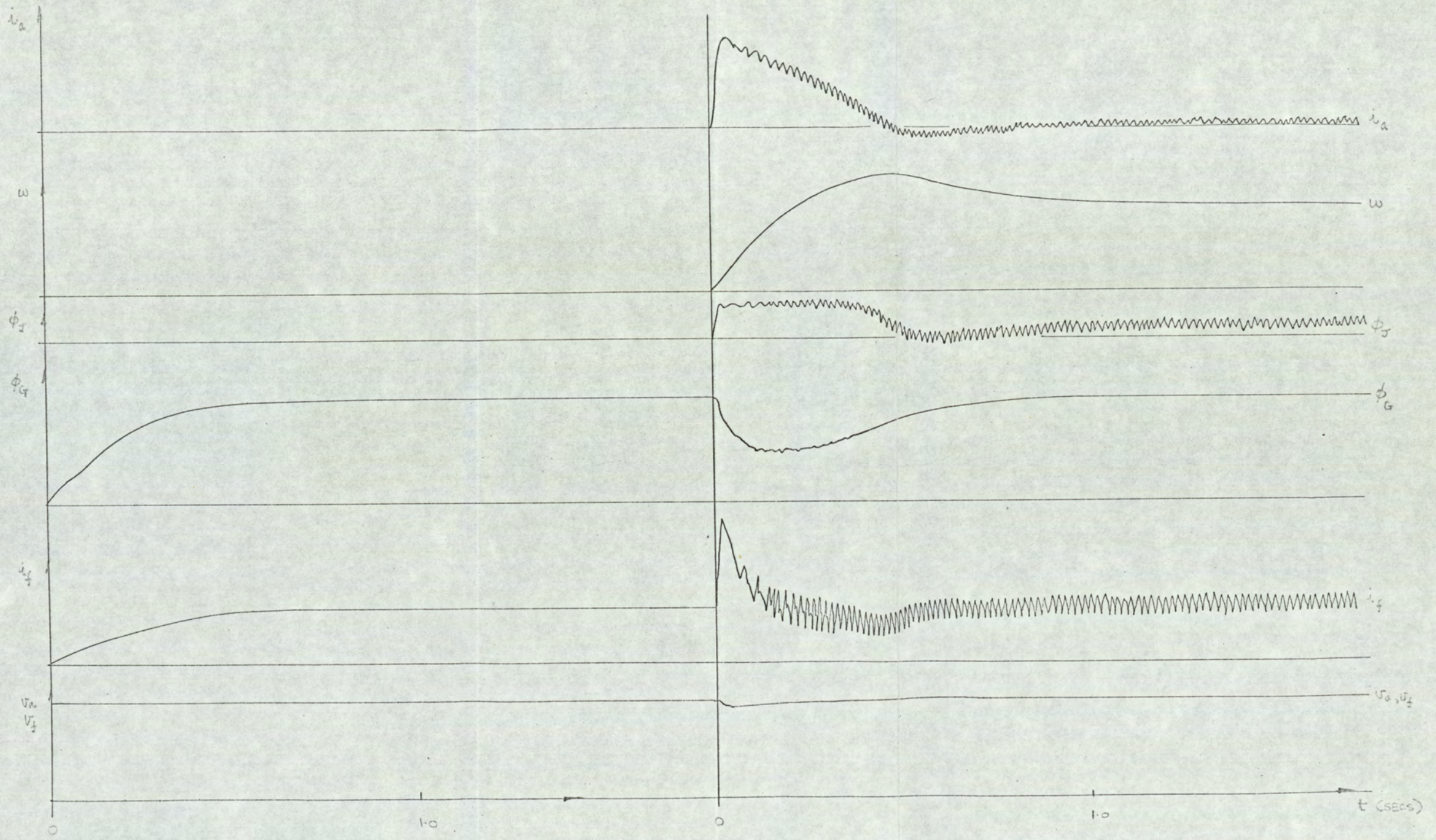


Fig. 3.19

TABLE 3.6

Current(i_a) amps.	Speed(ω) rad/sec.	Flux(ϕ_J) mWb.	Flux(ϕ_G) mWb.	Current(i_f) Amps.	Voltage($v_a=v_f$) Volts	Time Secs
0.0	0.0	0.0	6.7	0.405	232	0.0
42.3	27.7	1.04	5.7	0.765	215	0.025
40.5	55.4	1.09	5.35	0.64	217	0.05
33.8	79.6	1.09	5.0	0.59	224	0.075
28.9	102.0	1.13	5.05	0.48	230	0.1
12.5	152.0	0.955	5.35	0.31	232	0.2
0.9	164.0	0.41	6.05	0.338	232	0.3
-0.9	154.0	0.137	6.36	0.369	232	0.4
0.9	147.0	0.27	6.47	0.396	232	0.5
0.8	144.0	0.33	6.58	0.40	232	0.6
0.7	142.0	0.36	6.6	0.405	232	0.7
0.68	140.0	0.37	6.72	0.41	232	1.0

3.3.2.4 RELATION BETWEEN DIRECT-AXIS FLUX ϕ_G /M. M. F.
WITH THE MACHINE ACCELERATING FROM
REST.

From the transient tests, described in the last Section, the relation $\phi_G = f(i_f, i_a)$ was plotted for various initial conditions (FIG. 3.20 and FIG. 3.21).

The general effect of reduction of ϕ_G for increasing i_a was noted for a given value of i_f . However exact relationships were considered to be not readily defined by these results due to the time lag produced by eddy currents.

3.3.2.5 RELATION BETWEEN QUADRATURE AXIS FLUX
 ϕ_J /M. M. F. WITH THE MACHINE
ACCELERATING FROM REST.

The results from the transient tests provided information about the quadrature-axis flux in the region of the commutating pole. This flux (ϕ_J) represents only a proportion of the total quadrature-axis flux and was found to be virtually unaffected by the direct-axis m. m. f. due to i_f .

A typical relationship is shown in FIG. 3.22.

DIRECT-AXIS FLUX ϕ_g / i_f FOR GIVEN i_a WITH MACHINE
ACCELERATING FROM REST

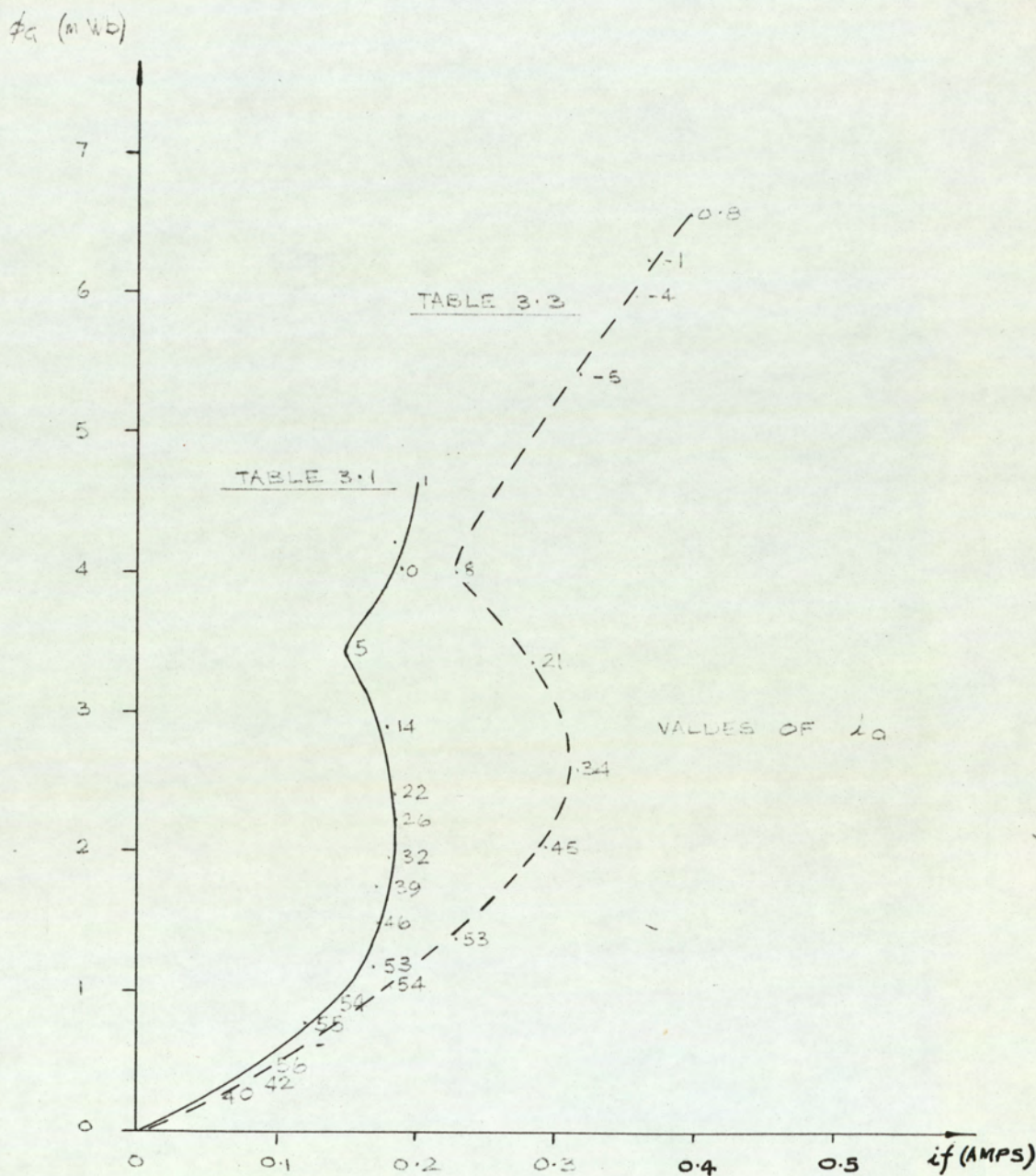


FIG 3.20

DIRECT-AXIS FLUX ϕ_a / i_f FOR GIVEN i_a WITH MACHINE ACCELERATING FROM REST

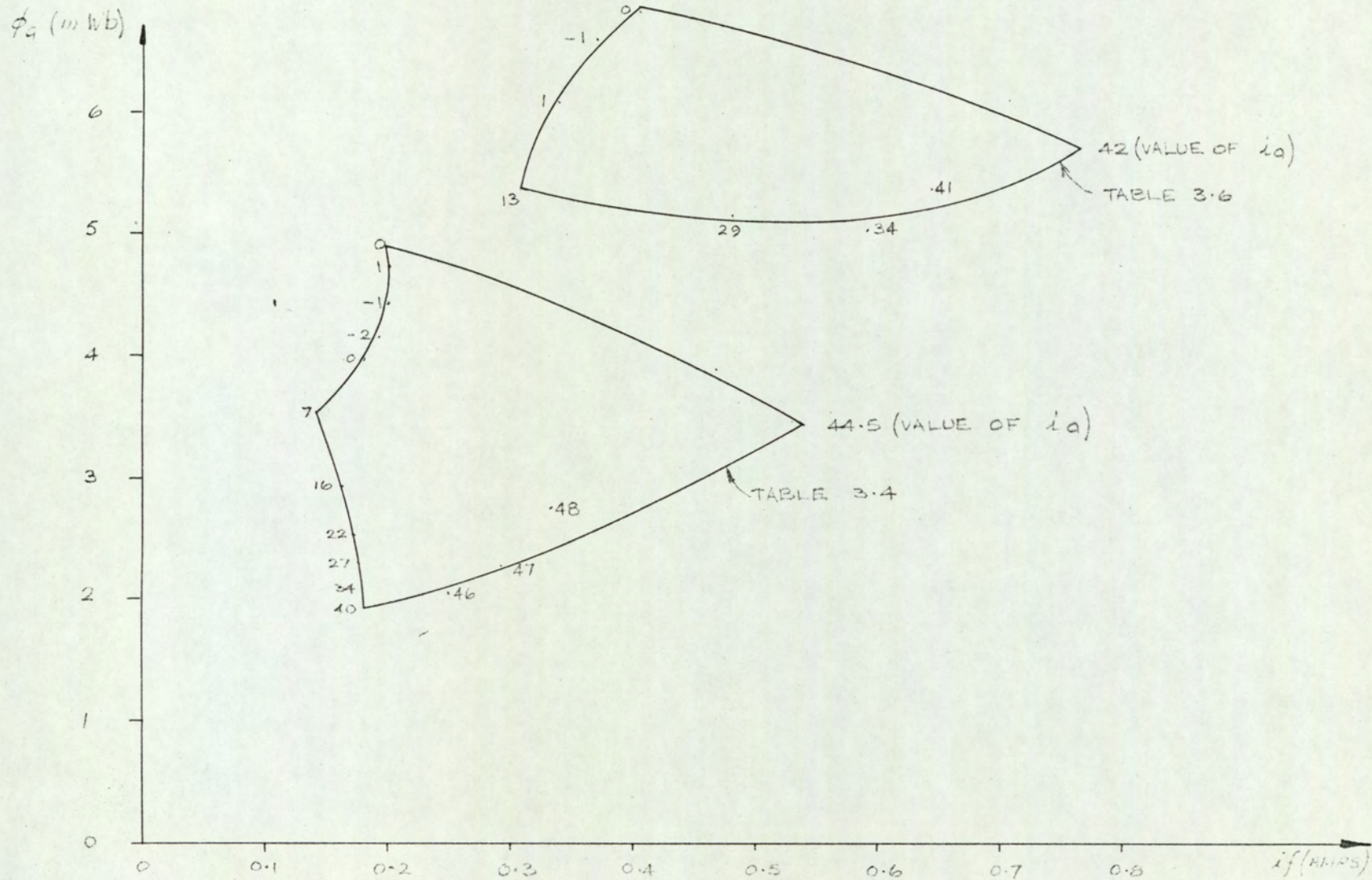


FIG. 3.21

ϕ_J (m Wb)

QUADRATURE-AXIS FLUX ϕ_J / I_a FOR A GIVEN i_f WITH THE MACHINE ACCELERATING FROM REST

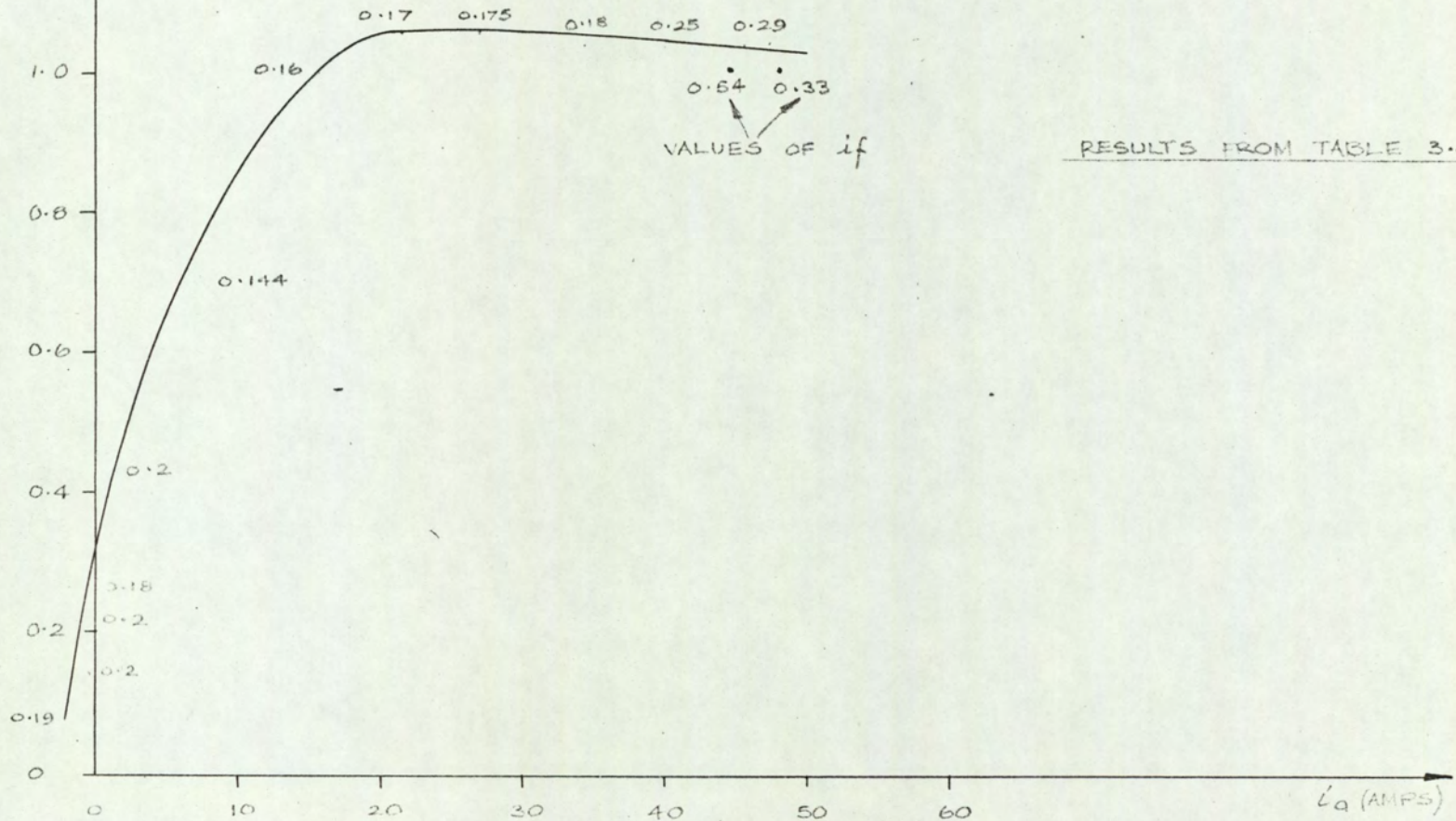


FIG. 3.22,

3.3.2.6. DIRECT-AXIS POLE-FACE FLUX-DENSITY
DISTRIBUTION WITH MACHINE ACCELERATING
FROM REST.

The flux-density distribution under the pole face was measured by use of search-coils (A-F) with the machine accelerating from rest under the initial conditions described by Table 3.2. and Table 3.5.

These results, which are shown in FIG. 3.23. and FIG. 3.24. respectively, indicate the considerable effect of high armature currents under saturated and initially non-saturated conditions. It was noted that even though the average flux-density returned to its initial value (when $t = 0$) the actual flux-density distribution was altered in the case when $i_f \neq 0$ at $t = 0$. This result was confirmed by a series of tests of which typical results are represented by FIG. 3.24 .

The marked saturation at the neck of the pole tips may be noted by reference to search coils B and E.

FLUX DENSITY (Wb/m^2)

DIRECT AXIS POLE FACE FLUX DENSITY DISTRIBUTION WITH THE MACHINE ACCELERATING FROM REST

INITIAL CONDITIONS $i_f = 0, t = 0$

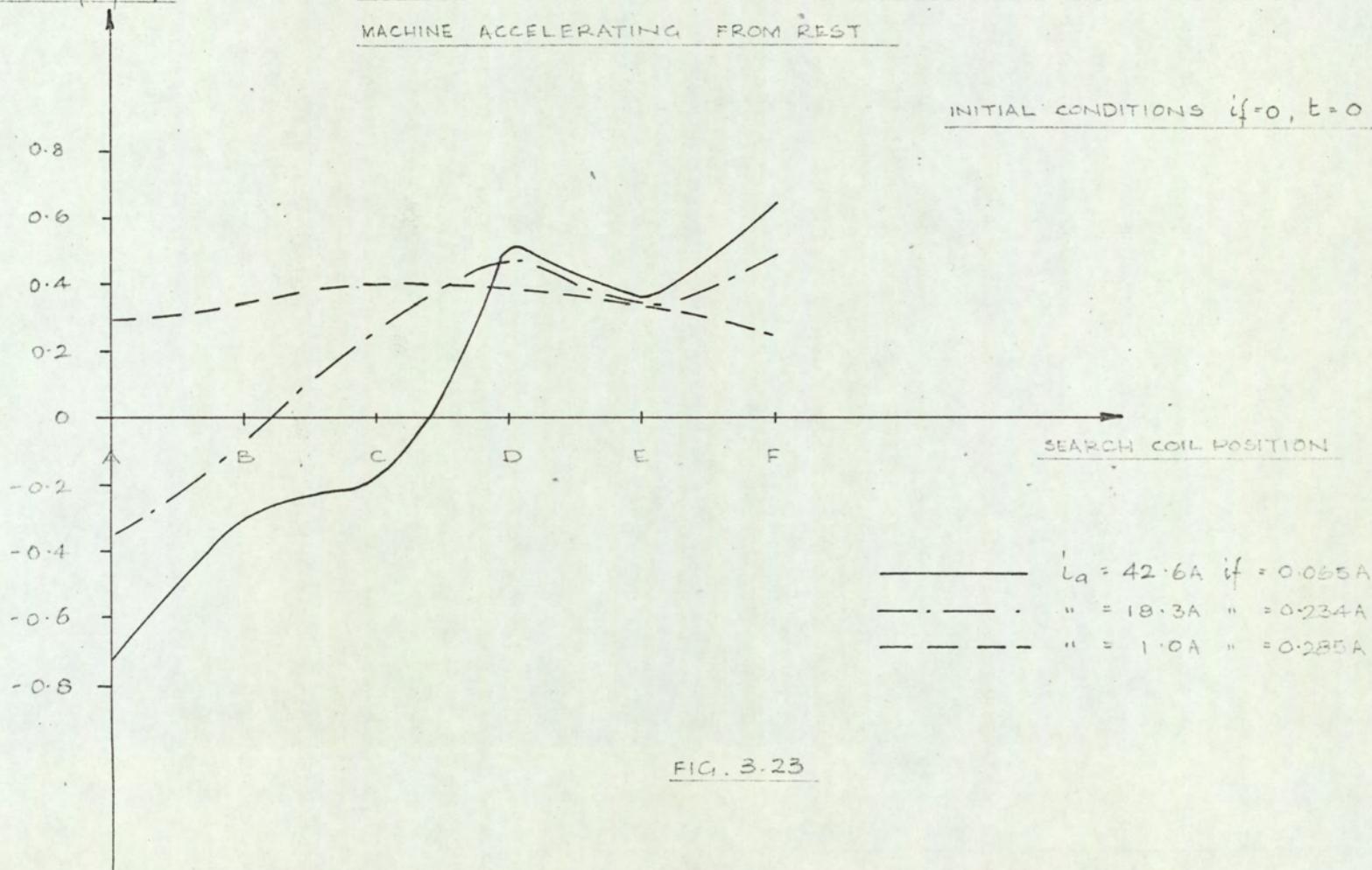
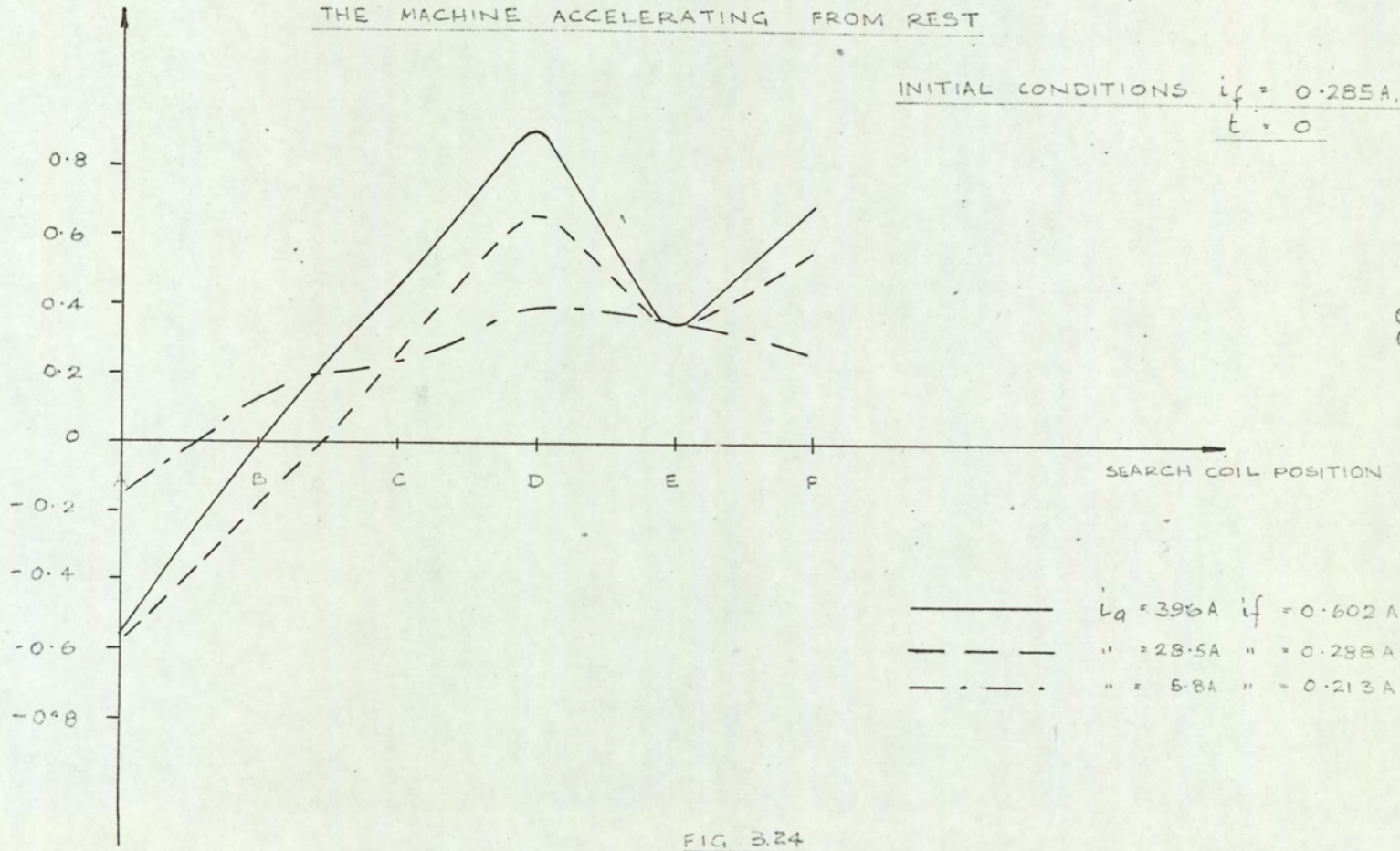


FIG. 3.23

FLUX DENSITY (Wb/m^2)

DIRECT AXIS POLE FACE FLUX DENSITY DISTRIBUTION WITH
THE MACHINE ACCELERATING FROM REST

INITIAL CONDITIONS $I_f = 0.285A$,
 $t = 0$



— $I_a = 39.6A$ $I_f = 0.602A$
- - - $I_a = 28.5A$ $I_f = 0.288A$
- . - $I_a = 5.8A$ $I_f = 0.213A$

FIG. 3.24

3.3.2.7 COMMUTATION.

To access the effect of poor commutation on the transient performance of the machine some of the quadrature-axis pole current was diverted until visual sparking was observed at the commutator.

Under these conditions a limited number of tests with the machine accelerating from rest were conducted in a manner similar to that described in Section 3.3.2.3.

A typical result is shown in FIG. 3.25 and Table 3.7 for initial conditions $i_f = .285$ A, $v_a = v_f = 221$ V, $r_f = 776 \Omega$, at $t = 0$. [% diversion of $i_a = 30\%$.]

TABLE 3.7

Current(i_a) amps.	Speed(ω) rad/sec.	Flux(ϕ_J) mWb.	Flux(ϕ_G) mWb.	Current(i_f) Amps.	Voltage($v_a=v_f$) Volts	Time(t) Secs.
0	0	0	5.64	0	221	0
40	46.7	0.465	3.73	.699	204	.05
34.7	95.2	0.682	2.92	.393	208	.1
29.8	130	0.71	2.72	.317	211	.15
24.9	156	0.737	2.72	.285	213	.2
21.4	175	0.737	2.97	.249	215	.25
16.0	192	0.71	3.22	.225	217	.3
10.7	204	0.682	3.52	.204	219	.35
5.35	211	0.573	4.03	.191	224	.4
- 1.78	204	0.355	4.83	.262	226	.50
- 1.33	190	0.218	5.13	.271	226	.60
-.45	178	.218	5.24	.262	226	.7
0	166	.273	5.43	.275	224	.8
0.5	164	.273	5.48	.28	224	.9
1.0	161	.273	5.54	.285	222	1.0

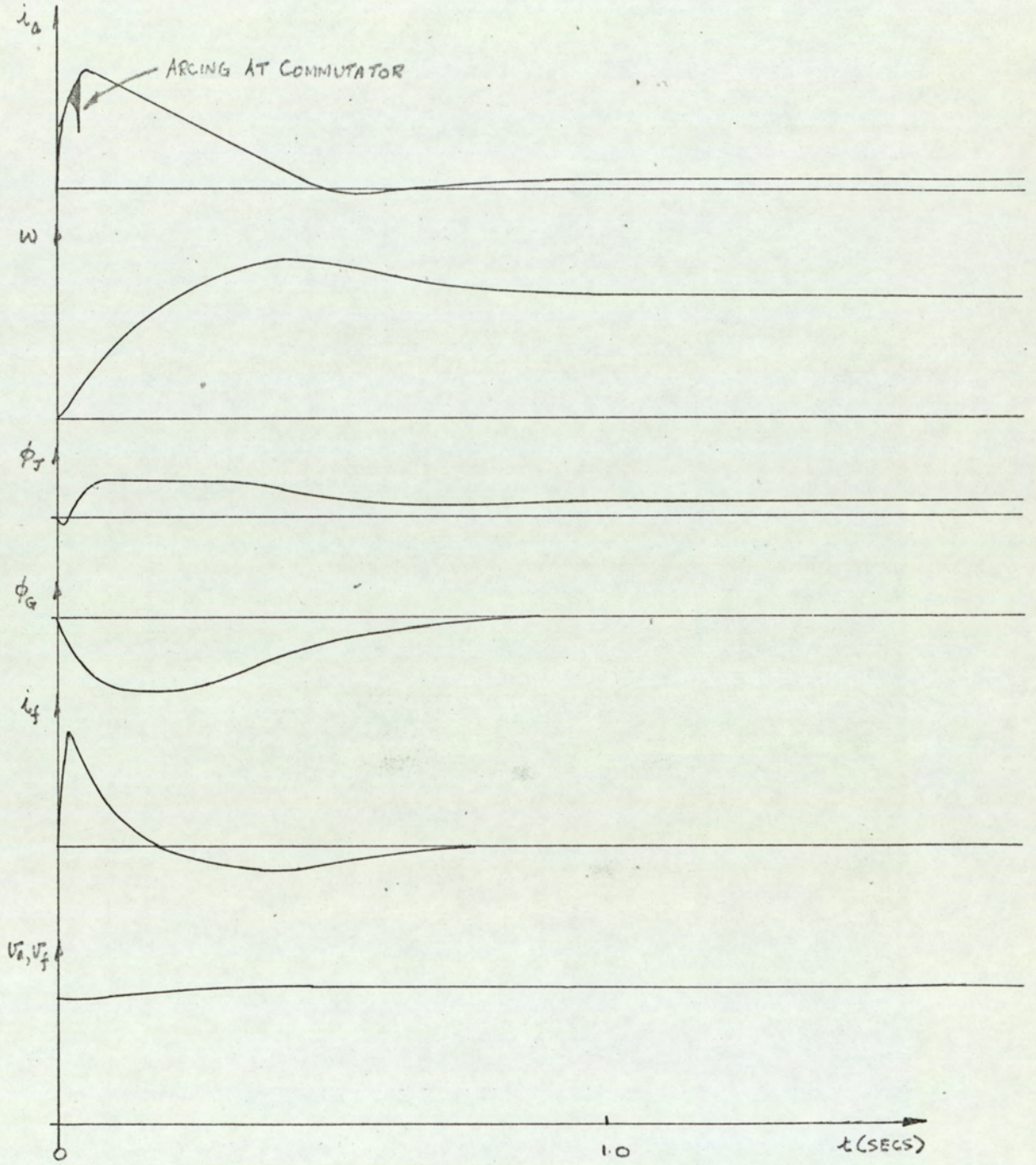


FIG. 3.25

3.4. SUMMARY

This chapter describes in detail the tests necessary to evaluate the parameters defined by the introduction of the block diagram FIG. 2.7.

Some of the relationships obtained are self explanatory in that they are defined directly by the curves shown or values obtained. Other tests, such as those described in sections 3.3. (1.4., 2.4.-2.6.), were included to establish sufficient evidence for the treatment of cross-axis interference.

Section 3.3.2.2. was included to establish how flux changes were influenced by eddy currents. The treatment, as explained, was based on the assumption that the delay in build up of flux due to eddy currents could be approximated to a single time constant. In the case of $T\phi_d$ there appeared to be very little change in the mean value obtained when the tests were repeated for different values of i_f . However, a measurable difference, as shown by FIG. 3.17, occurred when estimating $T\phi_q$ for different levels of i_a .

The measurement accuracy quoted on page 49 indicates the estimated error incurred in taking measurements from recording paper. Where steady-state measurements were involved, components and instruments were chosen such that together with reading error an accuracy of $\pm 2\%$ was maintained.

The measurements involved much work because of the difficulty of repeating each test under exactly the same initial conditions. In fact, consideration of the tests required will show that :-

- 1) Supply voltages are not easily controlled under all transient load conditions.
- 2) Component temperatures vary continuously after each test.
- 3) Residual flux varies as a function of the degree of forcing and the initial conditions.

Whereas it is possible to control some of these variables, it was found preferable to regard supply voltages as varying with time so that the method could be applied to different supply voltage waveforms e. g. thyristor control.

Other variables were fixed (e. g. i_f) and an appropriate parameter (e. g. r_f) changed to maintain a given initial condition.

CHAPTER 4.

ANALYSIS OF RESULTS

4.1 Introduction.

4.2 The average direct-axis flux-linkages (ψ_f)

4.2.1 Brief review of flux pattern produced by
currents i_f & i_a

4.2.2 Estimation of average airgap flux ϕ_g /total
m. m. f. relation under steady-state conditions.

4.3 Estimation of the armature flux linkages (ψ_a)
under steady-state conditions.

4.4 Effect of commutation.

4.5 Time delay introduced by eddy currents.

4.6 Summary.

CHAPTER 4.

ANALYSIS OF RESULTS.

4.1 INTRODUCTION.

A number of the tests which have been described in Chapter 3 require no further analysis since they provide the appropriate parameter evaluation. Certain exceptions exist, however, and these will now be examined in more detail.

4.2 THE AVERAGE DIRECT-AXIS FLUX-LINKAGES (ψ_f)

It was suggested in Section 2.2.1 that the airgap flux ϕ_g was a function of i_f and i_a . This statement applies only to steady-state conditions since the results of section 3.3.2 indicate that it is also a function of time under transient conditions.

In view of the difficulty of carrying out steady-state tests at very high armature currents it was decided that the steady-state characteristics should be estimated theoretically and then compared with the measured results.

4.2.1 BRIEF REVIEW OF FLUX PATTERN PRODUCED BY CURRENTS i_f AND i_a .

This topic is dealt with very adequately by current literature describing the basis of machine performance (e.g. (2, p.51), (4, p.386).)

The conclusion is that when the resultant flux-density waveform for the main pole of a single-axis d.c. machine is deduced the effect of armature current produces magnetic saturation at one pole tip and flux weakening at the other pole tip. The nett effect is a reduction of the total airgap flux which produces an induced e.m.f. in the direct-axis during transient conditions.

4.2.2 ESTIMATION OF AVERAGE AIRGAP FLUX ϕ_g /TOTAL AMPERE TURN RELATION UNDER STEADY-STATE CONDITIONS.

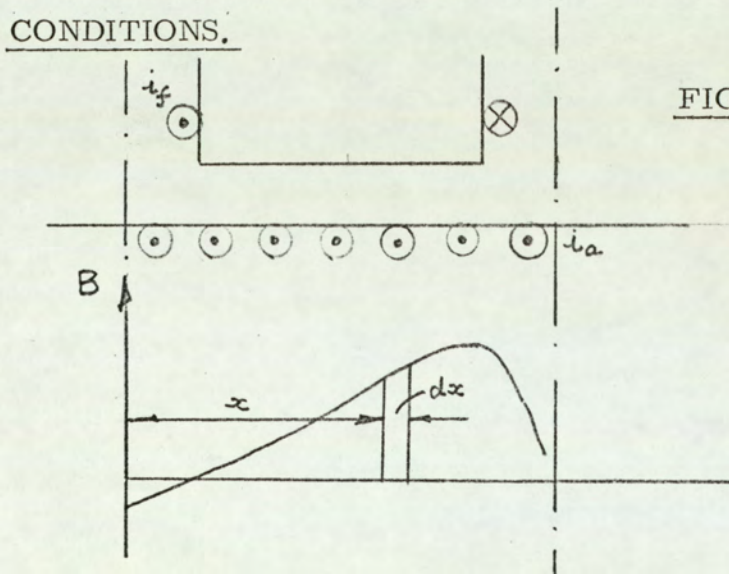


FIG. 4.1.

$$B \equiv B(x, i_a, i_f), \quad dB \equiv \left[\frac{\partial B}{\partial x} \right]_{i_a, i_f} dx + \left[\frac{\partial B}{\partial i_a} \right]_{x, i_f} di_a + \left[\frac{\partial B}{\partial i_f} \right]_{x, i_a} di_f$$

This expression can only be evaluated for specific values of the variables i_a , i_f and x , therefore the method adopted was to estimate the average flux density for different constant values of i_a and i_f .

The technique that was employed was similar to that suggested by Linville⁽¹⁶⁾ in which the flux density B was estimated for a specific value of x by finding the total contribution of ampere turns at x due to constant values of i_a and i_f .

From the resultant curve, B_x against x , the average flux density for known values of i_f and i_a was calculated.

In view of the large number of calculations involved, the characteristic was estimated by programming a digital computer.

The following section outlines the method, which incorporates FIG. 4. 2, and the computer program is shown in appendix 8. 1.

$$\begin{aligned} \text{M. M. F. due to } i_a &= \left[\text{M. M. F. /unit current } (i_a) \text{ at } x \right] \times i_a \\ &= [A T_x] \times i_a \\ \text{M. M. F. due to } i_f &= [A T_f] \\ \text{Total M. M. F. /pole' at } x &= [A T_{Tx}] = [A T_f] + [A T_x] \end{aligned}$$

To calculate the average airgap flux density as a function of i_f and i_a the curves shown in FIG. 3. 7 were employed and assumed to be symmetrical for positive and negative ampere turns. Very large m. m. f. 's were dealt with by fixing the slope of the upper part of the curve. The basis of this being that above a certain level of flux density

ARMATURE
TURNS/UNIT
 L_a

ARMATURE TURNS/UNIT L_a AGAINST SLOT POSITION

N- POLE

EQUIVALENT POSITION OF SEARCH COILS

A

B

C

D

E

F

200

100

-100

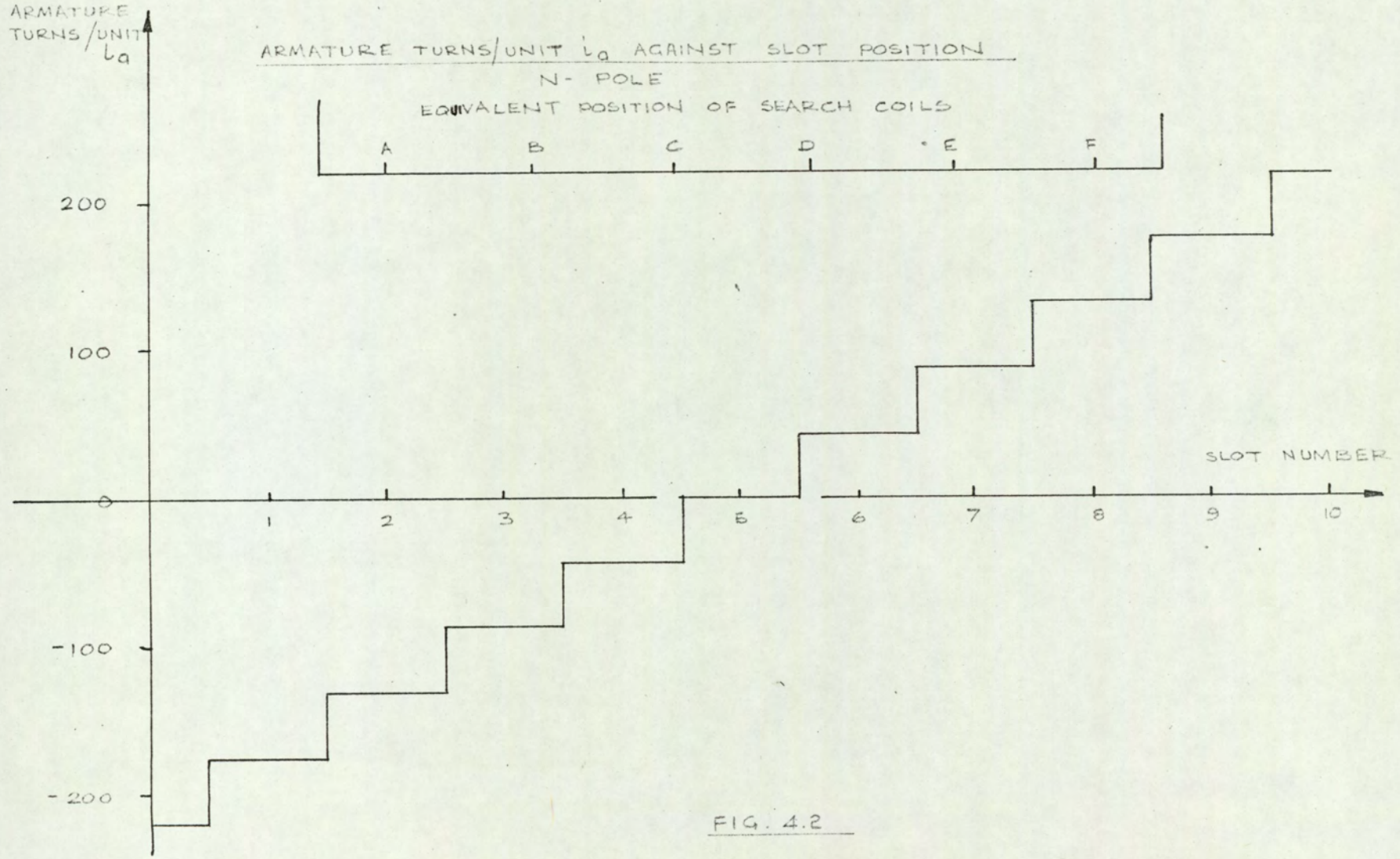
-200

SLOT NUMBER

1 2 3 4 5 6 7 8 9 10

FIG. 4.2

-12-



the armature teeth as though they are non-magnetic to further increase in flux. ⁽¹⁶⁾

Therefore using the curves shown in FIG. 3.7. the flux density at x (B_x) was calculated, which enabled the average flux density B_g to be computed.

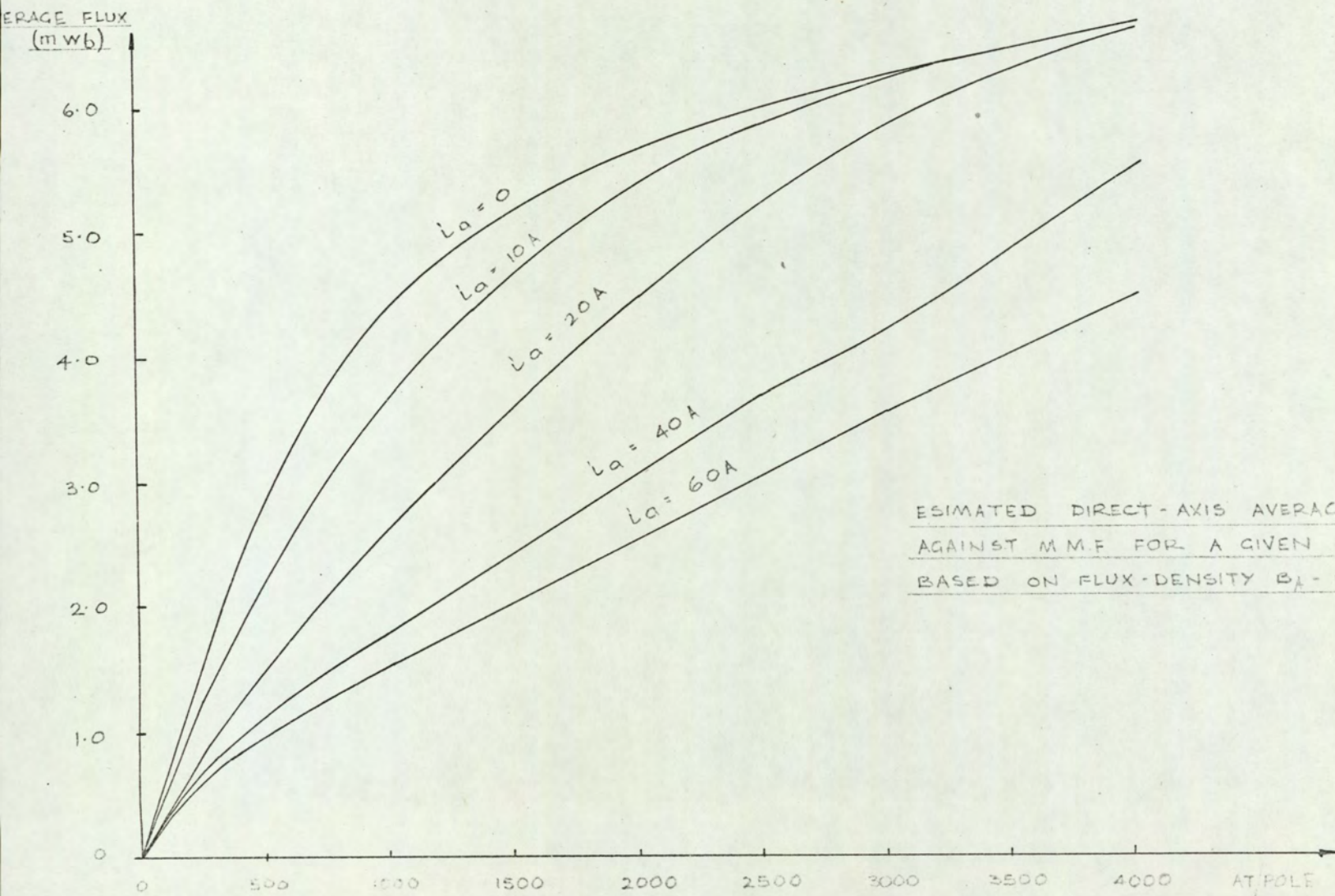
Identical calculations were repeated for other fixed values of i_a & i_f and the resultant curves, shown in FIG. 4.3., were produced by equating the average flux density/pole to the average flux/pole (ϕ_g) and the number of turns/pole (N_f).

4.3. ESTIMATION OF THE ARMATURE FLUX LINKAGES (γ_a)

UNDER STEADY-STATE CONDITIONS.

The estimation of the armature flux linkages as a function of i_a and i_f was considered to be similar to that described in Section 4.2.2. since the majority of the flux links the armature turns adjacent to the direct-axis pole face.

Calculations were therefore limited to two main regions
 (1) The direct-axis pole face and (2) The quadrature-axis pole face (commutating pole). The assumption being that the



ESTIMATED DIRECT-AXIS AVERAGE FLUX/POLE
 AGAINST M.M.F. FOR A GIVEN VALUE OF L_a
 BASED ON FLUX-DENSITY $B_A - B_F$ FIG 3.7

FIG. 4.3

flux linking the armature in the interpolar region, the end windings and the flux crossing the slots would be a very small proportion of the total.

The method of evaluating the flux linking the armature turns under the direct-axis pole face was to use the information obtained in section 4.2.2. For example the flux density $[B_x]$ for $[AT_{Tx}]$ gave a result similar to that shown in FIG. 4.4 for a given value of i_f and i_a

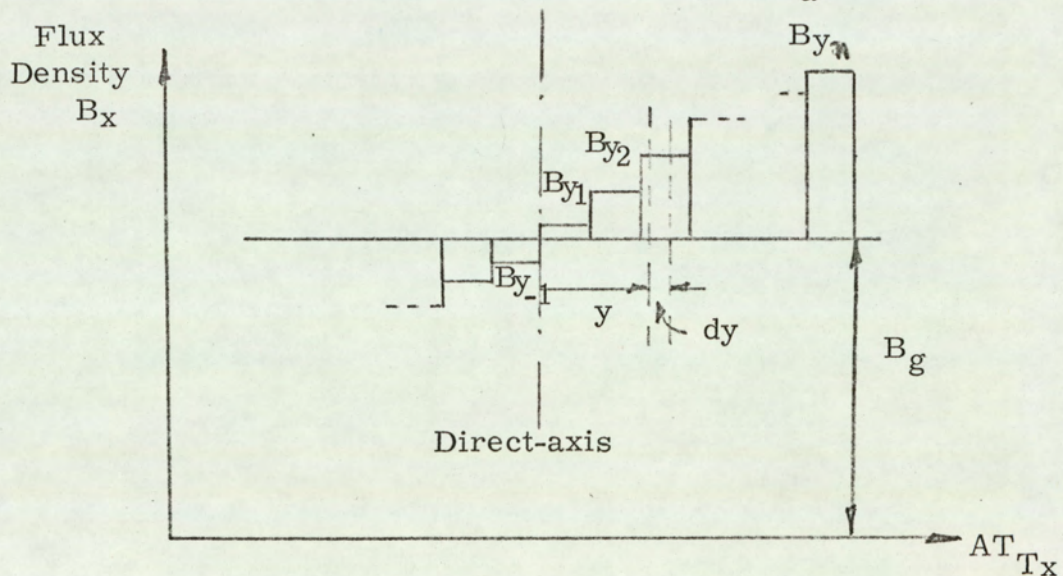


FIG. 4.4.

The flux density at y (B_y) = $B_x - B_g$.

Therefore $\phi_y = (B_y) \times (dy) \times (l)$ Wb where l = armature length (m).

If there are Z conductors/metre of armature periphery assumed uniformly distributed.

Then the number of linkages with the conductors between o and y by the flux which crosses area $l dy$ is $(B_y) l Z y dy$.

If y is divided into intervals of y_1 and the flux density is held constant during the interval, the total linkages for $2m$ poles and $2a$ parallel paths are

$$\begin{aligned} \gamma_{da} = \frac{2m}{2a} Zl & \left[\int_0^{y_1} (B_{y_1}) y dy + \int_{y_1}^{2y_1} (B_{y_2}) y dy + \int_{2y_1}^{3y_1} (B_{y_3}) y dy + \dots + \int_{(n-1)y_1}^{ny_1} (B_{yn}) y dy \right. \\ & \left. + \int_0^y (B_{-y_1}) y dy + \dots + \int_{(m'-1)y_1}^{m'y_1} (B_{-ym'}) y dy \right] \text{----(4.1.)} \\ \gamma_{da} = \frac{2m}{2a} Zl \frac{y_1^2}{2} & \left[(B_{y_1}) + 3 (B_{y_2}) + 5 (B_{y_3}) + \dots + (n^2 - (n-1)^2) (B_{yn}) \right. \\ & \left. + (B_{-y_1}) + 3(B_{-y_2}) + \dots + (m'^2 - (m'-1)^2)(B_{-ym'}) \right] \text{Wb turns} \end{aligned}$$

The results for a wide range of values of i_a and i_f were calculated by adding to the program described in section 4.2.2. as follows :-

$$\begin{aligned} |B_y| &= |B_x| - |B_g| \\ |\psi_{da}| &= |B_y| \cdot |B| \end{aligned} \quad \text{where } B \text{ is the matrix defined by the terms in equation 4.1.}$$

These results were added to the contribution from the quadrature-axis pole face flux-linkages to give the total armature flux linkages $\psi_a = f(i_a, i_f)$ (FIG. 4.5.). The contribution from this source was found by noting the fact that the quadrature-axis pole turns link the armature turns in opposite senses.

I_a (AMPS)

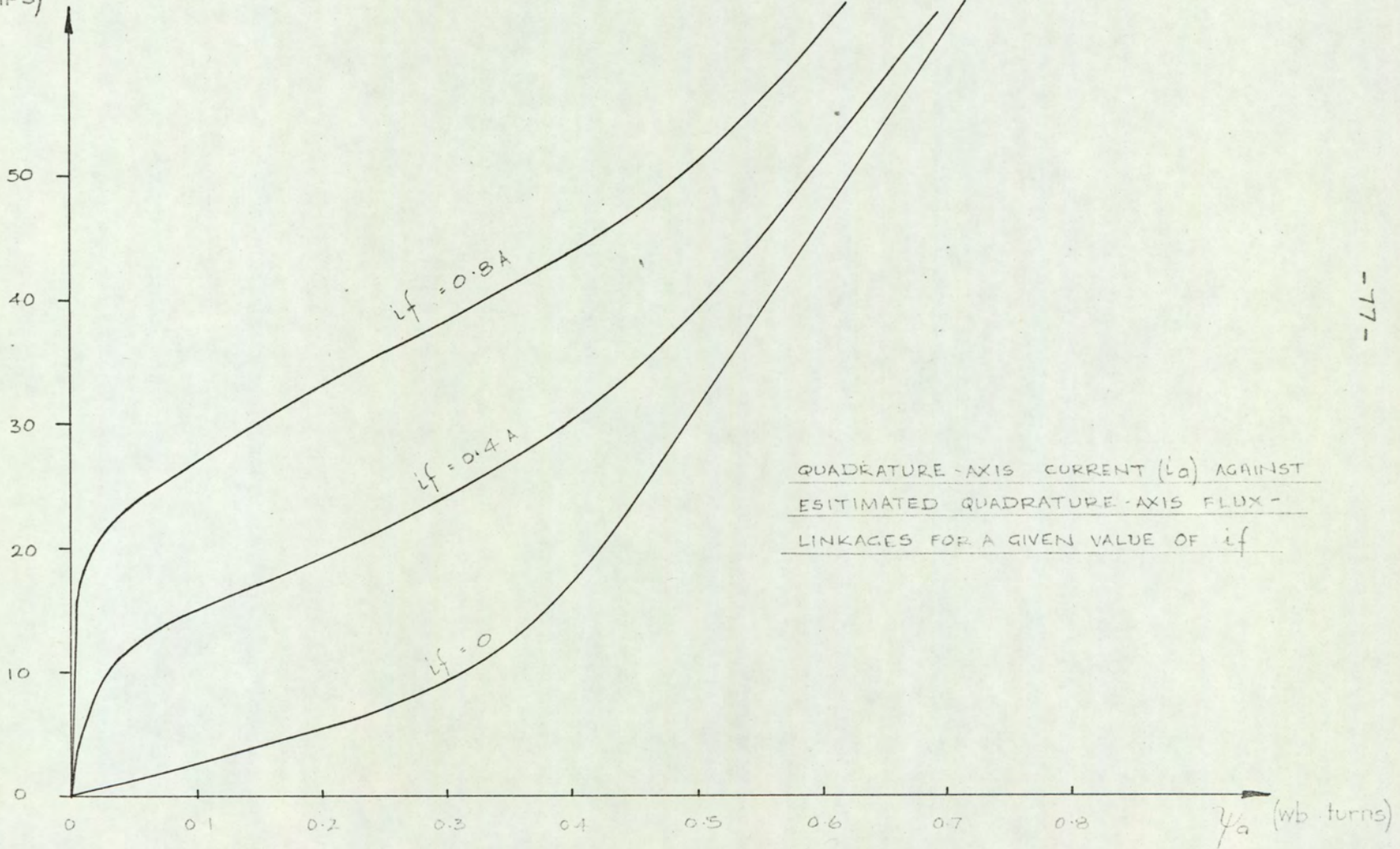


FIG. 4.5

4.4 Effect of Commutation

The process of commutation, when a machine is operating under steady-state conditions, is adequately explained in current literature (e.g. 14, p.189)

However under transient operating conditions the quadrature-axis current (i_a) is changing as well as the normal change that must take place as the conductor current reverses polarity. This condition is not readily amenable to exact analysis due to the vast amount of data required for different values of i_a and di_a/dt .

The direct-axis flux will be effected by commutation due to the additional m. m. f. produced in the direct-axis by the combined effects of currents in the coils short-circuited by the brushes. This m. m. f. depends on the shape of the current reversal curve ⁽¹⁷⁾ and can be calculated if this curve is known over the necessary range of quadrature-axis current.

The general effect of the short-circuit currents produced during commutation was considered to change the m. m. f. distribution at the direct-axis pole tips, which affects the characteristics described in sections 4.2 and 4.3. by virtue of the change in FIG. 4.2.

4.5. TIME DELAY INTRODUCED BY EDDY CURRENTS.

Various authors have postulated that the delay imposed by eddy currents on the build up of flux in an iron core due to impact excitation can be allowed for by treating the main magnetising winding as having a short circuited turn⁽¹⁸⁾, or as being coupled to a short circuited winding.⁽¹⁹⁾

The delay introduced by the short circuit is then added directly to the delay imposed by the main winding.

If such an approach is adopted, then consideration of FIG. 2.7. will show that $v = iR + p\psi$ is an equation which applies to the flux linkages produced in both the direct and quadrature axis.

If this equation is converted into a form in which the time delay due to eddy currents can be included then

$$v = iR + (1 + T\phi kR)p\psi$$

where $k =$ incremental slope A/Wb turn

$R =$ resistance of the main winding

$T\phi =$ measured time delay.

Applying the above expression to a number of measured values of $T\phi_d$, the factor $T\phi kR$ was found to lie between 0.05 and 0.4 for various levels of i_f and i_a .

When the same method was used for the measured values of $T\phi_q$, the factor $T\phi_q kR$ was found to be considerably greater than unity. A typical curve is shown in FIG. 4.6; the result was obtained by evaluating $T\phi_q$ for a number of steady-state levels as typified by FIG. 3.17.

It should be noted that even if the average value of $T\phi$ does not change appreciably, the factor $T\phi kR$ must change for different steady-state levels.

VARIATION OF EQUIVALENT TURNS AGAINST QUADRATURE-AXIS

FLUX LINKAGES

EQUIVALENT
TURNS

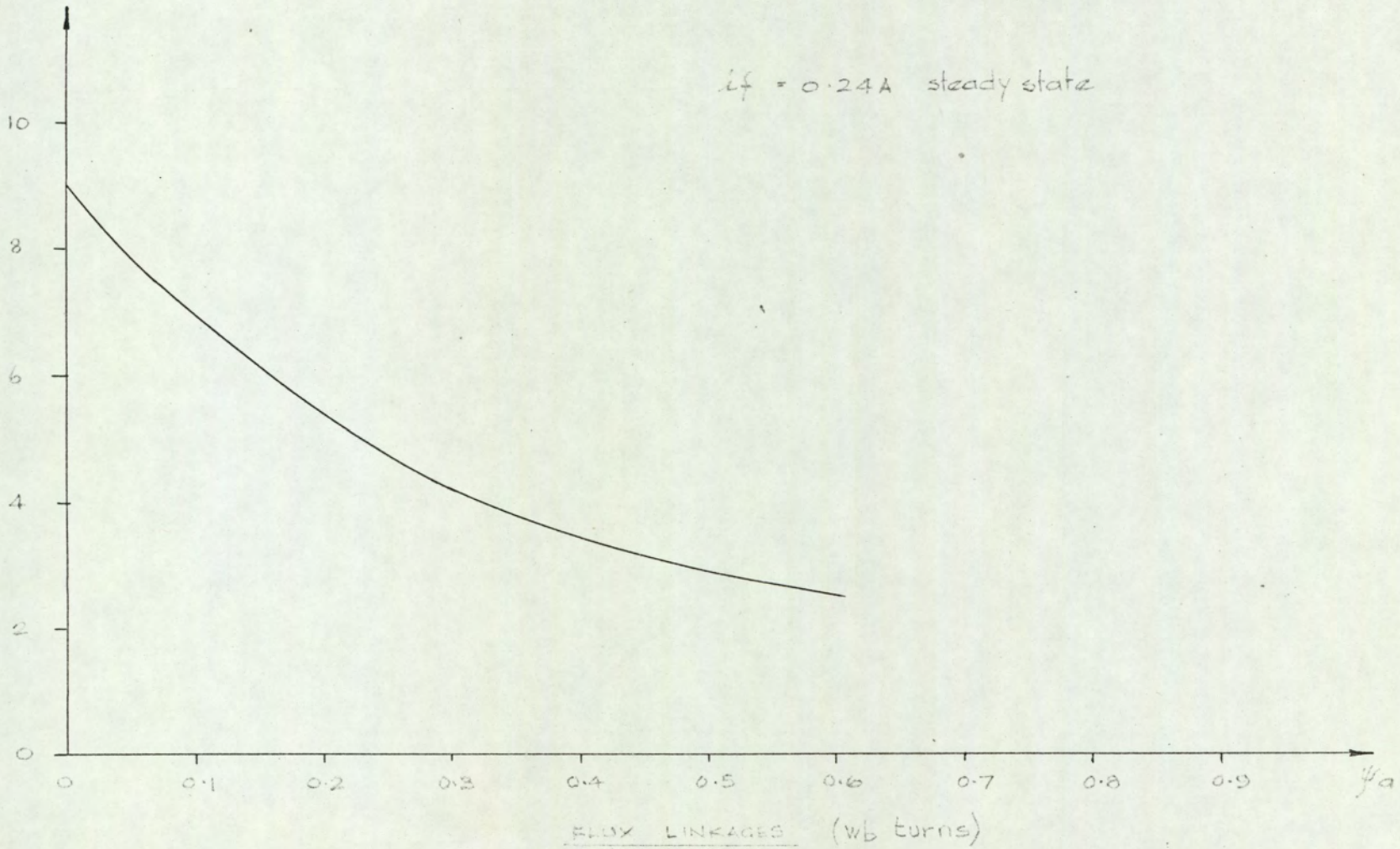


FIG. 4.6

4.6 Summary

It will be seen that the relationships between some of the variables are not readily obtained without a considerable number of calculations. However these calculations were deemed to be necessary in order to express the interrelated system variables with sufficient accuracy for simulation purposes.

The next chapter deals with the method of system simulation.

CHAPTER 5.
SYSTEM SIMULATION.

5.1. Introduction.

5.2. Non-linear functions.

5.2.1. Single valued functions of a single variable.

5.2.2. Single valued functions of two variables.

5.2.2.1. General method.

5.2.2.2. Alternative method of representation.

5.3. Method of integration.

5.3.1. Integration routine.

5.3.2. Integrator program.

5.4. Formulation of computer program.

5.4.1. Outline of program for block diagram (Fig. 2. 7).

5.4.2. Data for program.

5.5. Results from simulation.

CHAPTER 5.

SYSTEM SIMULATION

5.1 Introduction

The technique required to predict the performance of the system relies substantially on the mode of formulating the system equations. The block diagram (FIG. 2.7) consists of a set of first order non-linear differential equations which can be solved by integration. Two of the most important steps in deciding the method of solution are (a) the method of describing the non-linear functions and (b) the method of integration.

The complexity of the non-linear relationships between the variables ruled out the use of an analogue computer and therefore simulation was based on numerical solution by digital computer. ⁽²⁰⁾

5.2 Non-linear functions

The non-linear functions defined in chapters 3 and 4 fall into two categories :-

- (i) Single valued functions of a single variable, such as Fig. 3.13.
- and (ii) Single valued functions of two variables, such as Fig. 4.2.

It was found that these functions required considerable computation time and therefore a large number of ordinates were used so that straight line interpolation could be used to keep the program size down to a minimum.

All the functions were considered to be symmetrical about zero and the modulus of the independent variable was used to compute the required value. The sign of this value was then fixed after calculation.

5.2.1. Single valued functions of a single variable.

As an example the curve defined in Fig. 3.13 will be employed.

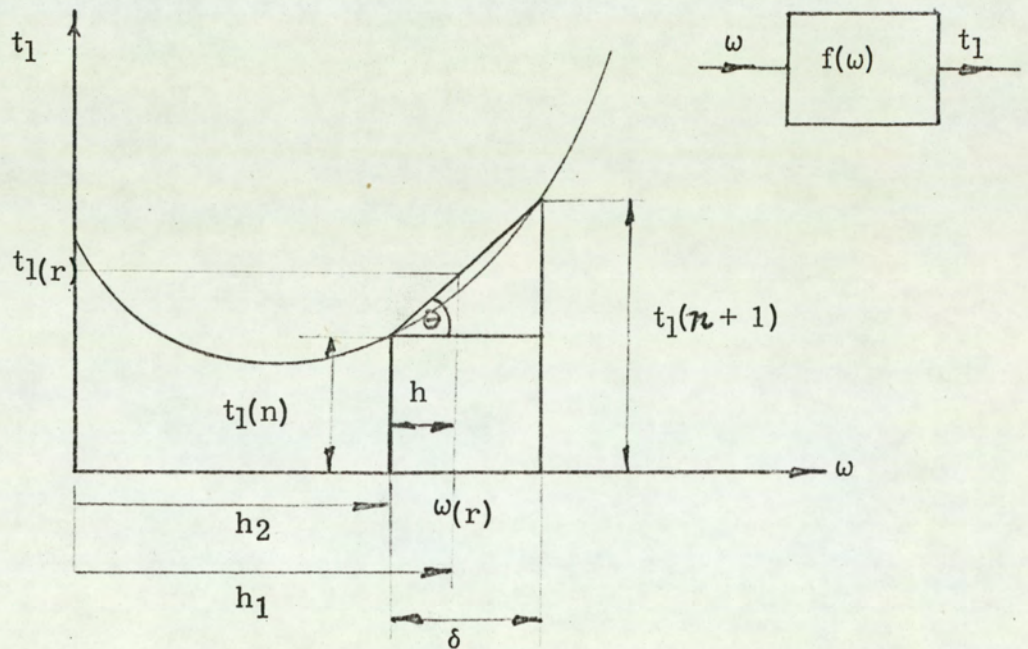


FIG. 5.1.

The independent variable ω was split into intervals of δ such that the n th interval defined ordinate $t_1(n)$.

If it is required to find $t_1(r)$ at ω_r then $h_1 = \omega_r / \delta =$ no of ordinates to ω_r .

$$h_2 = \text{Integer part of } h_1$$

$$h_1 - h_2 = h$$

$$\tan \theta = \frac{t_1(n+1) - t_1(n)}{\delta}$$

$$\therefore t_1(r) = t_1(n) + h \tan \theta$$

For convenience δ was made equal to unity such that

$$t_1(r) = [t_1(n+1) - t_1(n)] h + t_1(n)$$

For programing purposes the calculation was split into simple steps using the following flow chart shown in FIG. 5. 2. Examples of the actual computer program are given in appendix 8.2 under the general title NL1.

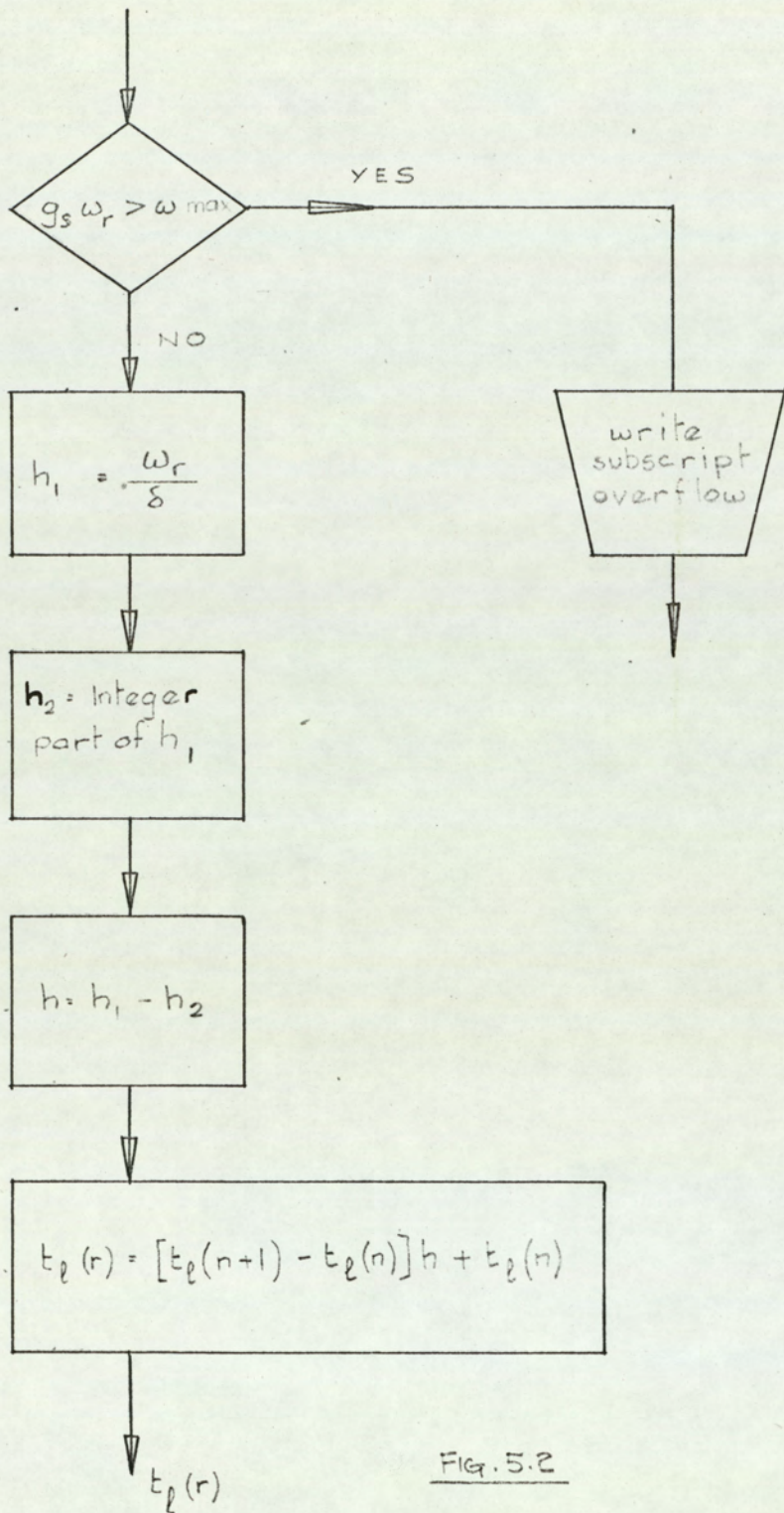


Fig. 5.2

It can be noted from the above that if the number of ordinates chosen is large then the accuracy of the prediction will consequently increase. From which it follows that if there are abrupt changes in the characteristic the number of ordinates may have to be increased to obtain stable calculations.

In some cases it was found necessary to change the value of δ during the calculation for certain characteristics in order to improve computation time or accuracy.

5.2.2 Single valued functions of two variables.

5.2.2.1. General Method.

As an example the curve defined in Fig. 4.3 is employed.

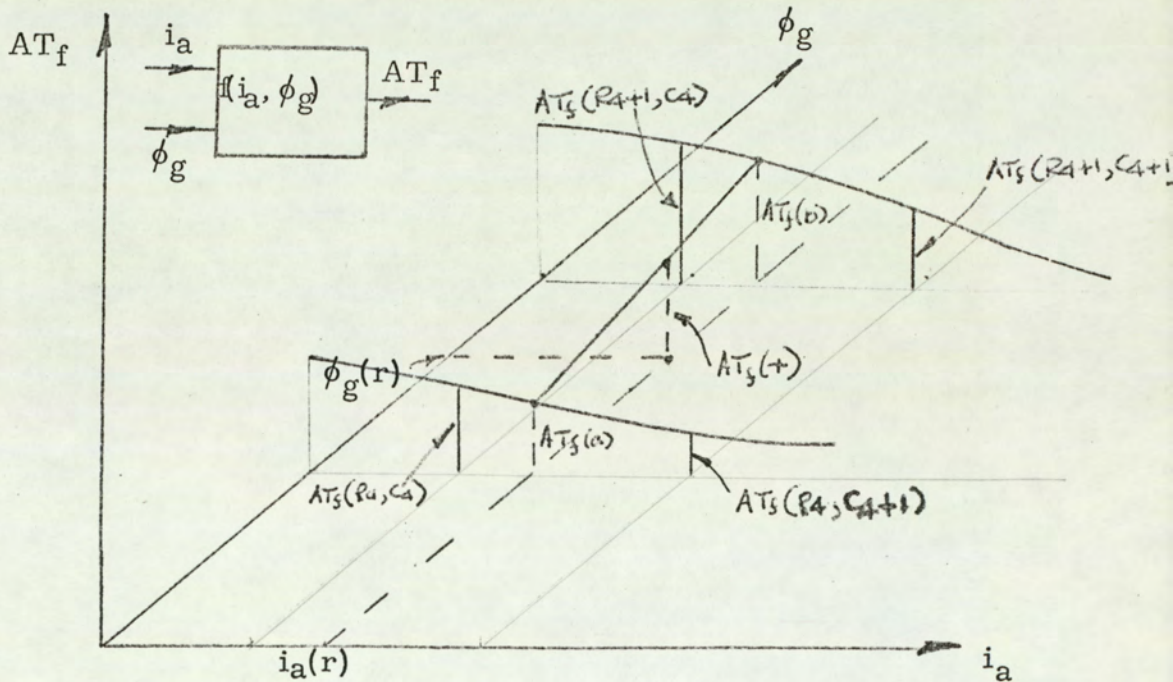


FIG. 5.3.

The calculation is based on the previous section for the function of a single variable except that it must be performed three times. The technique employed therefore was to calculate AT_{f_a} and AT_{f_b} for given values of ϕ_g and i_a and then to find $AT_{f(r)}$ at $i_{a(r)}$ and $\phi_{g(r)}$.

The method is illustrated in the flow diagram (Fig. 5.4) where each axis of Fig. 5.3 has been split into an equal number of ordinates and the array has been labeled K2 (Rows (R), COLUMNS (C)).

For examples of the actual program, see appendix 8.3 under general title NL2.

The technique described in this section and section 5.2.1. was used to express all non linear functions defined by FIG. 2.7. However other alternatives were also considered.

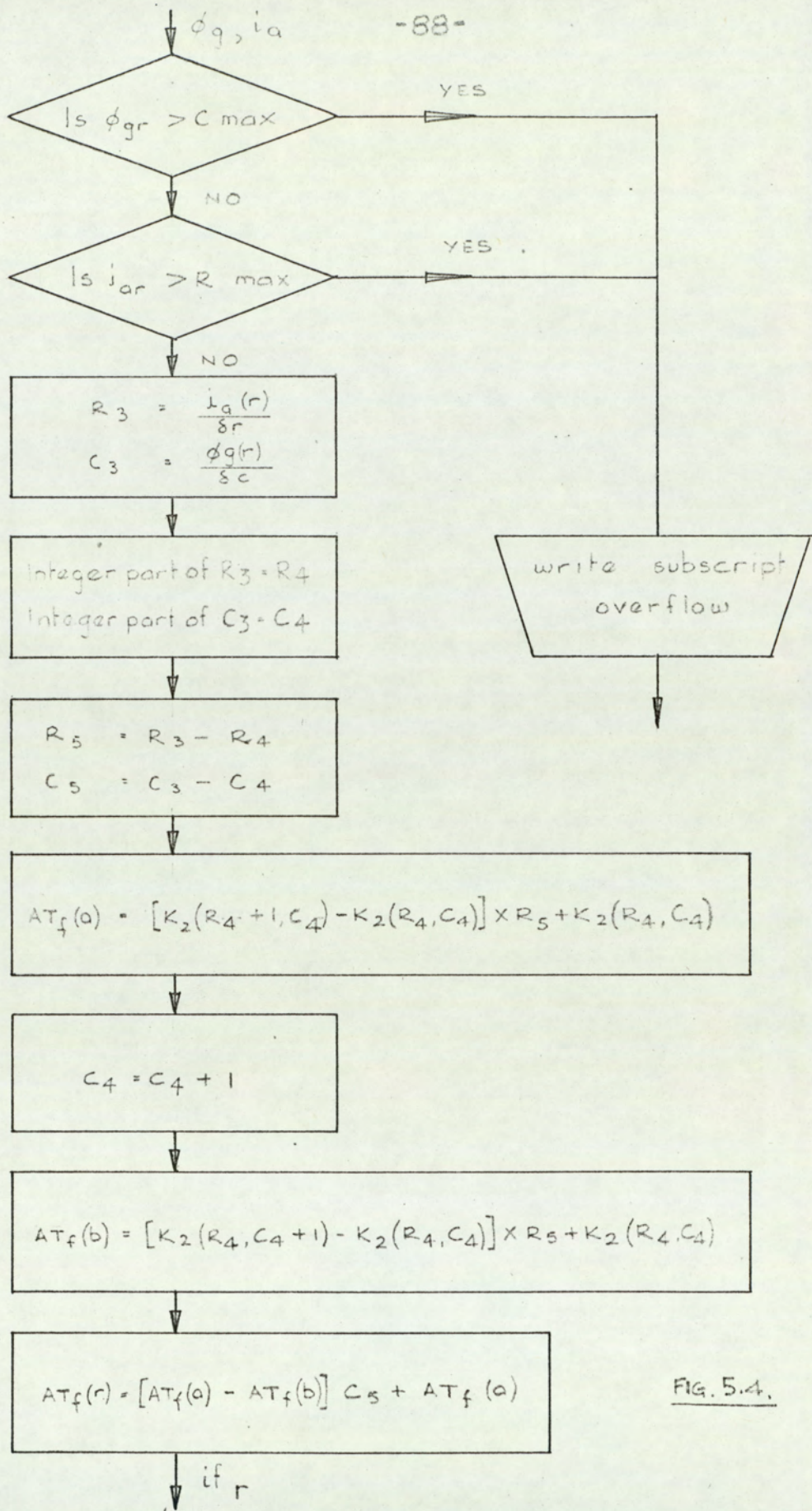


FIG. 5.4.

5.2.2.2. Alternative method of representation.

The equation which most simply represents the magnetisation characteristic, FIG. 4.3. is Froelich's equation

$$\phi_g = \frac{q i_f}{u + i_f}, \quad \text{where coefficients } q \text{ and } u$$

are constants which can be calculated for a given value of i_a .

When these coefficients were evaluated, the resultant expression

$$\phi_g = \frac{10^{-3} \times (8.3 + 0.575 i_a^{0.77}) i_f}{0.19 + 0.039 i_a + i_f} \quad \text{Wb/pole}$$

gave quite good results when the flux changes were restricted to levels of $\phi_g > 2.0$ mWb.

A further alternative method would be to use curve fitting techniques to find the best polynomial equation to satisfy $\phi_g = f(i_f)$ for each constant value of i_a . Then linear interpolation could be used between curves.

Both of the above alternatives have some advantage, over the storage of large arrays, with respect to reduction in calculation time and storage space.

5.2.2.3. Interaction between non-linear functions.

In treating the non-linear relationships, represented by FIGS. 4.3., and 4.5., in the manner indicated, it is clear that prediction of the new value of i_f depends upon knowing i_a and ϕ_g . Similarly, therefore, the prediction of i_a depends

upon known values of i_f and ψ_a . Clearly, this situation leads to an unstable numerical calculation, unless past values of i_a are used to predict the expected value, of i_a , which with ϕ_g known, also based on past values, will enable the new value of i_f to be calculated.

To achieve the necessary degree of prediction a routine of the form $f((r+1)T) = f(rT) + T \dot{f}(rT) + \frac{T^2}{2} \ddot{f}(rT) + \dots$, where T is the sampling interval, was used to predict the expected value of the required variable (i. e. i_a).

By calculating the gradient, based on past values, and ignoring derivatives of higher order than second, then

$$x_{r+1} = x_r + k (1.5 x_r - 2 x_{r-1} + 0.5 x_{r-2})$$

where k was taken as a weighting factor to enable partial prediction of x_{r+1} .

Prediction was then advanced by assigning x_{r-1} as x_r , and x_{r-2} as x_{r-1} .

5.3 Method of integration.

In analogue computers the process of integration is continuous and may be performed in a reasonably short space of time. However when such an operation is performed on a digital computer it is necessary to use an integration routine which will calculate the input and output of the integrator at discrete sampling intervals.

Even with very fast digital computers the time of computation may be considerable, especially since it is desirable to keep the errors introduced by the integration routine to a minimum. In other words the error incurred at one step propagates in later steps and produces an unstable calculation.

Therefore a routine is required which will be reasonably accurate and yet perform the operation in reasonable time.

One of the simplest methods⁽²⁰⁾ is to predict the input value of each integrator at the next sampling point based on past values. The new value of the output of each integrator can then be used to find the corrected input value which is used for the next prediction.

This method was found to be reasonably accurate provided the sampling time interval was kept to a value consistent with any sudden change in integrator input.

Other methods⁽²¹⁾ of course exist which are similar to the one chosen but an assessment of the best method for this particular problem was not undertaken.

5.3.1 INTEGRATION ROUTINE.

If the input to an integrator is $x(t)$ and it is sampled at points separated by time interval T , then the r th output sample is

$$I(rT) = \frac{1}{\tau} \int_0^{rT} x(t) dt.$$

τ = integrator time constant.

A forward integration routine may be used to predict $I[(r+1)T]$ by extra polating $x(t)$ beyond rT to $(r+1)T$ based on past values.

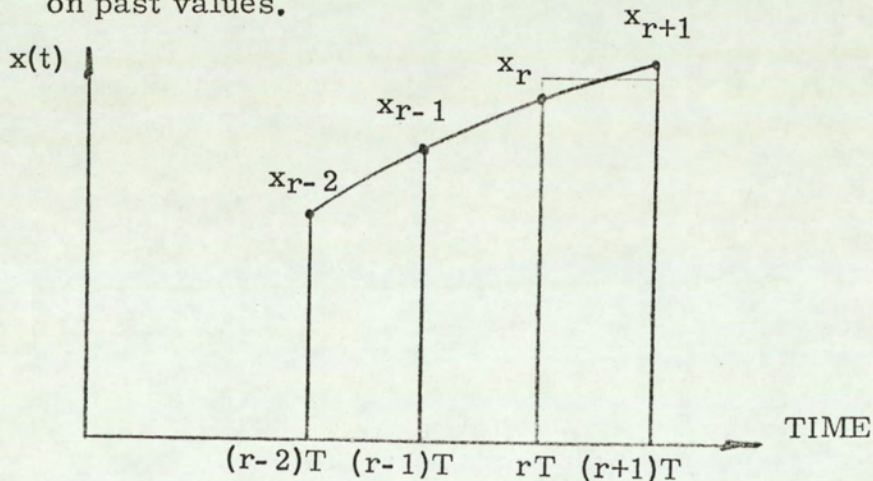


FIG. 5.5.

$$\text{If } I \left[(r+1)T \right] - I(rT) = \frac{T}{\gamma} \left[x_r + \frac{x_{r+1} - x_r}{2} \right] \quad \text{----- (5.1)}$$

and x_{r+1} is extrapolated from the expression

$$x_{r+1} = 3x_r - 3x_{r-1} + x_{r-2} \quad \text{----- (5.2)}$$

$$\text{then } I \left[(r+1)T \right] = I(rT) + \frac{T}{\gamma} \left[2x_r - 1.5x_{r-1} + 0.5x_{r-2} \right] \quad \text{--- (5.3)}$$

by combining equations (5.1) and (5.2).

Equation (5.2) being chosen as a reasonable compromise based on starting procedure and frequency response. ⁽²⁰⁾

The starting procedure must be considered in choosing a method of extrapolation due to the fact that no past values exist.

5.3.2 INTEGRATOR PROGRAM

Since the integration routine described in the last section was used for all integrations, the integrators were numbered from 1 to N such that equation (5.3) was assigned the form

$$I(N) \left[(r+1)T \right] = I(N)(rT) + \frac{T}{\gamma(N)} \left[2x(N)_r - 1.5x(N)_{r-1} + 0.5x(N)_{r-2} \right] \quad \text{-- (5.4)}$$

Integration was then advanced by following the procedure that $x(N)_{r-1}$ becomes $x(N)_r$

and $x(N)_{r-2}$ becomes $x(N)_{r-1}$

Integration errors were reduced to a minimum by keeping the sampling interval small, and printing out only a fraction of the total calculations. The choice of sampling interval was based on the percentage error produced when comparing the results obtained from the exact solution of a linear equation, with the solution of the same equation using numerical integration.

It was also found useful to program for a change in T such that when only slow changes were taking place the calculation time could be improved.

5.4. Formulation of Computer Program.

The construction of a particular program was based on the block diagram using Fortran 4 ^(22, 23) as the programming language. The choice of Fortran being determined so the best method available using a PDP9 computer.

5.4.1. Outline of program for block diagram (FIG. 2.7).

The program was devised such that the integration routine formed the main program, then the subroutine simulating the machine performance could be called to calculate the new integrator inputs.

The machine subroutine itself was employed to call subroutines NL1 and NL2 as well as subroutines containing new data.

The complete flow diagrams for the main program and the machine subroutine are shown in FIG. 5.6. and FIG. 5.7. respectively. The terms jump and control were used as start and stop instructions. Thus enabling data or titles to be read or printed once, or as required.

The actual computer programs appear in appendix.8.4.2.

5.5. Results from analysis.

Employing the initial conditions which gave rise to the measured results tabulated in Tables 3.1. - 3.7., the machine performance was predicted from the mathematical model and the results are shown, together with the measured result in FIGS. 5.8. - 5.14.

The predicted results compare favourably with the measured results in so far as general behaviour of the main variables is concerned. Even when comparatively heavy sparking occurred at the commutator brushes, by reduction of the quadrature axis pole flux, the transient performance could still be predicted with reasonable accuracy without knowing the values of the short circuit currents produced by the brushes. This is because the change in m. m. f. at the pole tips does not produce a significant change in the characteristics represented by FIGS. 4.3. and 4.5.

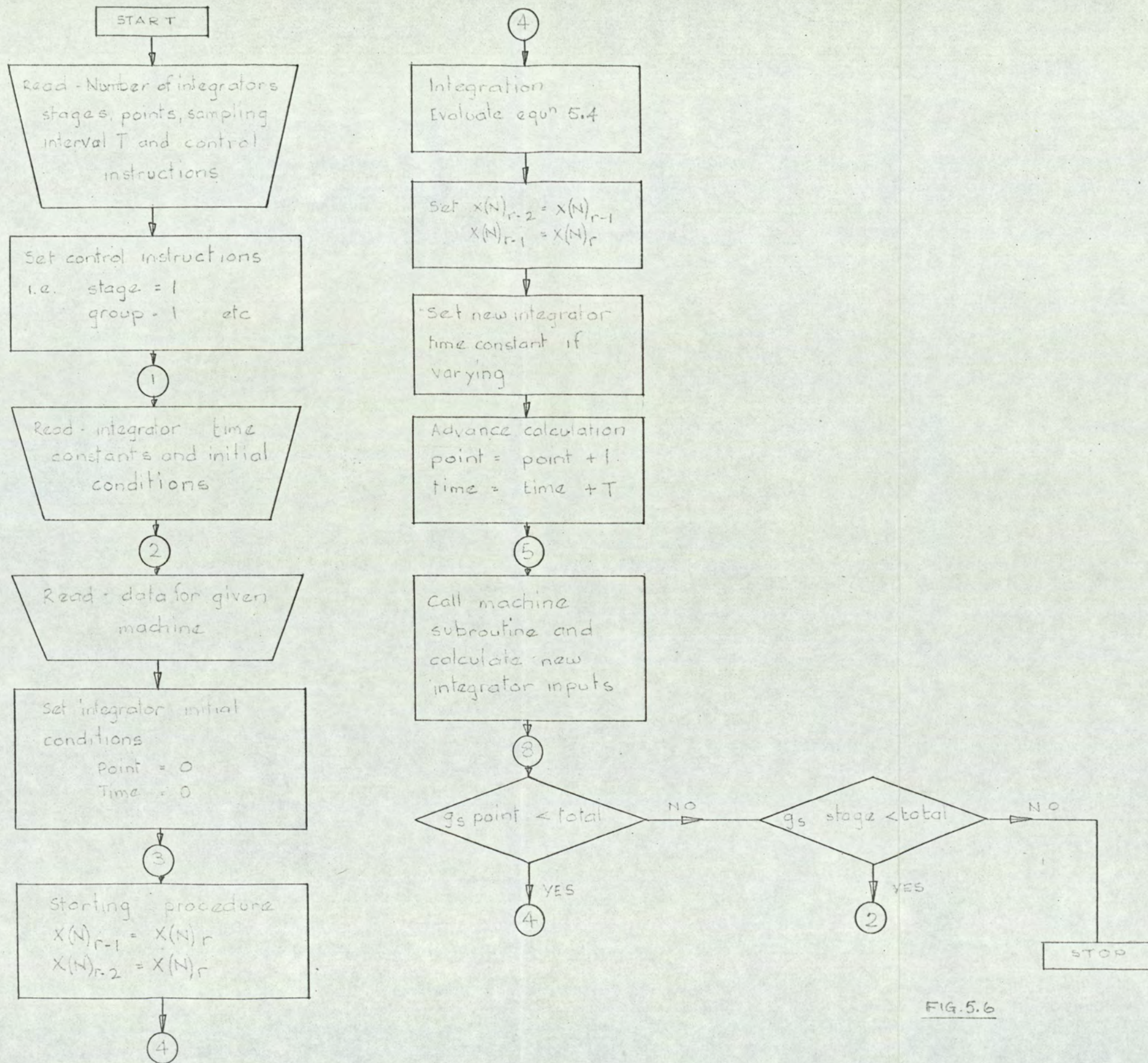


FIG. 5.6

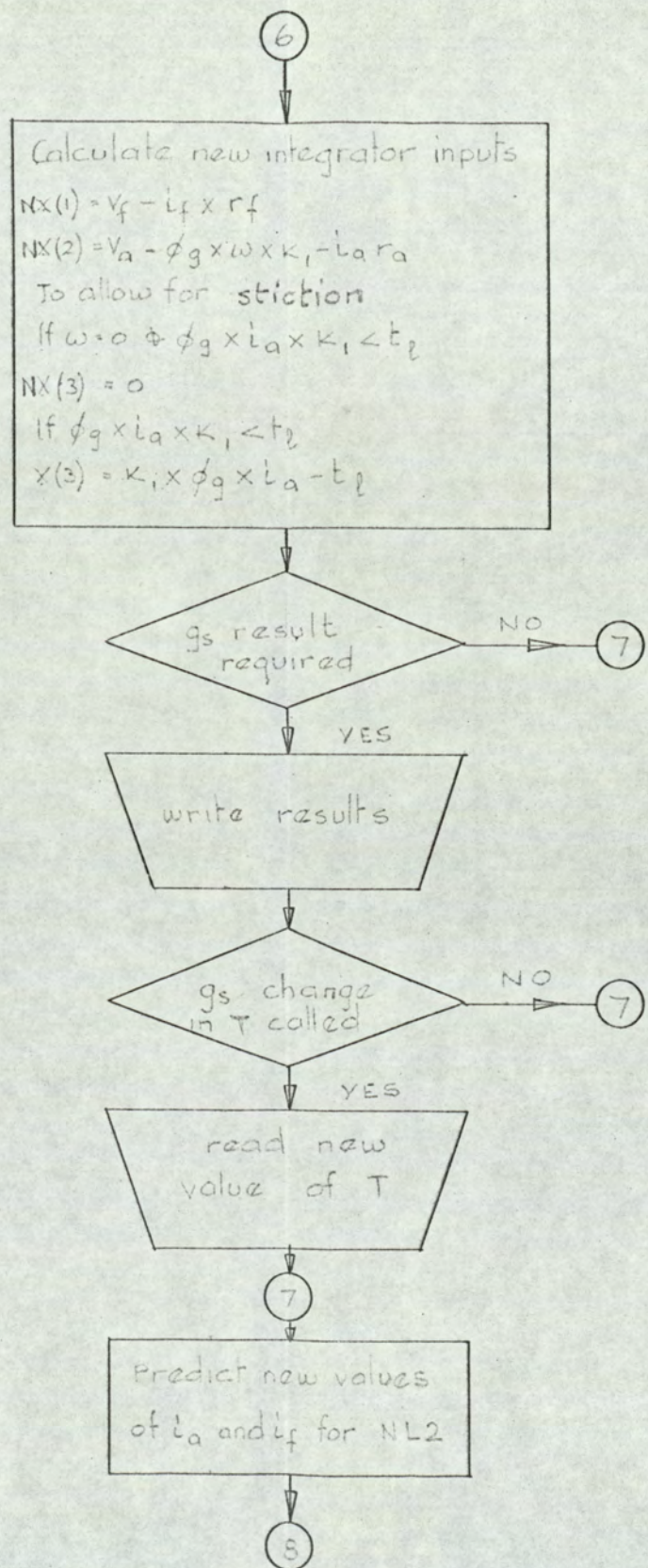
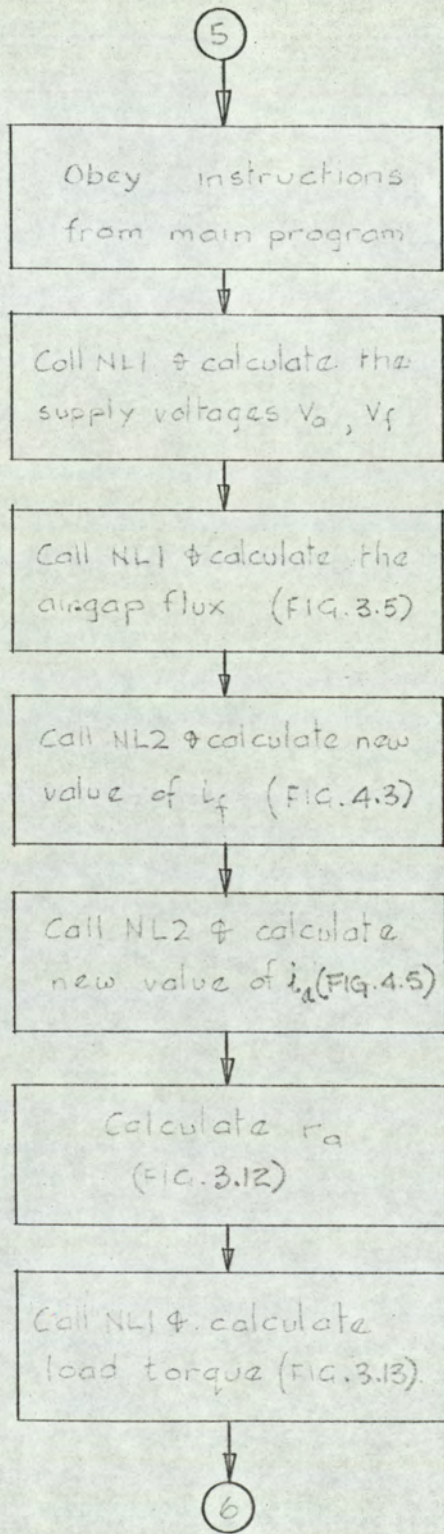


FIG. 5.7

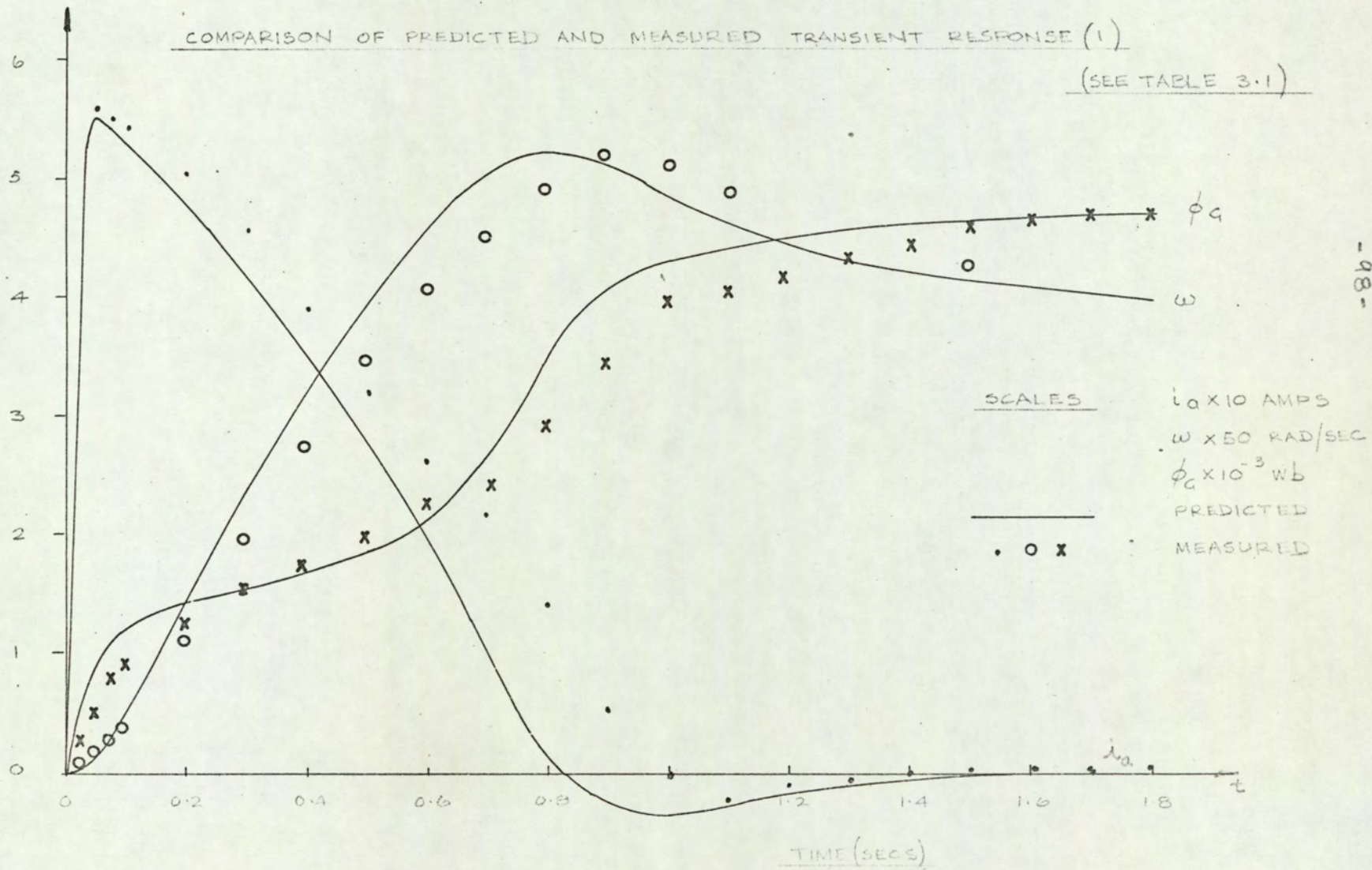
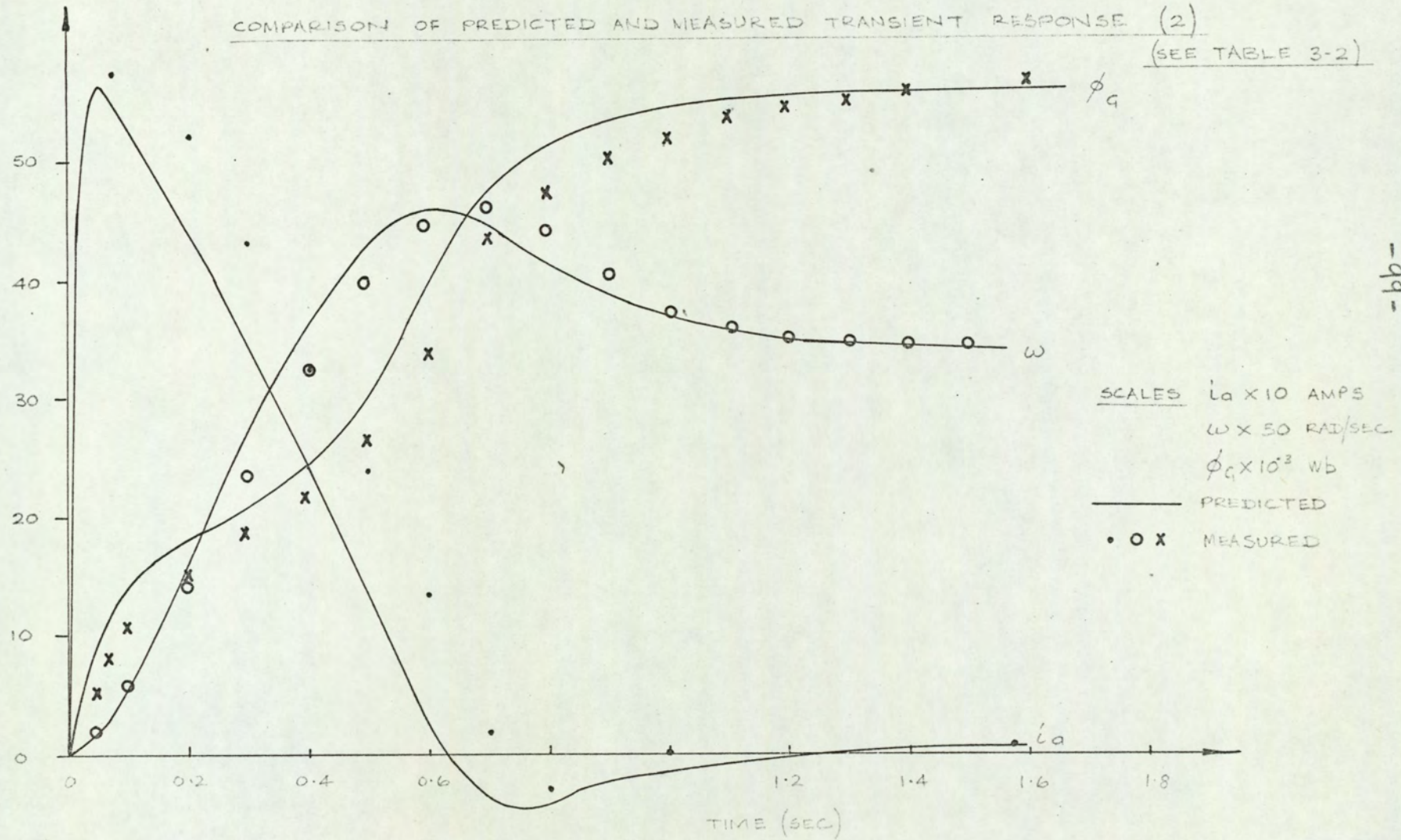


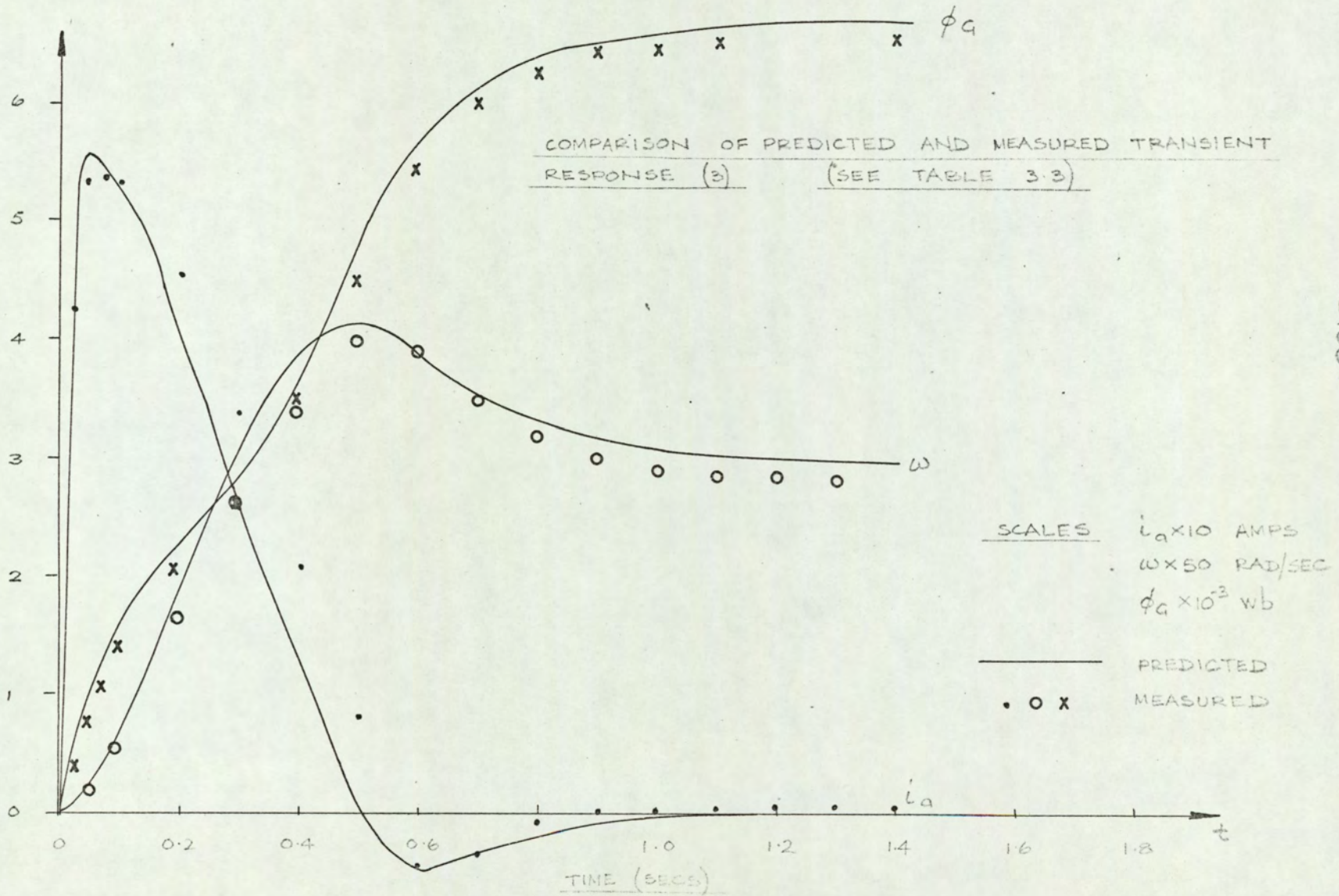
FIG 5.8

COMPARISON OF PREDICTED AND MEASURED TRANSIENT RESPONSE (2)
 (SEE TABLE 3-2)



-bb-

FIG. 5.9



100-

FIG. 5.10

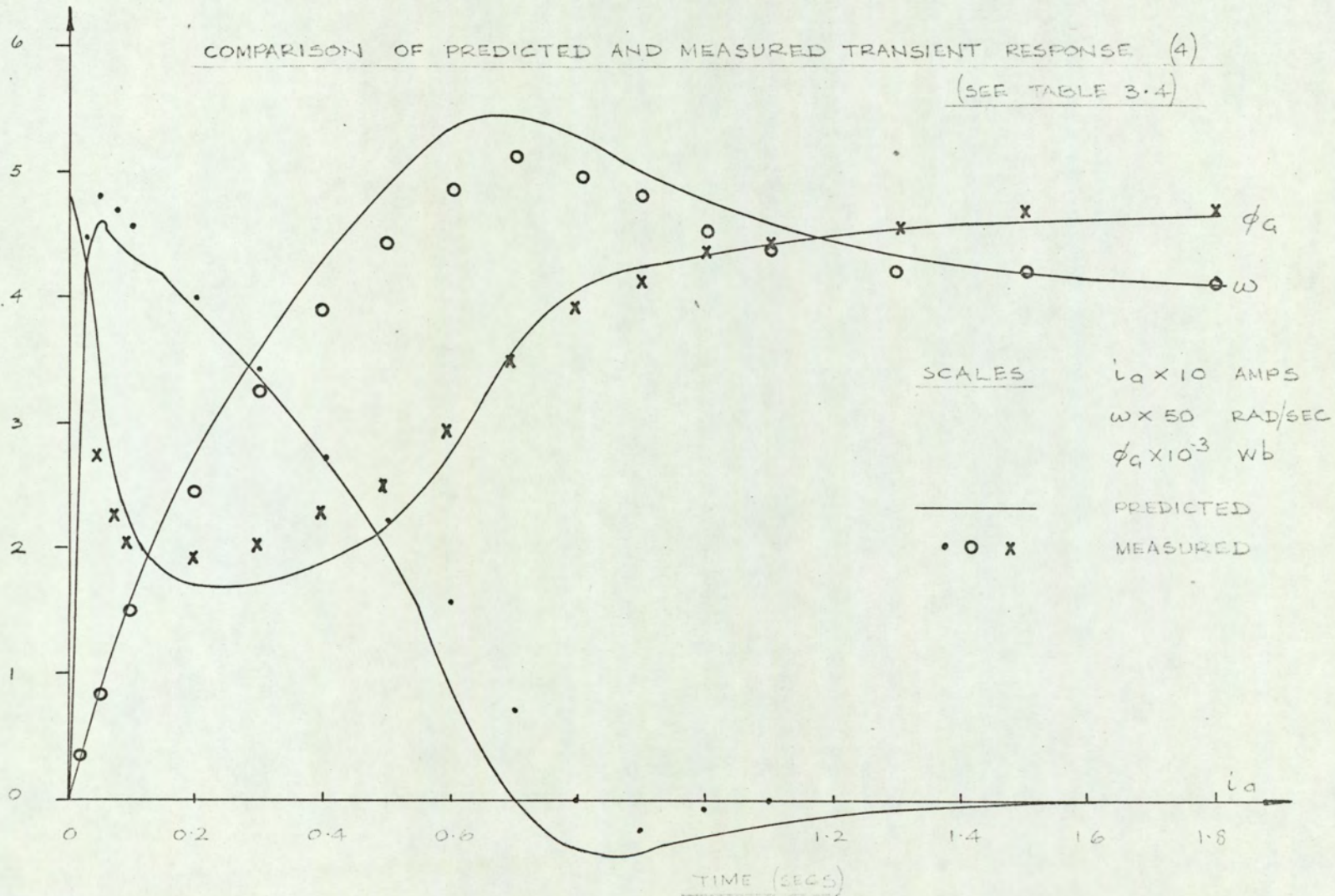


FIG. 5.11

COMPARISON OF PREDICTED AND MEASURED TRANSIENT RESPONSE (5)

(SEE TABLE 3.5)

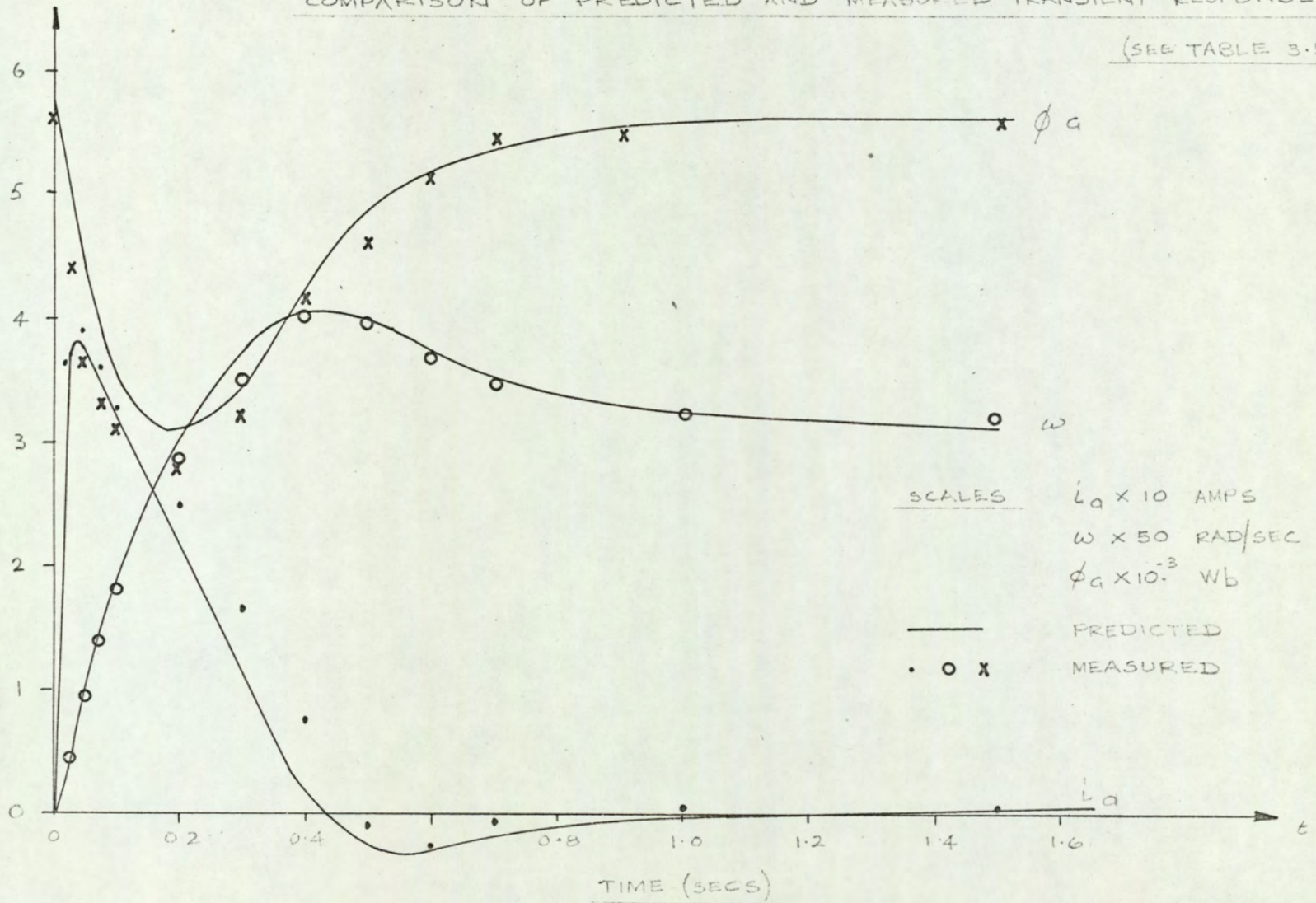
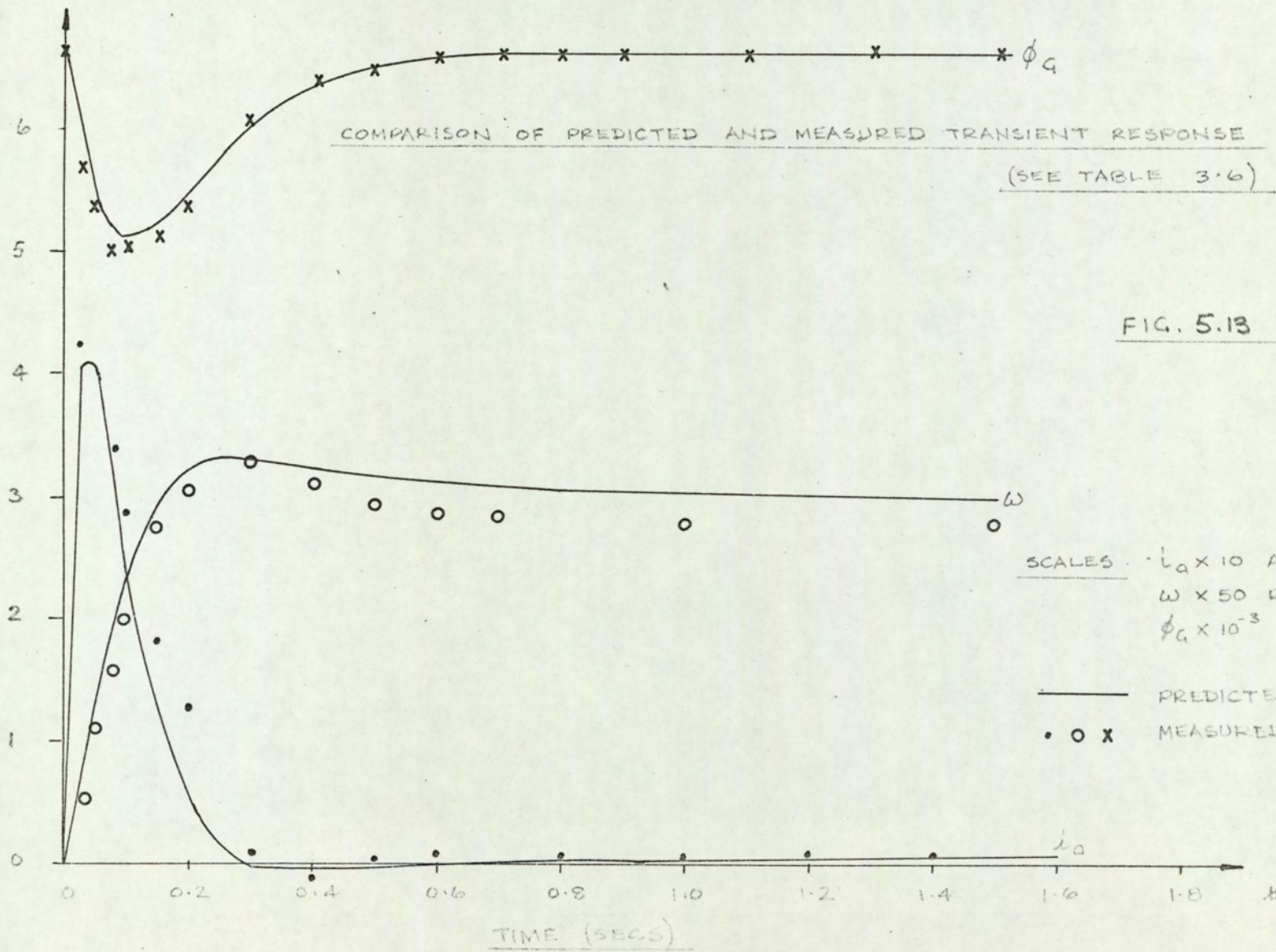


FIG. 5.12



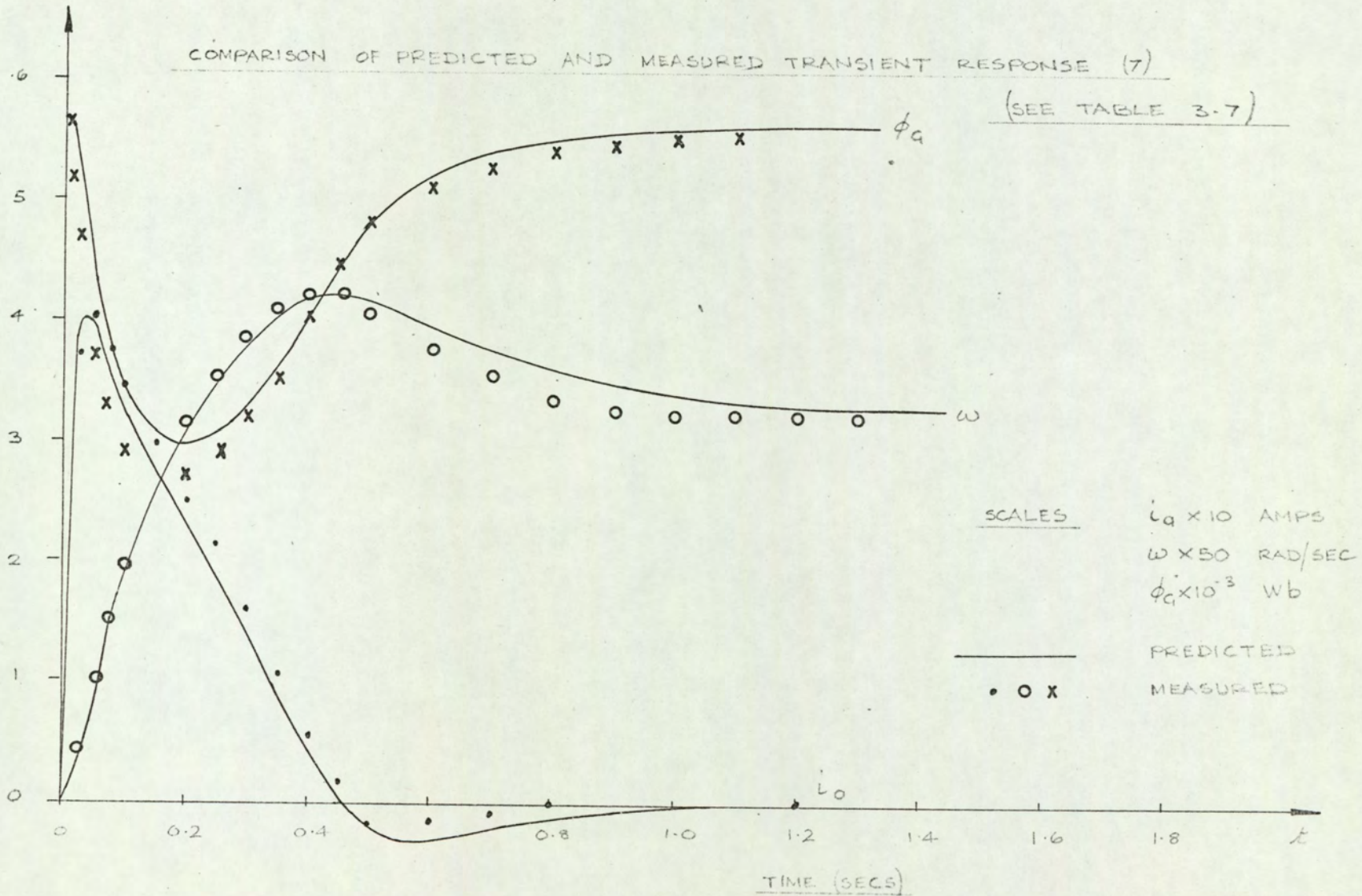


FIG. 5.14

5.6. Summary.

The method of simulation and hence the prediction of system performance was made possible by the following :-

- 1) Adopting the mathematical model shown in FIG. 2.7.
- 2) Use of a numerical sampling process for prediction of new values of the variables and for integration.
- 3) Linear interpolation between points in two dimensional and three dimensional arrays.
- 4) Eliminating numerically unstable calculations by employing predictive methods or small step lengths between calculations.

The non-linear relations described to be of type NL1 were read as arrays with sufficient elements to allow acceptable accuracy for linear interpolation. This also applied to non-linear relations of type NL2 except that a two dimensional array of about 300 points was required.

Using the model as a system to be controlled, the next chapter deals with a method of controlling the transient performance.

CHAPTER 6.

Control Strategy to produce a given performance.

- 6.1. Introduction.
- 6.2. Review of steepest descent method.
- 6.3. Computer program to realise steepest descent calculations.
- 6.4. Application of steepest descent to the system.
- 6.5. Interaction between stages.
- 6.6. Computer program to realise control strategy.
- 6.7. Choice of desired trajectory.
- 6.8. Results.
- 6.9. Errors encountered in the prediction process.
- 6.10. Summary.

CHAPTER 6.

CONTROL STRATEGY TO PRODUCE A GIVEN PERFORMANCE.

6.1. Introduction.

The system to be controlled was taken to be the mathematical model of the machine.

The overall control objective was to demand a given transient speed response $\omega(t)$. The control effort was to be predicted such that the speed attained should give minimum deviation from the desired speed characteristic. The deviation in speed was treated as the index of performance, and the control strategy required to minimise this index was taken to be the optimum.

The specific methods employed for optimisation, of which there are many, vary in degree of sophistication and rigor. The most important available for non-linear systems are hill climbing methods⁽²⁴⁾ and dynamic programming⁽²⁵⁾. A comparison of methods for discrete and continuous systems is given in the literature, (eg. 26) and the conclusion, generally, is that hill climbing methods are usually better except in the simplest problems.

Gradient methods^(27, p. 288) form the basis of most climbing procedures and they have the inherent advantage of avoiding saddle points^(27, p. 296). In most engineering problems the gradient is relatively easy to measure but the disadvantage of the method is that convergence can be slow. Despite this disadvantage

it was decided to adopt a gradient method because a result could be obtained. Particularly as approximate location of the optimum could be forecast from engineering knowledge of the system.

6.2. Review of steepest descent method.

The method assesses slopes in different directions and takes steps of chosen length in the "steepest" direction.

The index of performance (ρ) is considered to be a surface in control parameter space and successive parameter changes are made proportional to the gradient of ρ ($\nabla\rho$). The method requires that ρ be reduced after each step of the procedure.

$$\rho(y)_{r+1} < \rho(y)_r$$

$\nabla\rho$ defines the direction in which a given magnitude change in control parameter vector y is most effective in improving ρ over discrete changes. As the elements of $\nabla\rho$ were not functionally available; a change was made in one value of control parameter in y , with all other values of y held constant, and the corresponding change in ρ calculated. This calculation was repeated for all other values of y to enable $\nabla\rho$ to be determined. From the result the new value of y , $y_{r+1} = y_r - s \nabla\rho$ was determined.

Where s is the magnitude of the step size

y_r is the present value of y

d_r is the direction vector which establishes the extent, in terms of the various values of y , to which s is apportioned.

The method of steepest descent adopted was to choose

a step size based on the predicted value of ρ , with $d_r = \nabla \rho_r$.

A typical trial run therefore consisted of operating the system, represented by the model, over a given period with certain initial conditions to calculate the value of ρ . A trial change in initial conditions was then made to estimate $\nabla \rho$ for each value of y , and corrective adjustments in y made proportional to $\nabla \rho$. The process was repeated until a sufficiently low value of ρ had been reached.

6.3. Computer program to realise steepest descent calculations.

The program was based on the flow chart proposed by Eveleigh⁽²⁸⁾.

The control parameter state y_r was adjusted to minimise the value of ρ , and the notation used to specify the adjustment is shown below.

- Δy_r = test perturbation in y_r
- δy_r = corrective adjustment in y_r
- $\delta \rho_p$ = predicted change in ρ due to δy_r
- $\delta \rho_a$ = actual change in ρ due to δy_r
- $\delta \rho_r$ = change in ρ due to Δy_r

Control of s was based on the assumption that the ρ surface, near to the test point, could be considered as a plane. This assumption is valid only if Δy_r is made sufficiently small.

By computing at each step adjustment $\delta \rho_p = \nabla \rho_r \times \delta y_r$, where $\nabla \rho_r = \delta \rho_r / \Delta y_r$, and comparing with the actual change ($\delta \rho_a$) produced by $\delta y_r = -s \times \nabla \rho_r$ a decision was made about

whether adjustment in s was necessary.

If the ratio $(\delta\rho_p - \delta\rho_a)/\delta\rho_a$ differed by:-

- (a) more than 50% s was reduced
- (b) more than 20% s was kept fixed
- (c) less than 20% s was increased.

Control parameter state was then incremented after appropriate adjustment of the step length and the procedure repeated.

A flow chart of the computer program is shown in FIG. 6.1.

The initial control state was read in as $X_0(M)$ together with Δy and a stopping condition. Present values of y were retained as $Y(M)$ while predicted changes in y were made equal to $X(M)$. When step length adjustments had been finalised y was updated by putting $Y(M) = X(M)$.

Constraints were allowed for by fixing the max. value of y . If this value was exceeded, y was reduced by a small amount and allowed to climb back to its maximum value. In this way, at a later state, a reduction in y could be made if required.

The steps in computation were as follows :-

- 1) Control parameter y_r was set to x_{0r} and program count signified by J being set to zero.
- 2) $\rho(y_r)$ was calculated.
- 3) $\rho(y_r + \Delta y_r)$ was calculated to find $\nabla\rho_r$.

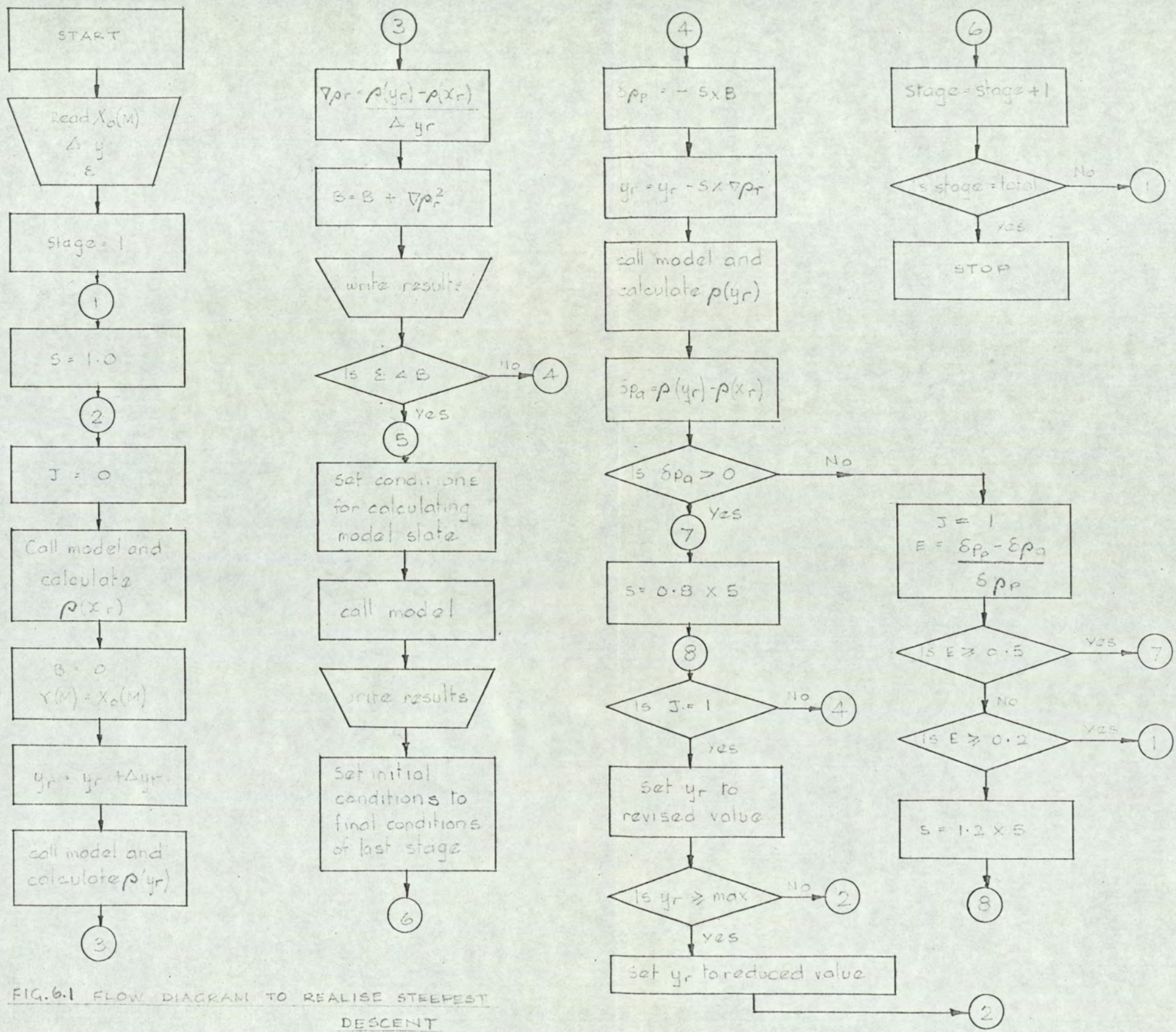


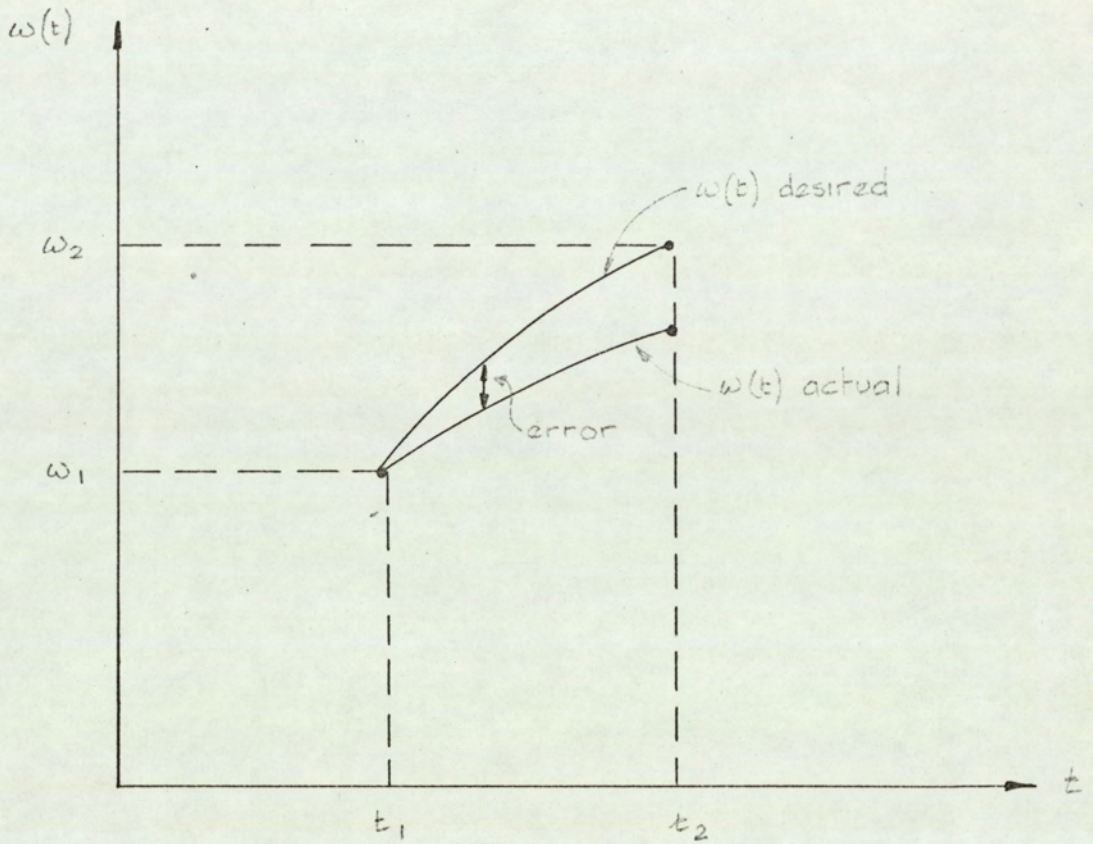
FIG. 6.1 FLOW DIAGRAM TO REALISE STEEPEST DESCENT

- 4) y_r , $\rho(y_r)$, s and $\sum_{i=1}^n \nabla \rho_{r_i}^2$ were printed out.
- 5) If next stage was not called δy_r and $\delta \rho_p$ were computed.
- 6) A new control parameter $y_r = y_r + \delta y_r$ was used to compute $\rho(y_r)$.
- 7) $\delta \rho_a$ was then found and if an improvement had been achieved, J was set to one.
- 8) Otherwise s was reduced and the process repeated from 5).
- 9) The step length s was then adjusted depending upon the degree of accuracy of the prediction.
- 10) The process was then repeated from 1).

6.4. Application of steepest descent to the system.

The control strategy required to produce the desired transient speed response will clearly be time varying. Therefore if the control interval is divided into, for example, ten equal stages and adjustment of two control input states is required. Then the problem of evaluating the optimum policy involves a decision process in twenty dimensions. It was necessary to reduce the number of dimensions in order to cut down computing time. This can be done by optimising over one stage before moving onto the next. But for this to be correct the interaction between stages must be small. Otherwise a decision taken at an earlier stage may influence the result at a later stage.

Reference to FIG. 6.2. will show that, if the model is used to calculate the actual trajectory over a given stage, the error can be evaluated. In fact the mean squared error was

FIG. 6.2

calculated over the period t_1 to t_2 and used as a measure of ρ . The mean square error was chosen because it penalises large errors and hence produces an increase in $\nabla\rho$; with consequent faster convergence. It also has a well established minimum by virtue of its second order nature.

In general, therefore, the system control input function combination which extremalised an assigned index of performance ρ was desired. This was obtained computationally by using the extremum search program, described in section 6.3., to converge to the appropriate minima.

6.5. Interaction between stages.

Control was afforded by variation of the control input voltages v_f and v_a , the field and armature voltages respectively. Since these control inputs are time varying it was decided to compute the response for fixed values of v_f and v_a for each stage.

These control inputs were then adjusted over the fractional period of the transient response (one stage), until the desired response was obtained for that period. This process was repeated for further stages until the best fit was obtained.

In an attempt to reduce interaction between stages, each stage was divided into two parts. The control inputs v_f and v_a were assigned two values, one each for the first half period of the stage and two new values for the second half period of the stage. FIG. 6.3. illustrates the arrangement with the control inputs taking four values to be adjusted for the minimisation of ρ .

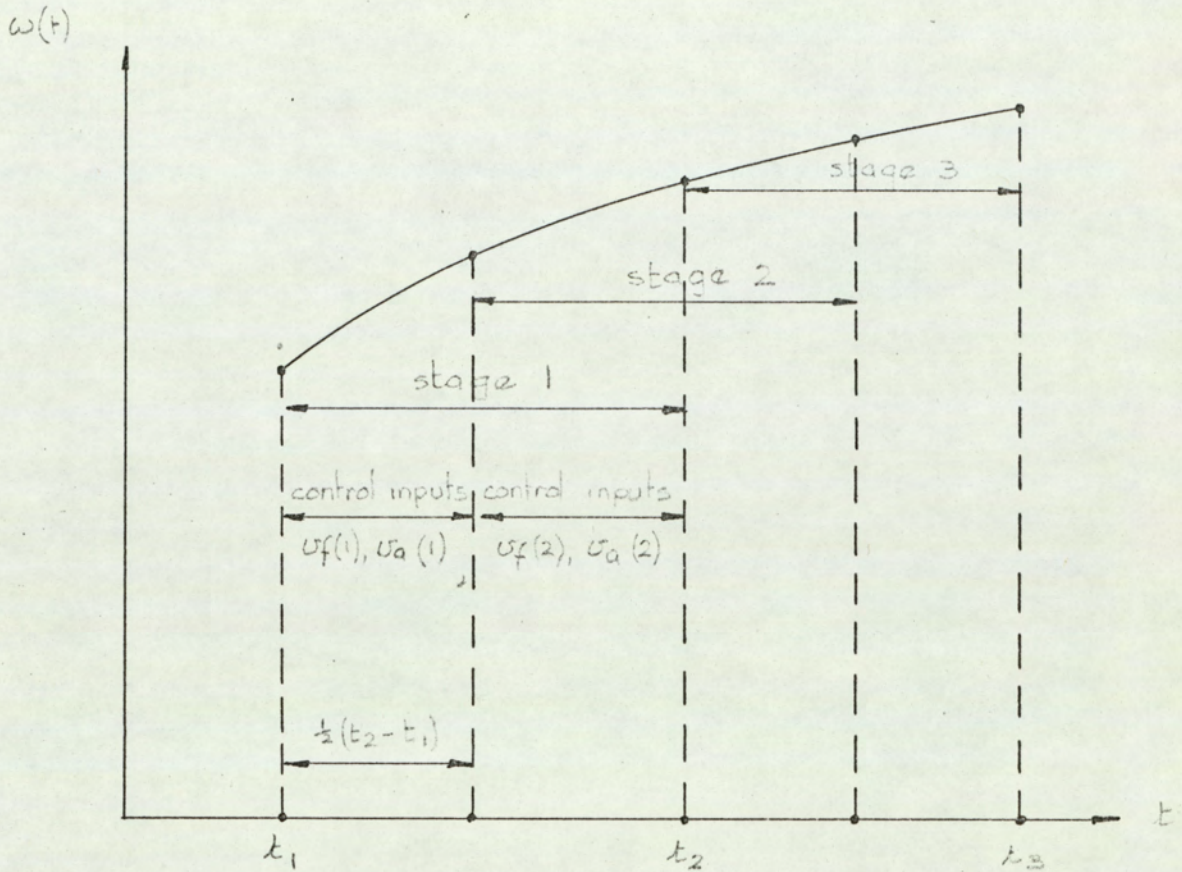


FIG. 6.3

Transfer to the next stage was made only when the gradient had reached an acceptably low value. Then the new stage was started with initial conditions as for the mid point of the previous stage.

6.6. Computer program to realise control strategy.

A computer program was formulated to enable the following calculations :-

- 1) Evaluation of the transient response of the model over the period t_1 to t_2 , with given initial conditions ω , i_a and ϕ_g , for v_a and v_f .
- 2) Calculation of the mean squared error between the desired trajectory and actual trajectory over the same period.
- 3) Repeat of 1) and 2) for new values of v_a and v_f as predicted by extremum search.
- 4) The process was repeated until a sufficiently close fit with the desired trajectory was obtained.

The flow diagram for this program is shown in FIG. 6.4. and should be read in conjunction with FIG. 6.1.

6.7. Choice of desired trajectory.

The desired trajectory was chosen from the point of view that the speed of the machine was to follow a prescribed variation. The main reason for this approach was based on a number of practical observations. Industrial applications exist where practical limits impose conditions such that direct, or related, reference to the speed-time curve is required.

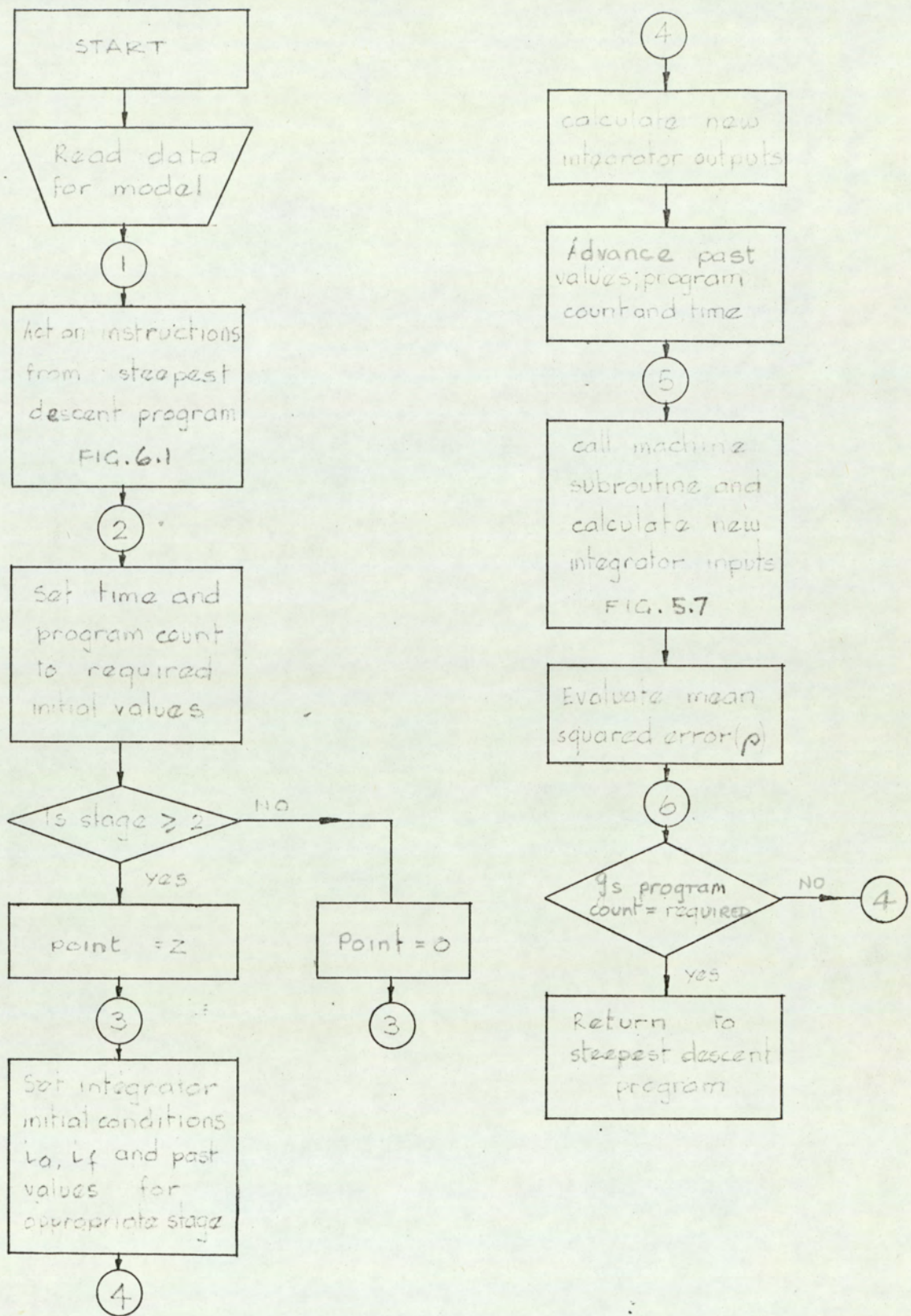


FIG 6.4 FLOW DIAGRAM FOR MODEL USED IN CONJUNCTION WITH STEEPEST DESCENT DIAGRAM

Examples include traction, mine winding and steel mill controls, where acceleration and deceleration are of prime concern when considering a method of control.

The curves showing the results indicate the desired trajectory chosen and the control strategy necessary to attain it. Clearly when dealing with a continuous process the number of stages n should be as large as possible to obtain reasonable accuracy of analysis. When the control interval was split into time intervals of 0.025 sec reasonably accurate prediction was possible.

6.8. Results.

The results obtained are shown in FIGS. 6.5-6.10., and they include the desired trajectory, the control strategy and the actual speed predicted from the model. All results were checked separately, by calculating $\omega(t)$ using the control strategy predicted, and in all cases conformed to the desired characteristic.

One point worth noting is that control must be continued well after $\omega(t)$ has reached its desired level, because other state variables have not reached their steady state values.

Another point is that interaction between stages is fairly small, which indicates that the decision process may be reduced to two variables without appreciable loss of overall accuracy.

The results shown in FIG. 6.9 indicate that when the system is required to follow a function of $\text{SIN } t$ that initially the

acceleration required demands large control voltages. But over the next stage this voltage has to be reduced drastically because acceleration becomes greater than required.

6.9. Errors encountered in the prediction process.

The curve shown in FIG. 6.11 is included to show how the function $\nabla \rho_r^2$ fluctuates during the process of predicting a reduction in ρ .

Results were taken from a typical stage where the initial step length chosen was too small. The errors encountered here are those produced by evaluation of data representing non-linear functions and the round-off error introduced by numerical integration. Therefore the limits that determine the termination of the search must be chosen with reference to more than one factor. For example very small changes in control voltage may be a guide, if the value of ρ is acceptably small, and from a knowledge of the model it is known that small changes in control voltage produce virtually no change in speed characteristic.

6.10. Summary

This chapter outlines the method adopted to derive the control strategy required to produce a desired transient response.

The results show the feasibility of splitting a desired transient characteristic into a number of stages and predicting the control strategy required for one stage separately. This has the considerable advantage of reducing the extremum search to comparatively few dimensions.

The next chapter summarises and concludes the thesis.

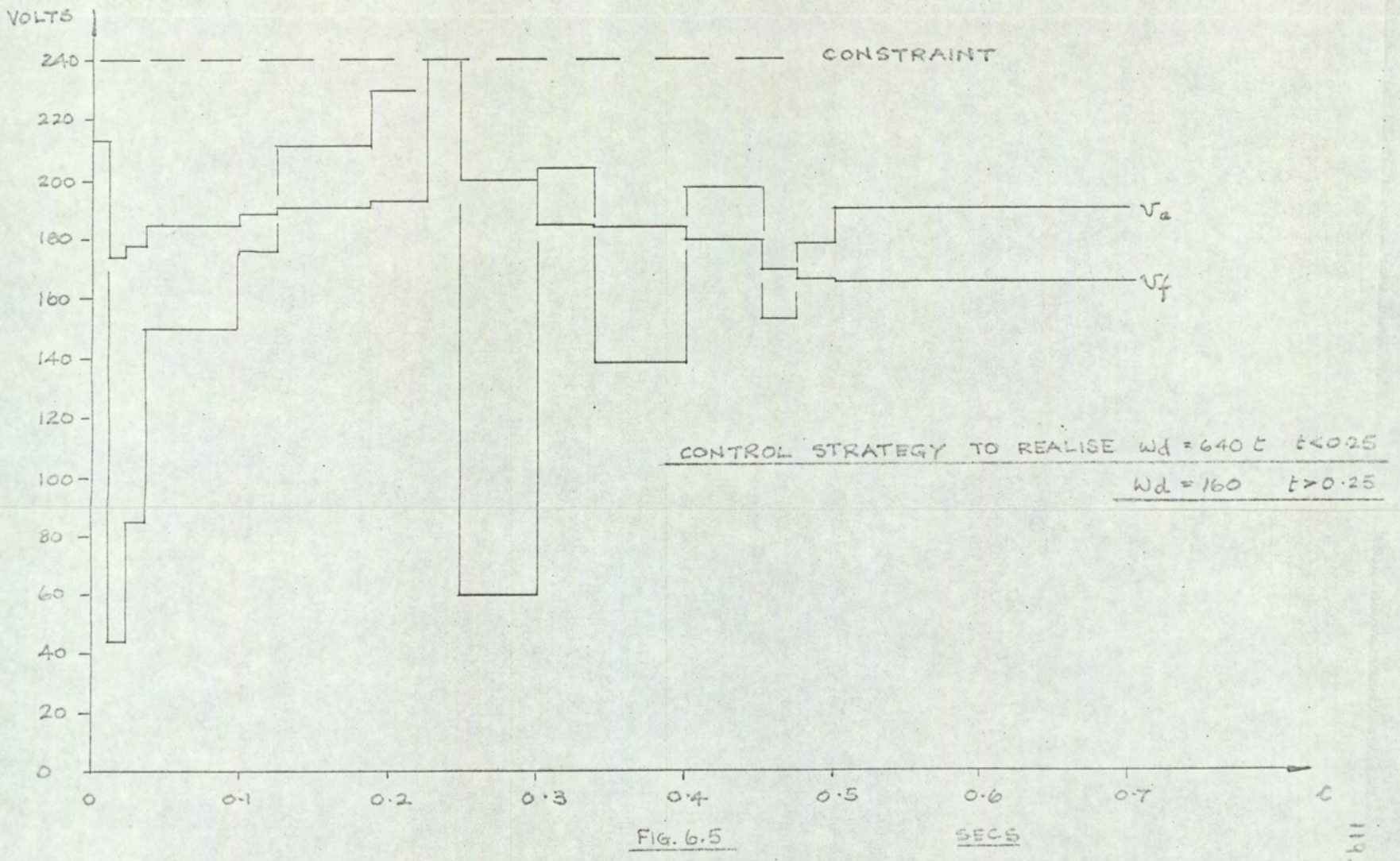
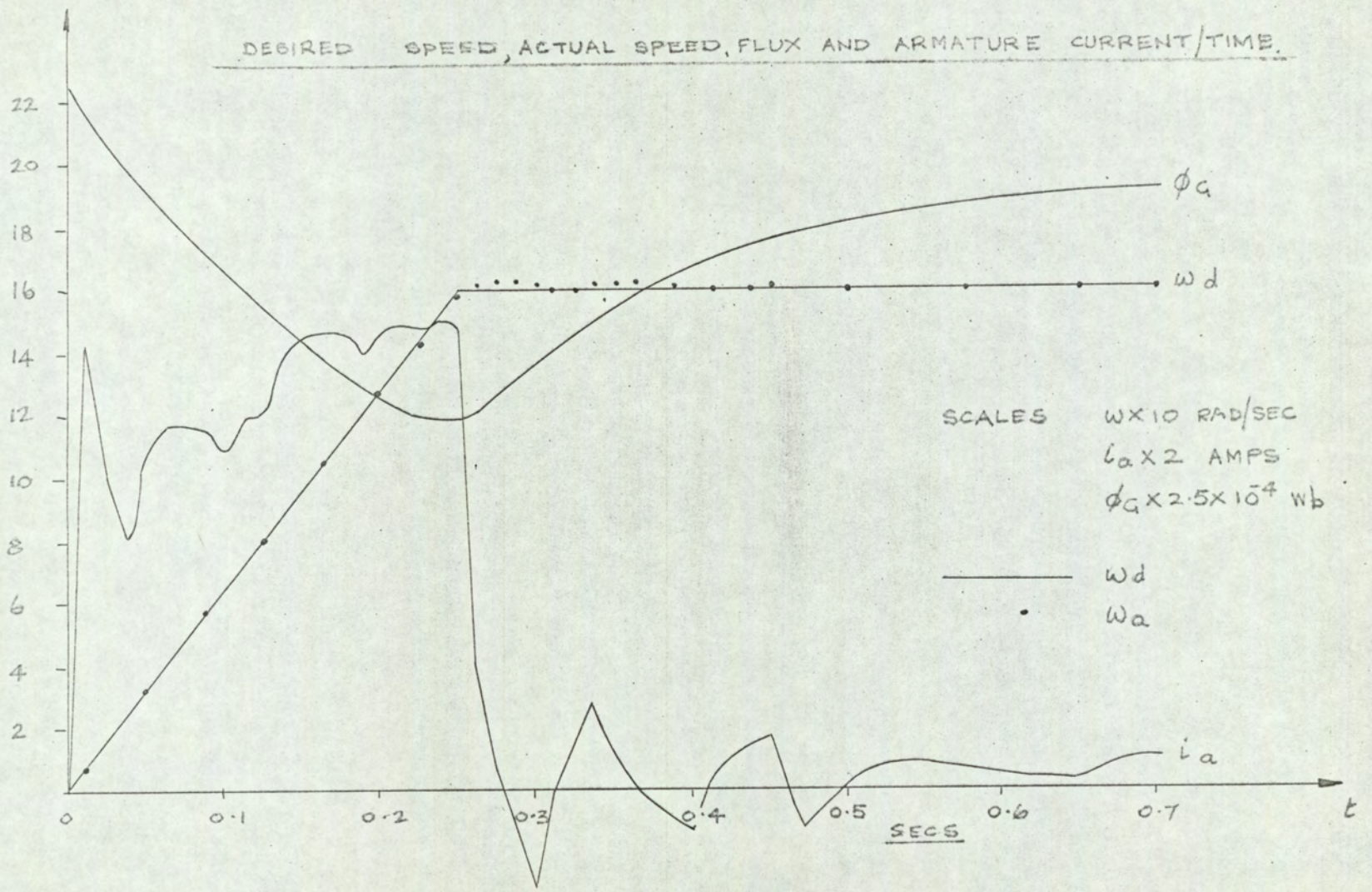


FIG. 6.5

% ERROR

% ERROR IN SPEED AGAINST TIME

$$\% \text{ ERROR} = \frac{\omega_d - \omega_a}{\omega_d} \times 100$$

(SEE FIG. 6.5)

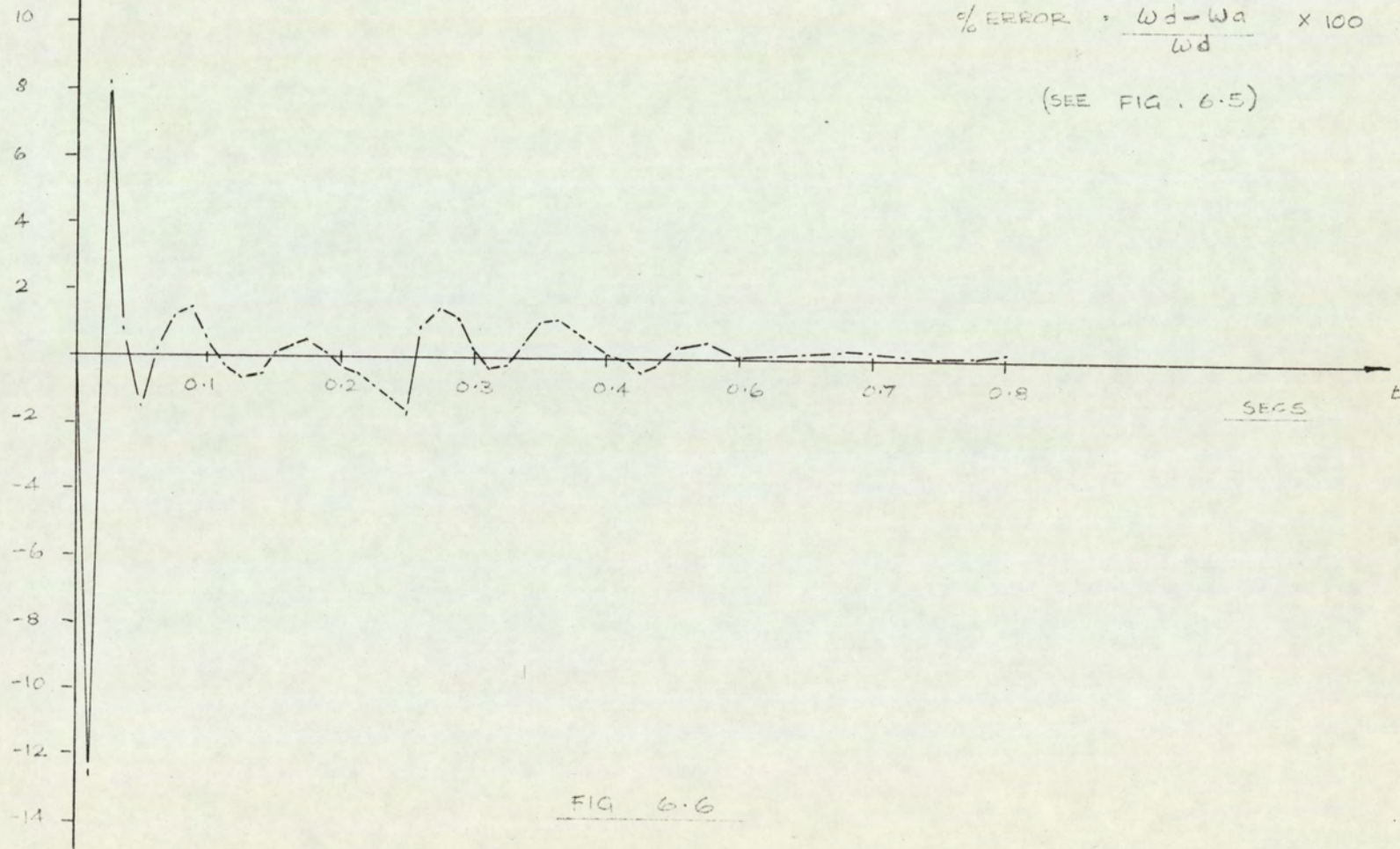


FIG 6.6

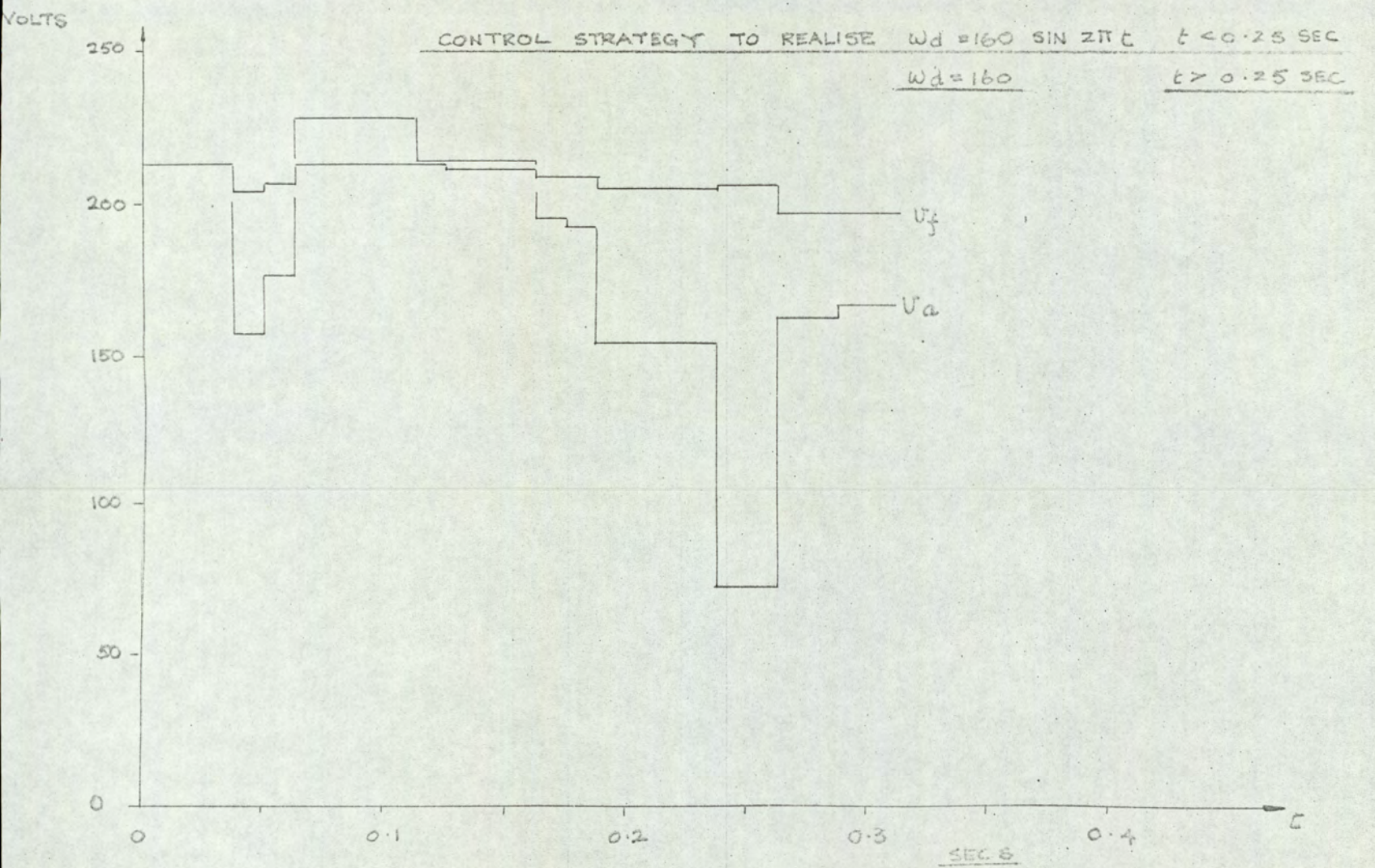
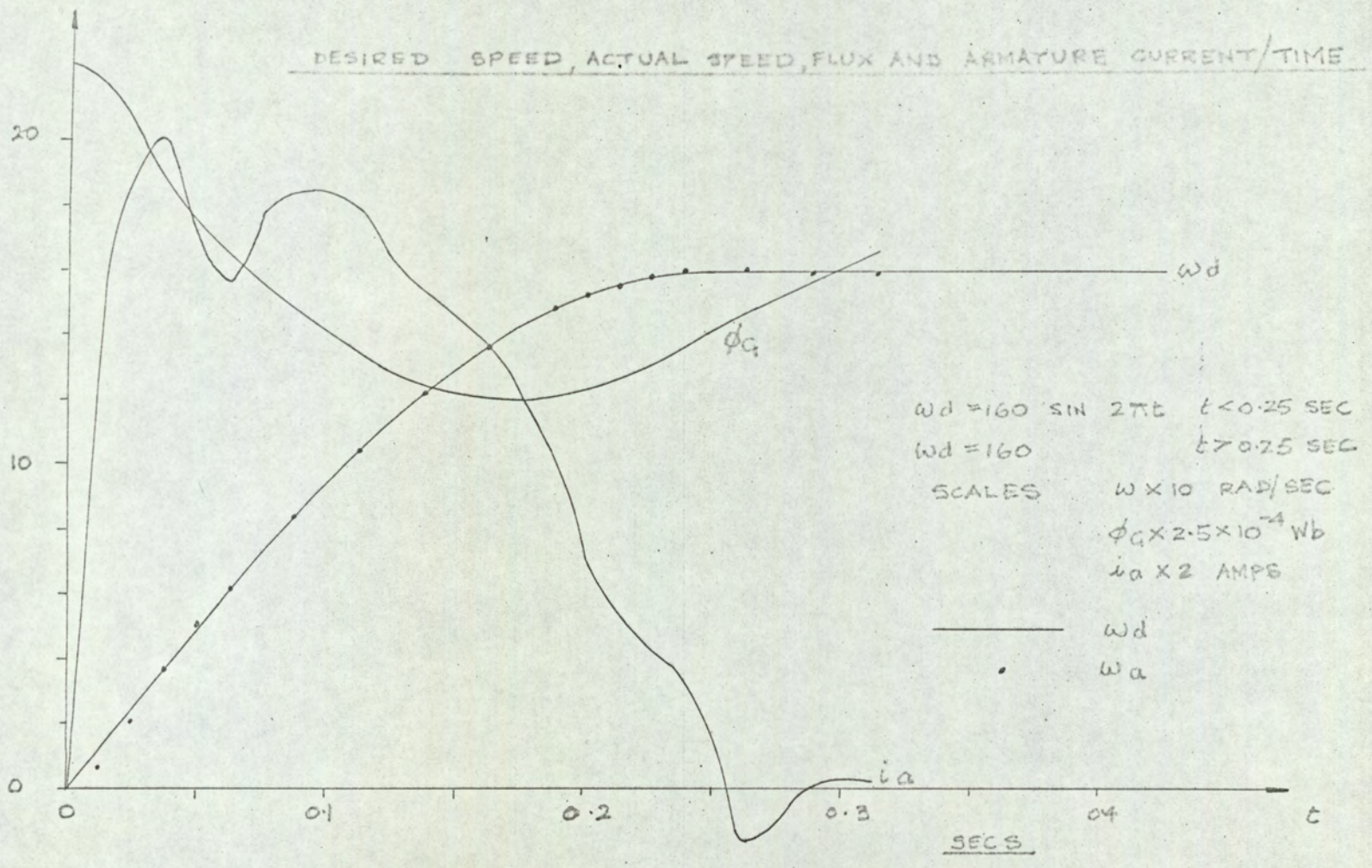
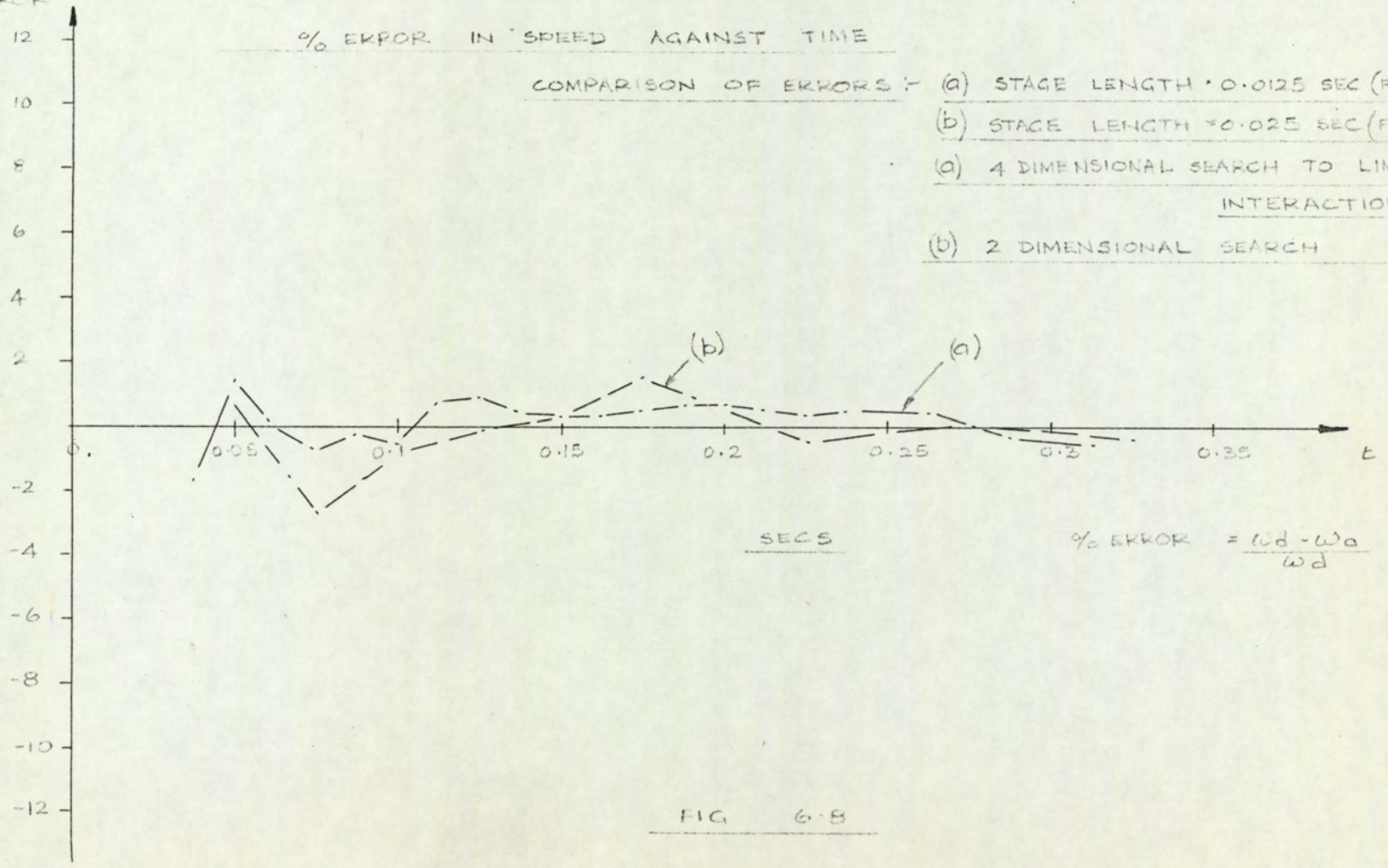


FIG 6.7

% ERROR

% ERROR IN SPEED AGAINST TIME

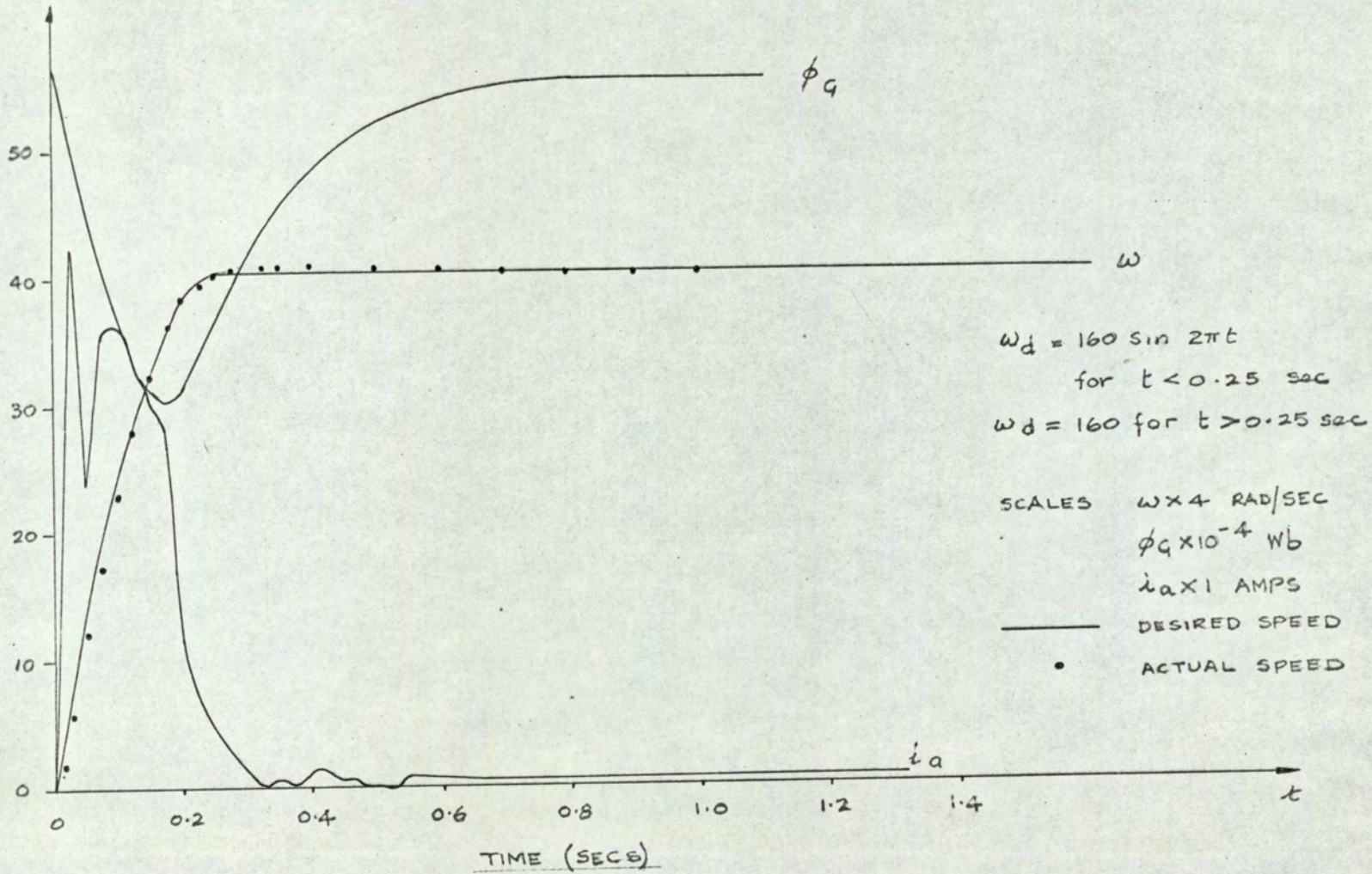
- COMPARISON OF ERRORS :-
- (a) STAGE LENGTH = 0.0125 SEC (FIG. 6.7)
 - (b) STAGE LENGTH = 0.025 SEC (FIG. 6.9)
 - (a) 4 DIMENSIONAL SEARCH TO LIMIT INTERACTION
 - (b) 2 DIMENSIONAL SEARCH



$$\% \text{ ERROR} = \frac{\omega_d - \omega_a}{\omega_d} \times 100$$

FIG 6.8

DESIRED SPEED, ACTUAL SPEED, FLUX AND ARMATURE CURRENT / TIME.



CONTROL STRATEGY REQUIRED TO PRODUCE ABOVE RESPONSE.

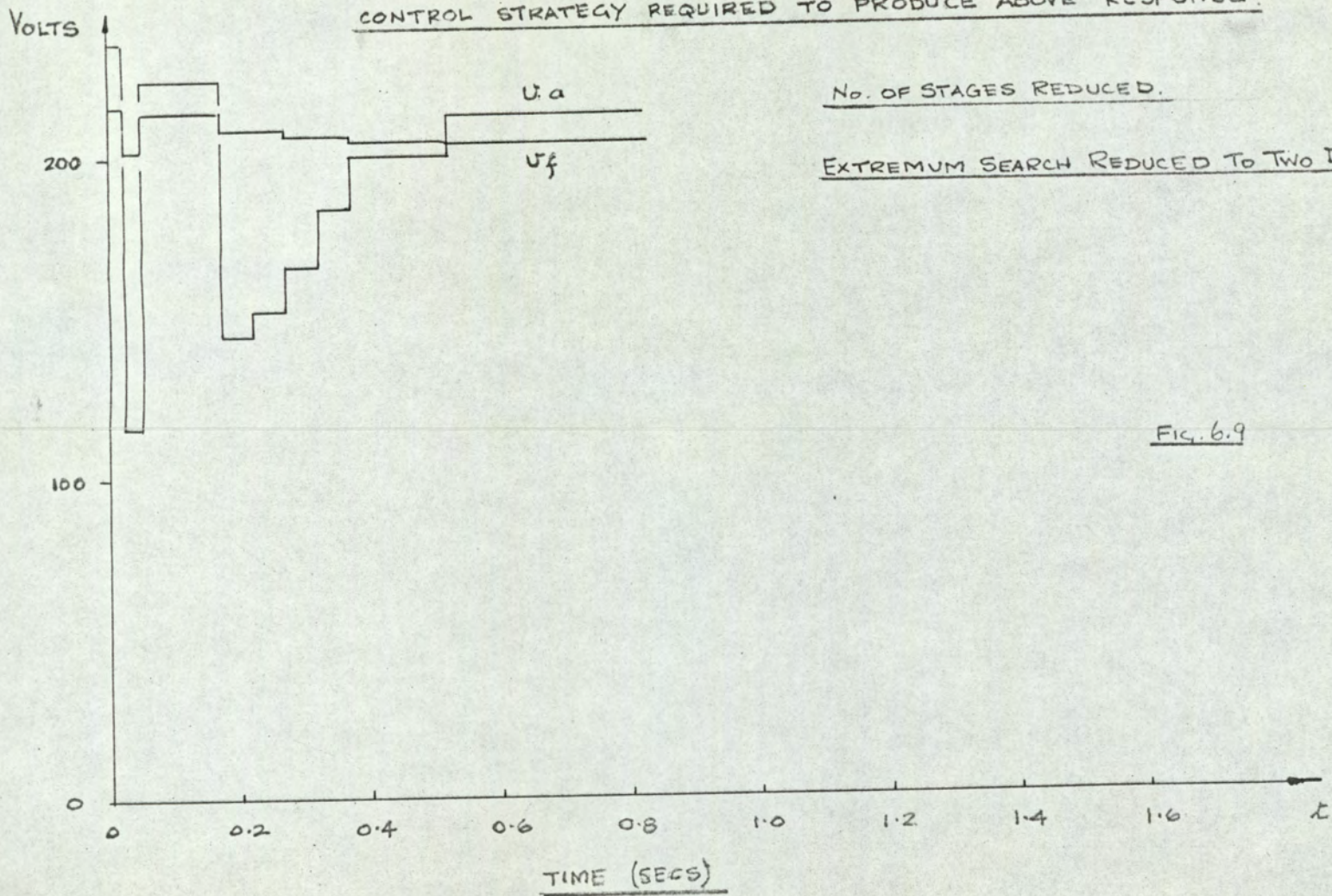
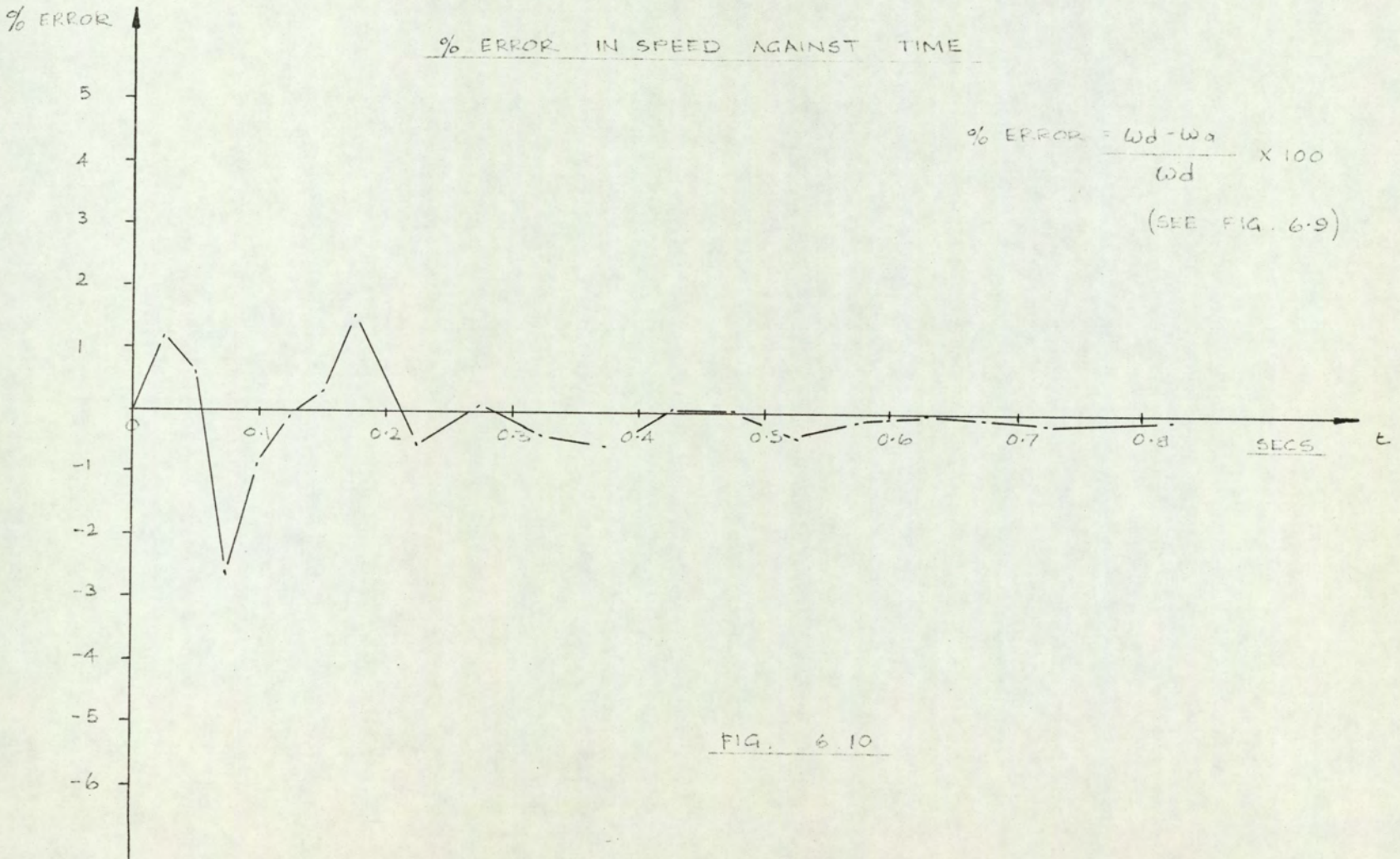


FIG. 6.9

% ERROR IN SPEED AGAINST TIME



$$\% \text{ ERROR} = \frac{\omega_d - \omega_a}{\omega_d} \times 100$$

(SEE FIG. 6.9)

FIG. 6.10

FLUCTUATION IN $\nabla p_r^2, \rho$ AGAINST NUMBER OF TRIAL
ADJUSTMENTS

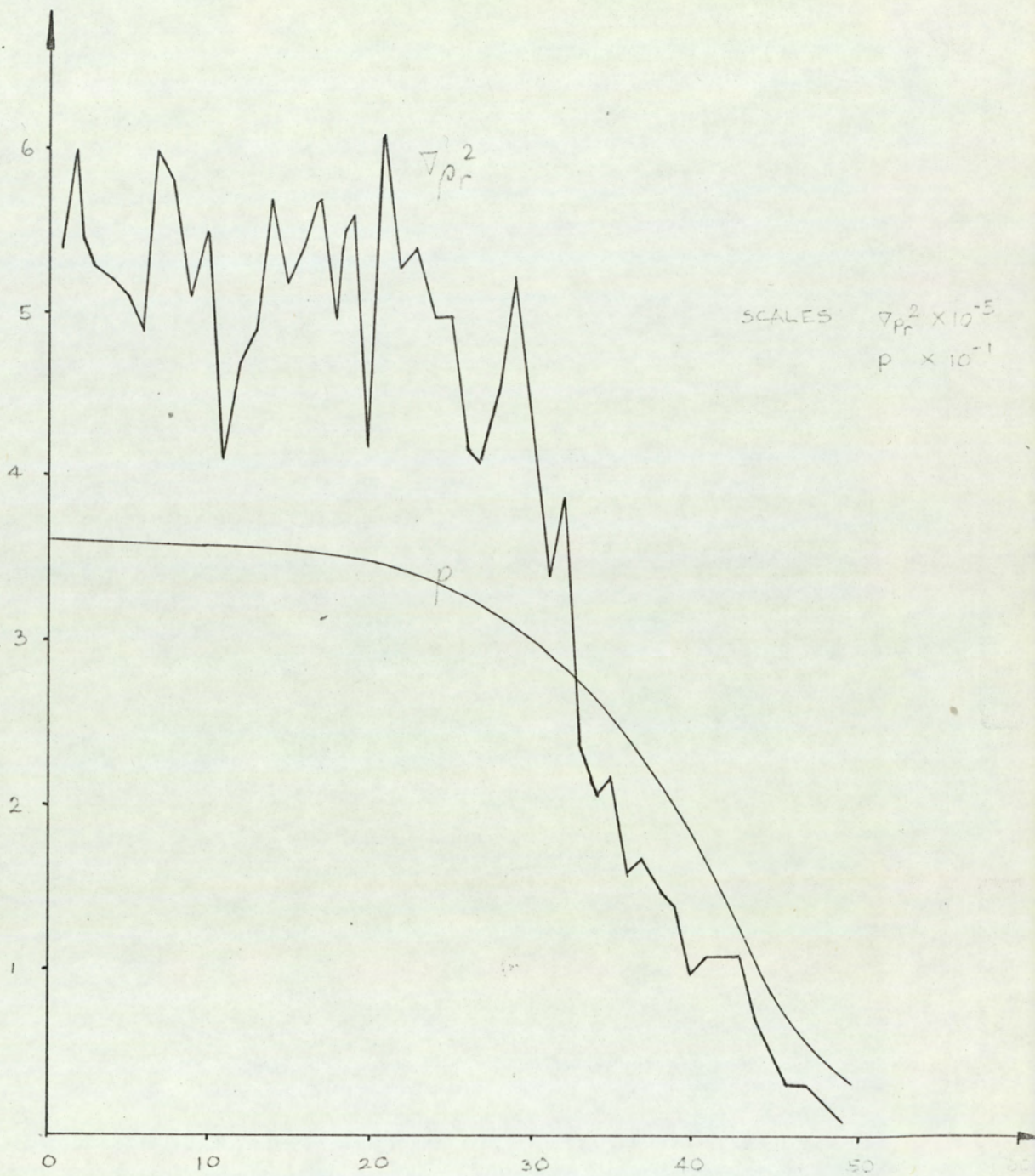


FIG. 6.11

CHAPTER 7.

Summary of research and general conclusions

7.1. Object of research.

7.2. Discussion on the method adopted to deal with cross-axis interference.

7.3. Discussion on the treatment of eddy currents.

7.3.1. The effect of eddy currents on flux changes.

7.3.2. The effect of eddy currents on r_a .

7.4. Method of simulation of machine performance.

7.5. Discussion on prediction of control strategy.

7.6. General comments.

7.7. Suggestions for further work.

7.8. Conclusions.

CHAPTER 7SUMMARY OF RESEARCH AND GENERAL CONCLUSIONS7.1. Object of research

The objectives under consideration were :-

- 1) To examine the validity of the assumptions associated with linear theory.
- 2) To represent a single-axis d. c. machine as a control system element by evolving a mathematical model based on new assumptions.
- 3) To undertake measurements of transient performance on the machine at widely different initial conditions.
- 4) To analyse the results of measurements and where necessary predict the form of the parameters not directly measurable.
- 5) To simulate the performance of the machine by treating the mathematical model as a multivariable non-linear interacting control system.
- 6) To correlate the measurements of the variables with those predicted by simulation.
- 7) To evolve a method of predicting the control strategy.

The above list represents the order in which the work was carried out and has been described in chapters 1 to 6 of the thesis.

The original work may be identified with the development of, 1) an adequate model to predict the transient characteristic of a saturated single-axis d. c. machine, and 2) a method of predicting the control strategy to produce a desired transient response.

7. 2. Discussion on the method adopted to deal with cross-axis interference.

As soon as the presence of saturation in a machine is acknowledged, it follows that the flux produced on both the direct-axis and quadrature-axis will be subject to cross-axis interference. That this interference must be considered ⁽²⁹⁾ is amply demonstrated by the reduction in direct-axis flux, due to i_a , shown in FIGS. 5. 11. - 5. 14.

The method of predicting this interference was to employ the measured magnetisation characteristic at various points in the air-gap and to compute the flux density at each point by assuming a fixed concentration of M. M. F. at each slot. The flux linkages in the direct-axis were then deduced as a function of quadrature-axis current. The corresponding relation in the quadrature-axis was found by using the same calculation to derive the flux-linkages adjacent to the direct-axis pole face and then adding this contribution to the quadrature-axis poles.

Alternative methods which have been used consist of treating the magnetic circuit as a field problem having certain boundary conditions, ^(30, 31) or deducing the interference on the direct-axis only for limited forcing ⁽²⁹⁾.

Some of the methods suggested ^(30, 31) would probably produce a more accurate result than the method adopted, ⁽¹⁶⁾ but with a considerable increase in computing time. However, research has shown that greater accuracy need only be demanded if other relationships can be expressed with similar accuracy.

Under transient conditions eddy currents effect the flux distribution and hence the change in flux in both the main pole and the commutating pole. Therefore these currents will produce a change from the steady-state results obtained by either method.

7.3. Discussion on the treatment of eddy currents

7.3.1. The effect of eddy currents on flux changes

The time lag produced by eddy currents was deduced by measuring the average time delay encountered in flux build-up for different initial conditions.

Allowance was made for this delay by changing the time constant of the appropriate integrator when computing the flux linkages ψ_f and ψ_a . This method must be regarded as a rather crude approximation since it treats the eddy currents as being equivalent to a short-circuited turn, ⁽¹⁸⁾ which enables the new equivalent turns to be recalculated from $T\phi_d$ and $T\phi_q$.

The allowance with respect to ψ_f , which is associated with a laminated circuit was comparatively small. But, the change with respect to ψ_a was considerable due to the solid iron commutating pole.

Consideration of the results of section 3.3.2.2. and FIG. 4.6. will show that a family of curves would most likely be required to simulate the changing time constant more precisely.

The only justification for maintaining an approximate relation was that when changes, of the order of 10%, in slope and magnitude were tried during simulation, it produced only very small changes in the predicted values of i_a , ϕ_G and ω .

It appears that very little work has been done on the transient behaviour of flux in the presence of eddy currents, except under no load conditions. ⁽³²⁾

7.3.2. The effect of eddy-currents on r_a .

The measurements described in section 3.3.1.5. indicate the considerable variation in r_a as a function of speed and current. Various authors ^(e.g. 14, p. 179, 11) have discussed this relationship in terms of eddy currents or commutation and some have illustrated that the effective resistance is somewhat greater than the standstill value.

However, separation of the amount by which the resistance is increased due to eddy currents and that due to chattering of the brushes makes any predicted value of r_a open to considerable error.

7.4. Method of simulation of machine performance.

The results obtained by numerical analysis confirm that the non-linear equations, presented by the model, can be solved with sufficient engineering accuracy to justify the approach. Unfortunately analysis of this type produces a number of problems that are not readily solved. Such problems include the choice of the method of integration and step length, and estimation of errors. The method of integration was chosen as being easy to apply and

had the virtue that the prediction and starting routine was based on frequency response.⁽²⁰⁾ Various tests were carried out on different systems of equations both linear and non-linear to justify the method used. These tests revealed that provided the step length was chosen with respect to the smallest time constant and the maximum rate of change of any non-linear function, then acceptable accuracy could be achieved. Accuracy had to be checked in the non-linear case by comparison with known results. This is because no practical estimate of the error is possible. In fact it has been suggested⁽³³⁾ that the only means of checking the solution of non-linear differential equations is to substitute the computed values back into the original equations.

A number of the routines that were used for calculation could have been made to produce more accurate results by developing prediction correction sub-routines to choose the step length. However all the work was carried out on a computer with an 8K store, which proved to be a limit to the production of the "ultimate" program.

It should also be borne in mind that the approximations employed to express some of the varying parameters of the model will produce errors, perhaps of more significance, than those introduced by computation.

7.5. Discussion on prediction of control strategy.

Consideration of the introductory comments in chapter 6 will indicate that the subject of optimisation by extremum search techniques is a large and expanding one. Therefore the choice of method adopted for a particular system presents a problem similar to that posed in choosing a method of numerical integration.

The choice, as far as this problem was concerned, was based on the principle that the search should be restricted in dimen-

sion. So that during the development stages of establishing the search technique it was decided to try a straight forward gradient method. The idea being that step length adjustment methods could be tried when it became necessary to speed up convergence. But it was found that useful results could be obtained in reasonable computing time without refining the method used for adjusting the step length. On some stages no change in s was required at all, but on others considerable adjustments were required. By printing out results after a given number of iterations the trend can be assessed and on-line adjustments initiated to speed convergence. This of course is only possible if the process dynamics are predictable with reasonable certainty.

Perhaps the most common method of speeding convergence is to employ curvature estimating methods. (27, p. 323)

For most engineering applications of this type an upper and lower limit of deviation in speed over a given stage would probably permit the number of stages to be reduced. But this limit would have to be chosen carefully otherwise violent fluctuations in control effort would be required between stages.

The final comment also applies if the deviation in the speed from the desired is specified to be very small.

Constraints were applied by limiting the maximum control input. But these limits only applied for a limited range because the model parameters were chosen to constrain the state variables to values within the extremes measured on the actual machine under test. In other words it was considered that the machine was tested under maximum, or near maximum, forcing conditions, and any attempt to exceed those limits would drive the calculations beyond

the data limits available.

One way of treating constraints in a system of this type is to apply them directly to the model. Allowance can then be made in the hill climbing routine by adjusting the limits on performance measure. Flexibility of control can also be improved by adjustment of other parameters (e. g. r_f) when a maximum input voltage level is reached.

7.6. General Comments.

The importance of modelling in automatic control is an accepted fact, because it is a means of filling existing gaps between theory and practice. From the first assessment of the problem the use of first principles, followed by measurement, together with an early introduction of the digital computer seemed the better course.

The method of analysis is applicable to most machines of similar configuration if machine design data is available. However certain parameters, such as r_a and T_ϕ , would have to be estimated. Tests were conducted on two other machines to verify that the same trends, with respect to ϕ_G , i_a and ω , occurred, although detailed analysis was not undertaken.

The prediction of the control strategy should be regarded as the first step in designing the optimum controller for a closed-loop control configuration. Disturbances in the form of load torque can be built into the model and the appropriate strategy obtained.

Therefore the controller would store the optimum control strategy for a number of desired steady state speeds. The optimum trajectory would also be stored for comparison with the actual

trajectory such that any deviation could be corrected by transfer to the correct strategy. This may involve transfer to a neighbouring optimum strategy if any constraints are violated.

7.7. Suggestions for further work.

Improvement of the model would probably result if comparison with results from other machines were obtained, and also if some of the cruder assumptions, mentioned earlier, were refined.

Numerical integration is a time consuming process which could be eliminated by adopting a hybrid computing arrangement. Then integration would be performed on an analogue machine and non-linear calculations on the digital machine. This would lead to a considerable reduction in computation time.

An automatic method of speeding convergence to the optimum in the hill climbing procedure could be developed.

Considerable practical work on the design of optimum controllers for specific applications remains to be done.

The main contributions of this thesis are :

- 1) The development of a new model for the d. c. motor that is superior, in simulation studies, to any model available hitherto.
- 2) A new computer program based on this model, that readily predicts the transient performance of d. c. machines in traction and similar applications.
- 3) A computer program, which could be used with limited storage space, for predicting the time optimal control strategy for d. c. motor speed control.

These contributions can be applied as follows :

- 1) The model is a general design contribution for any industrial or military system incorporating d. c. machines. The analyses on which this model was derived may also prove of value in establishing new concepts of d. c. machine design; i. e., choice of flux level, pole shape, laminated regions, class of insulation and additional windings.
 - 2) The transient performance prediction program has been requested by the University of Bristol for their traction studies; and could be of equal value to other institutions investigating other applications of d. c. machines.
 - 3) There seems to be no fundamental reason why the method developed for predicting the optimal control strategy should not be applied to the control of industrial plant such as rolling mills. Then if an adequate model of the rolling process is used it might be possible to maintain correct strip thickness during the accelerating and decelerating periods where rolling conditions, and hence control requirements, are changing continuously.
 - 4) The computer program used for the prediction of control strategies was developed on a PDP 9 computer; which is typical of the low-priced limited storage computers becoming increasingly available for industrial control applications. For instance these methods could be economically feasible in mine hoists, missile controls, traction and similar applications where digital computing facilities are readily available. Where computing facilities are absent the predicted control strategies could be used for the design of conventional control hardware. These strategies could be particularly valuable when it is desired to obtain maximum performance from an existing system, i. e.: uprating the transient performance of an existing drive.
- In some circumstances, where utmost exploitation of machine capacity is not a prime factor, these concepts will not make too valuable a contribution. A typical example is an industrial system where the cost of oversized (i. e.: underated) machines can be used. However, where maximisation of machine effort is a criterion, these concepts will be of value.
- 5) The modelling and simulation techniques that have been adopted are being used to investigate currently unexplored problems, such as the transient performance of eddy current couplings.

8.0. Appendices.

Computer Programs.

8.1. Average Flux Calculations.

8.2. Single Valued Functions of a Single Variable .

8.3. Single Valued Functions of Two Variables .

8.4. Simulation of Model.

8.4.1. Read Data.

8.4.2. Integration Routine.

8.4.3. Machine Subroutine .

8.5. Extremum Search

8.5.1. Read Data.

8.5.2. Steepest Descent Routine.

8.5.3. Integration Routine.

8.5.4. Machine Subroutine .

8.5.5. Print Results

8.5.6. Typical Data

8.0 APPENDICESCOMPUTOR PROGRAMS8.1 AVERAGE FLUX CALCULATIONS (SEE PAGE 70)

```

C      CALCULATE FLUX DENSITY - FLUX LINKAGES - TITLE FLUX
      INTEGER M, I, J, N, R
      REAL F(50), BA(54), BB(54), BC(54), TA(7), Z(7), ATT(7),
1     ATF, IA, DB, DIA, A, B, C, D, E, G, H, P, Q(7), FAV, BAV
      COMMON/P/ATT, BA, BB, BC, F, J, BAV
      READ(3,100)(F(M),M=1,16)
      READ(3,101)(TA(M),M=1,7)
      READ(3,102)(BA(M),M=1,54)
      READ(3,103)(BB(M),M=1,54)
      READ(3,104)(BC(M),M=1,54)
      READ(3,105)ATF, DIA
      DO 1 I=1,11
      DO 2 N=1,14
      DO 3 J=1,7
      ATT(J)=DIA*TA(J)+ATF
      CALL NL1A(P,1)
      Z(J)=P
3     CONTINUE
      BAV=(Z(1)+Z(2)+Z(3)+Z(4)+Z(5)+Z(6)+Z(7))/7.0
      CALL NL1A(FAV,2)
      DO 4 R=1,7
4     Q(R)=Z(R)-BAV
      IF(Q(3).GT.0.0)GOTO 5
      IF(Q(3).EQ.0.0)GOTO 6
      IF((Q(4).GT.0.0).AND.(Q(3).LT.0.0))GOTO 7
      IF(Q(4).EQ.0.0)GOTO 8
5     A=3.0
      B=1.0
      C=1.0
      D=3.0
      E=5.0
      H=7.0
      G=9.0
      GOTO 9
6     A=4.0
      B=2.0
      C=0.0
      D=2.0
      E=4.0
      H=6.0
      G=8.0
      GOTO 9

```

8.1 CONTINUED.

```
7      A=5.0
      B=3.0
      C=1.0
      D=1.0
      E=3.0
      H=5.0
      G=7.0
      GOTO 9
8      A=6.0
      B=4.0
      C=2.0
      D=0.0
      E=2.0
      H=4.0
      G=6.0
9      AFL=(A*ABS(Q(1))+B*ABS(Q(2))+C*ABS(Q(3))+D*ABS(Q(4))+
1E*ABS(Q(5))+H*ABS(Q(6))+G*ABS(Q(7)))
      IA=DIA
      WRITE(2,104)IA,FAV,AFL
      DIA=DIA+5.0
2      CONTINUE
      ATF=ATF+450.0
1      CONTINUE
100     FORMAT(8F5.0)

101     FORMAT(7F7.0)
102     FORMAT(9F9.0)
103     FORMAT(9F9.0)
104     FORMAT(9F9.0)
105     FORMAT(2F4.0)
      STOP
      END
```

8.2 SINGLE VALUED FUNCTIONS OF A SINGLE VARIABLE.GENERAL TITLE - NL1 (SEE PAGE 84).

```

SUBROUTINE NL11F(C,K)
C DATE 26/2/69
  INTEGER H2,K,STAGE,N(4),Z,POINT,P,J
  REAL H1,H3,TIME,B1,I(3),C,IO(3),K1(16),K6(30),A1,
1  A(8),ITIM(3),B(5),X(4),S,OLDX1(3),OLDX2(3),NEWT,
2  Y(4),DRO(4),RO
  COMMON POINT,I,TIME,A,IO,X,STAGE,N,B,ITIM,OLDX1,
1  OLDX2,NEWT,Z,RO,S,P,J,Y,DRO,K1,K6
  IF(K.EQ.2)GOTO 3
  GOTO 4
3  A1=I(1)
  B1=0.2
  GOTO 6
4  A1=I(3)
  B1=0.1
6  H1=ABS(A1*B1)
  H2=H1
  H3=H1-AINT(H1)
  IF(K.EQ.2)C=(K1(H2+2)-K1(H2+1))*H3+K1(H2+1)
  IF(K.EQ.3)C=(K6(H2+2)-K6(H2+1))*H3+K6(H2+1)
  RETURN
END

```

8.3 SINGLE VALUED FUNCTIONS OF TWO VARIABLES.GENERAL TITLE - NL2 (SEE PAGE 86).

```

SUBROUTINE NL21F(A1,X1,K)
C DATE 26/2/69
INTEGER H2,C2,L,K,STAGE,N(4),P,J,POINT,ZA
REAL H1,C1,H3,C3,A1,Z,H4,H5,X1,K2(14,14),K3(9,30),
1 A(8),RO,ITIM(3),B(5),X(4),Y(4),DRO(4),S,K1(16),
2 K6(30),TIME,IO(3),OLDX1(3),OLDX2(3),NEWT,I(3)
COMMON POINT,I,TIME,A,IO,X,STAGE,N,B,ITIM,OLDX1,
1 OLDX2,NEWT,ZA,RO,S,P,J,Y,DRO,K1,K6,K2,K3
IF(K-1)10,11,10
11 H1=ABS(A1*0.2)
C1=ABS(B(2)*2000.0)
GOTO 12
10 H1=ABS(A1*10.0)
C1=ABS(I(2)*40.0)
12 H2=H1
C2=C1
H3=H1-AINT(H1)
C3=C1-AINT(C1)
DO 1 L=1,2
IF(K.EQ.1)GOTO 4
IF(K.EQ.2)GOTO 5
4 Z=(K2(H2+2,C2+1)-K2(H2+1,C2+1))*H3+K2(H2+1,C2+1)
GOTO 6
5 Z=(K3(H2+2,C2+1)-K3(H2+1,C2+1))*H3+K3(H2+1,C2+1)
6 IF(L-1)2,3,2
3 H4=Z
C2=C2+1
GOTO 1
2 H5=Z
1 CONTINUE
X1=(H5-H4)*C3+H4
RETURN
END

```

8.4 SIMULATION OF MODEL.8.4.1 READ DATA.

```

C MAIN PROGRAM - READS DATA-CHECK RESPONSE-TITLE-CHECK1
C DATE 1/3/69
  INTEGER N(3),M,STAGE,POINT,P
  REAL ITIM(3),IO(3),K1(16),K2(14,14),K3(9,30),K6(35),
1 TIME,I(3),A(8),B(5),V1(15),V2(15),NEWX(3),OLDX1(3),
2 K4(3),T(15),OLDX2(3)
  COMMON POINT,I,TIME,A,IO,STAGE,N,ITIM,B,V1,V2,T,P,NEWX,
1 K1,K6,K2,K3,OLDX1,OLDX2,K4
  READ(3,100)(N(M),M=1,3)
  READ(3,102)(A(M),M=1,8)
  READ(3,103)(ITIM(M),M=1,3)
  READ(3,104)(IO(M),M=1,3)
  READ(3,107)(V1(M),M=1,15)
  READ(3,108)(V2(M),M=1,15)
  READ(3,109)(T(M),M=1,15)
  PAUSE 1
  READ(3,105)(K1(M),M=1,15)
  CALL CHAIN(2)
100  FORMAT(3I4)
102  FORMAT(8F8.0)
103  FORMAT(3F8.0)
104  FORMAT(3F8.0)
105  FORMAT(5F10.0)
107  FORMAT(5F8.0)
108  FORMAT(5F8.0)
109  FORMAT(5F8.0)
  STOP
  END

```

8.4.1 CONTINUED.

C-MAIN PROGRAM-CHAIN 2 -READ DATA-TITLE-CHECK2

C DATE 1/3/69

```
    INTEGER N(3), STAGE, M, M1, POINT, P
    REAL ITIM(3), IO(3), K1(16), K2(14, 14), K3(9, 30), V1(15),
    1K6(35), TIME, I(3), A(8), B(5), T(15), NEWX(3), OLDX1(3),
    2K4(3), V2(15), OLDX2(3)
    COMMON POINT, I, TIME, A, IO, STAGE, N, ITIM, B, V1, V2, T, P, NEWX,
    1K1, K6, K2, K3, OLDX1, OLDX2, K4
    READ(3, 106)((K2(M, M1), M1=1, 14), M=1, 13)
    READ(3, 107)((K3(M, M1), M1=1, 30), M=1, 9)
    READ(3, 108)(K6(M), M=1, 30)
    P=1
    CALL CHAIN(3)
106  FORMAT(14F5.0)
107  FORMAT(10F5.0)
108  FORMAT(10F5.0)
    STOP
    END
```

8.4.2 INTEGRATION ROUTINE (SEE PAGE 93).

```

C PROGRAM - INTEGRATION ROUTINE - NON-LINEAR MODEL TITLE-INCK
C DATE 1/3/69
      INTEGER STAGE,N(3),POINT,P
      REAL IO(3),K4(3),ITIM(3),NEWX(3),OLDX1(3),OLDX2(3),I(3),
1A(8),TIME,K1(16),K2(14,14),K3(9,30),K6(35),V1(15),
2B(5),T(15),V2(15)
      COMMON POINT,I,TIME,A,IO,STAGE,N,ITIM,B,V1,V2,T,P,NEWX,
1K1,K6,K2,K3,OLDX1,OLDX2,K4
      GOTO(1,2),P
1  STAGE=1
      POINT=0
      TIME=0.0
      DO 13 M=1,3
13  I(M)=IO(M)
      A(5)=A(7)
      A(6)=A(8)
      CALL NLMAC
      DO 11 M=1,3
11  K4(M)=A(1)/ITIM(M)
      OLDX1(M)=NEWX(M)
      OLDX2(M)=NEWX(M)
11  CONTINUE
      K4(2)=A(1)/(9.0-(ABS(I(2))*10.0))
2  DO 12 M=1,3
      I(M)=I(M)+K4(M)*((2.0*NEWX(M))-(1.5*OLDX1(M))+(0.5*OLDX2(M)))
      OLDX2(M)=OLDX1(M)
      OLDX1(M)=NEWX(M)
12  CONTINUE
      K4(2)=A(1)/(9.0-(ABS(I(2))*10.0))
      POINT=POINT+1
      TIME=TIME+A(1)
      CALL NLMAC
      P=2
      IF(POINT.EQ.(STAGE*N(2))) CALL CHAIN(4)
      GOTO 2
      STOP
      END

```

```

SUBROUTINE NLMAC
C TRANSIENT RESPONSE OF DC MACHINE -MACK-1/3/69
INTEGER N(3),POINT,STAGE,P3,M,P
REAL A(3),TIME,AT,IA1,RK1,IF2,B4,B5,T(15),OI(4),
1 K5,I(3),NEWX(3),DR,RK6,IO(3),ITIM(3),V1(15),V2(15)
COMMON POINT,I,TIME,A,IO,STAGE,N,ITIM,IA1,RK1,IF2,
1 B4,B5,OI,V1,V2,T,P,NEWX
P3=2*N(2)*STAGE-(2*N(2)-1)
CALL NL1CK(RK1,2)
IF(I(1).LT.0.0) RK1=-RK1
M=N(3)
IF(TIME.GE.T(M))N(3)=N(3)+1
M=N(3)
VF=V1(M)
VA=V2(M)
CALL NL2CK(A(5),AT,1)
IF2=AT/4500.0
CALL NL2CK(A(6),IA1,2)
IF(I(2).LT.0.0)IA1=-IA1
IF(ABS(IA1).LT.0.5) GOTO 17
DR=0.042/ABS(IA1)**0.69
GOTO 18
17 DR=0.064
18 K5=3.6+(DR*I(3))
CALL NL1CK(RK6,3)
IF(I(3).LT.0.0)RK6=-RK6
NEWX(1)=(VF-(IF2*743.0))
NEWX(2)=(VA-((RK1*I(3))*275.0)-(IA1*K5))
IF((I(3).EQ.0.0).AND.(((RK1*IA1)*275.0).LT.RK6)) GOTO 21
NEWX(3)=((IA1*RK1*275.0)-RK6)
GOTO 22
21 NEWX(3)=0.0
22 IF(POINT.EQ.P3)GOTO 12
GOTO 13
12 OI(1)=IA1
OI(2)=IA1
OI(3)=IF2
OI(4)=IF2
13 A(5)=IA1+0.1*(1.5*IA1-2.0*OI(1)+0.5*OI(2))
A(6)=IF2+0.1*(1.5*IF2-2.0*OI(3)+0.5*OI(4))
OI(4)=OI(3)
OI(3)=IF2
OI(2)=OI(1)
OI(1)=IA1
RETURN
END

```

8.4.4 PRINT RESULTS.

```

C MAIN PROGRAM - CHAIN 4 PRINT RESULTS -TITLE-CHECK3-1/3/69
  INTEGER N(3),STAGE,P,POINT
  REAL ITIM(3),IO(3),K1(16),K2(14,14),K3(9,30),K6(35),
  1TIME,I(3),A(8),B(5),F,V1(15),V2(15),T(15),OLDX1(3),
  2OLDX2(3),NEWX(3),K4(3)
  COMMON POINT,I,TIME,A,IO,STAGE,N,ITIM,B,V1,V2,T,P,NEWX,
  1K1,K6,K2,K3,OLDX1,OLDX2,K4
  IF(N(3).EQ.2)GOTO 1
  GOTO 2
1  WRITE(2,100)
100 FORMAT(33H TRANSIENT RESPONSE OF DC MACHINE
  1//5X,5HSPEED,8X,2HIA,10X,7HFLUX(G),8X,2HIF,10X,4HTIME,
  28X,4HI(2)//)
2  F=I(1)/9000.0
  WRITE(2,102)I(3),A(5),F,B(3),TIME,I(2)
102 FORMAT(F10.1,F12.2,F16.5,F12.4,F13.3,F10.3)
  N(2)=N(2)+50
  CALL CHAIN(3)
  STOP
  END

```

8.5 EXTREMUM SEARCH.8.5.1 READ DATA.

```

C MAIN PROGRAM - READS DATA-CONTROL STRATEGY-TITLE-RIF
C   DATE 26/2/69
   INTEGER N(4),M,STAGE,P,J,POINT,Z
   REAL X(4),ITIM(3),IO(3),K1(16),K2(14,14),K3(9,30),K6(30),
1 TIME,I(3),A(8),B(5),S,Y(4),DRO(4),RO,ROY,NEWT,OLDX1(3),
2 OLDX2(3)
   COMMON POINT,I,TIME,A,IO,X,STAGE,N,B,ITIM,OLDX1,OLDX2,
1 NEWT,Z,RO,S,P,J,Y,DRO,K1,K6,K2,K3,ROY
   P=1
   READ(3,100)(N(M),M=1,4)
   READ(3,101)(X(M),M=1,4)
   READ(3,102)(A(M),M=1,8)
   READ(3,103)(ITIM(M),M=1,3)
   READ(3,104)(IO(M),M=1,3)
   READ(3,106)NEWT,Z
   PAUSE 1
   READ(3,105)(K1(M),M=1,15)
   CALL CHAIN(2)
100  FORMAT(4I4)
101  FORMAT(4F6.1)
102  FORMAT(4F10.0)
103  FORMAT(3F8.0)
104  FORMAT(3F8.0)
105  FORMAT(5F10.0)
106  FORMAT(F8.0,I4)
   STOP
   END

```

8.5.1 CONTINUED.

```
C-MAIN PROGRAM-CHAIN 2 -READ DATA-TITLE-R2F-26/2/69
  INTEGER N(4),STAGE,P,J,M,M1,POINT,Z
  REAL X(4),ITIM(3),IO(3),K1(16),K2(14,14),K3(9,30),
  1K6(30),TIME,I(3),A(8),B(5),S,Y(4),DRO(4),RO,ROY,NEWT,
  2OLDX1(3),OLDX2(3)
  COMMON POINT,I,TIME,A,IO,X,STAGE,N,B,ITIM,OLDX1,OLDX2,
  1NEWT,Z,RO,S,P,J,Y,DRO,K1,K6,K2,K3,ROY
  READ(3,106)((K2(M,M1),M1=1,14),M=1,13)
  READ(3,107)((K3(M,M1),M1=1,30),M=1,9)
  READ(3,108)(K6(M),M=1,30)
  CALL CHAIN(3)
106  FORMAT(14F5.0)
107  FORMAT(10F5.0)
108  FORMAT(10F5.0)
      STOP
      END
```

8.5.2 STEEPEST DESCENT ROUTINE (SEE PAGE 109).

```

C HILL-CLIMBING ROUTINE - TITLE - HC1F-26/2/69
  INTEGER J,STAGE,Z,POINT,N(4),P,M
  REAL S,RO,B(5),ROY,NEWT,TIME,IO(3),DROP,DROA,E,I(3),
  1X(4),Y(4),DRO(4),A(8),ITIM(3),K1(16),K2(14,14),
  2K3(9,30),K6(30),OX1(3),OX2(3),OLDX1(3),OLDX2(3)
  COMMON POINT,I,TIME,A,IO,X,STAGE,N,B,ITIM,OLDX1,OLDX2,
  1NEWT,Z,RO,S,P,J,Y,DRO,K1,K6,K2,K3,ROY/AA/OX1,OX2
  GOTO(200,201),P
200  STAGE=1
7    S=1.0
1    J=0
     CALL PIN1F(RO)
     B(5)=0.0
     DO 10 II=1,4
     Y(II)=X(II)
     DO 11 K=1,4
     IF(K.EQ.II)X(K)=Y(K)+A(3)
11   CONTINUE
     CALL PIN1F(ROY)
     DRO(II)=(ROY-RO)/A(3)+0.00001
     B(5)=B(5)+DRO(II)**2
     X(II)=Y(II)
10   CONTINUE
     IF(B(5).LT.A(4))GOTO 3
     GOTO 2
3    N(4)=2
     CALL PIN1F(RO)
     N(4)=4
     P=2
     CALL CHAIN(4)
201  NEWT=TIME
     Z=POINT
     A(7)=A(5)
     A(8)=A(6)
     DO 14 M=1,3
     IO(M)=I(M)
     OX1(M)=OLDX1(M)
     OX2(M)=OLDX2(M)
14   CONTINUE

```

8.5.2 CONTINUED.

```
STAGE=STAGE+1
IF(STAGE.EQ.N(1))STOP
GOTO 7
2   DROP=-S*B(5)
    DO 12 II=1,4
12  X(II)=Y(II)-S*DRO(II)
    CALL PINIF(ROY)
    DROA=ROY-RO
    IF(DROA.GE.0.0)GOTO 4
    J=1
    E=ABS((DROP-DROA)/DROP)
    IF(E.GE.0.5)GOTO 4
    IF(E.GT.0.2)GOTO 6
    S=1.2*S
    GOTO 5
4   S=0.8*S
5   IF(J.NE.1)GOTO 2
6   DO 8 M=1,4
    X(M)=Y(M)-S*DRO(M)
    IF(X(M).GE.240.0)X(M)=238.0
8   CONTINUE
    GOTO 1
END
```

8.5.3 INTEGRATION ROUTINE (SEE PAGE 93).

```

SUBROUTINE PINIF(RO)
C PROGRAM - INTEGRATION ROUTINE - NON-LINEAR MODEL TITLE-PINIF
C   DATE 3/3/69
      INTEGER STAGE,N(4),POINT,Z,M,P3
      REAL IO(3),K(3),ITIM(3),NEWX(3),OLDX1(3),OLDX2(3),I(3),
      IRO,A(8),TIME,NEWT,X(4),OX1(3),OX2(3),B(5)
      COMMON POINT,I,TIME,A,IO,X,STAGE,N,B,ITIM,OLDX1,OLDX2,
      INEWT,Z/AA/OX1,OX2/CC/NEWX,P3
      P3=Z
      TIME=NEWT
      IF(STAGE.GE.2) GOTO 7
      POINT=0
      GOTO 8
7     POINT=Z
8     DO 13 M=1,3
13    I(M)=IO(M)
      A(5)=A(7)
      A(6)=A(8)
      CALL MAC1F(RO)
      IF(POINT.EQ.0)GOTO 14
      GOTO 4
14    DO 10 M=1,3
      OX1(M)=NEWX(M)
      OX2(M)=NEWX(M)
10    CONTINUE
4     DO 11 M=1,3
      K(M)=A(1)/ITIM(M)
      OLDX1(M)=OX1(M)
      OLDX2(M)=OX2(M)
11    CONTINUE
      K(2)=A(1)/(9.0-(ABS(I(2)*10.0))
2     DO 12 M=1,3
      I(M)=I(M)+K(M)*((2.0*NEWX(M))-(1.5*OLDX1(M))+(0.5*OLDX2(M)))
      OLDX2(M)=OLDX1(M)
      OLDX1(M)=NEWX(M)
12    CONTINUE
      K(2)=A(1)/(9.0-(ABS(I(2)*10.0))
      POINT=POINT+1
      TIME=TIME+A(1)
      CALL MAC1F(RO)
      IF((N(4).EQ.2).AND.(POINT.EQ.N(2)*STAGE))RETURN
      IF(POINT.EQ.(N(2)+STAGE*N(2))) RETURN
      GOTO 2
      END

```

8.5.4 MACHINE SUBROUTINE (SEE PAGE 116).

```

SUBROUTINE MACIF(R)
C TRANSIENT RESPONSE OF DC MACHINE -MACIF-3/3/69
  INTEGER N(4),POINT,STAGE,P3
  REAL A(3),TIME,AT,IA1,RK1,IF2,B4,B5,
1  X5,I(3),NEWK(3),DR,RK6,I(3),R),X(4),IN,IT,
2  II,IP,INT,DINT,VA,VF,OI(4)
  COMMON POINT,I,TIME,A,I),X,STAGE,N,IA1,
1  RK1,IF2,B4,B5,OI/CC/NEWK,P3
  CALL NL11F(RK1,2)
  IF(I(1).LT.0.0) RK1=-RK1
  CALL NL21F(A(5),AT,1)
  IF2=AT/4500.0
  CALL NL21F(A(6),IA1,2)
  IF(I(2).LT.0.0)IA1=-IA1
  IF(ABS(IA1).LT.0.5) GOTD 17
  DR=0.342/ABS(IA1)**0.69
  GOTD 18
17  DR=0.064
18  X5=3.6+(DR*I(3))
  CALL NL11F(RK6,3)
  IF(I(3).LT.0.0)RK6=-RK6
  IF(N(4).EQ.2)GOTD 1
  IF(POINT.LE.(N(2)*STAGE)GOTD 1
  GOTD 2
1  VF=X(1)
  VA=X(2)
  GOTD 3
2  VF=X(3)
  VA=X(4)

```

8.5.4 CONTINUED.

```

3      NEWX(1)=(VF-(IF2*743.0))
      NEWX(2)=(VA-((RK1*I(3))*275.0)-(IA1*K5))
      IF((I(3).EQ.0.0).AND.(((RK1*IA1)*275.0).LT.RK6)) GOTO 2
      NEWX(3)=((IA1*RK1*275.0)-RK6)
      GOTO 22
21     NEWX(3)=0.0
22     DINT=(160.0*SIN(6.2832*TIME+0.000001))-I(3)
      IF(TIME.GT.0.25)DINT=160.0-I(3)
      IF(ABS(DINT).LE.0.0001)GOTO 8
      GOTO 9
8      DINT=0.0001
9      INT=A(2)*((DINT)**2)
      IF(POINT.EQ.P3)GOTO 4
      IF(POINT.EQ.P3+1)GOTO 6
      GOTO 7
6      IN=0.0
      IP=0.0
7      II=(INT+IP)*0.5*A(1)
      IT=II+IN
      IN=IT
      IP=INT
      RO=IN
      GOTO 5
4      RO=0.0
5      IF(POINT.EQ.P3)GOTO 12
      GOTO 13
12     OI(1)=IA1
      OI(2)=IA1
      OI(3)=IF2
      OI(4)=IF2
13     A(5)=IA1+0.1*(1.5*IA1-2.0*OI(1)+0.5*OI(2))
      A(6)=IF2+0.1*(1.5*IF2-2.0*OI(3)+0.5*OI(4))
      OI(4)=OI(3)
      OI(3)=IF2
      OI(2)=OI(1)
      OI(1)=IA1
      RETURN
      END

```

8.5.5 PRINT RESULTS.

```

C MAIN PROGRAM - CHAIN 4 PRINT RESULTS -TITLE-R3F-27/2/69
  INTEGER N(4), STAGE, P, J, POINT, Z
  REAL X(4), ITIM(3), IO(3), K1(16), K2(14, 14), K3(9, 30), K6(30),
  1 TIME, I(3), A(8), B(5), S, Y(4), DR0(4), RO, F, ROY, NEWT,
  2 OLDX1(3), OLDX2(3)
  COMMON POINT, I, TIME, A, IO, X, STAGE, N, B, ITIM, OLDX1, OLDX2,
  1 NEWT, Z, RO, S, P, J, Y, DR0, K1, K6, K2, K3, ROY
  IF(N(3).EQ.1)GOTO 1
  GOTO 2
1  WRITE(2,100)
100 FORMAT(46H OPTIMISATION USING METHOD OF STEEPEST DESCENT
  1//3X, 4HX(1), 6X, 4HX(2), 6X, 4HX(3), 6X, 4HX(4), 8X, 2HRO, 8X, 1HS,
  29X, 5HFGRAD//)
  N(3)=2
2  WRITE(2,101)X(1), X(2), X(3), X(4), RO, S, B(5)
101  FORMAT(4F10.4, F9.5, F10.4, F12.7)
  F=I(1)/9000.0
  WRITE(2,102)I(3), A(5), F, B(3), TIME, I(2), ROY
102  FORMAT(F8.1, F12.2, F13.5, F12.4, F10.3, F10.3, F10.6)
  WRITE(2,103) STAGE
103  FORMAT(//11H END STAGE I3)
  CALL CHAIN(3)
  STOP
  END

```

8.5.6 TYPICAL DATA.

80	25	1	4		
193.61230	.12187	.58112	.91		
0.0005	1.0	0.001	0.001		
29.43	0.3241	29.43	0.3241		
1.0	7.5	0.0373			
26.73	0.427	142.7			
0.225	0				
0.0	0.00050	0.00105	0.00160	0.00210	
0.00260	0.00305	0.00350	0.00394	0.00440	
0.00480	0.00516	0.00547	0.00578	0.00605	
0.0	80.0	160.	250.	330.	400.
		530.	680.		
	850.	1050.	1380.	1830.	2470.
		3480.			
0.0	90.0	180.	280.	385.	480.
		615.	770.		
	975.	1200.	1480.	1910.	2520.
		3480.			
0.0	100.	200.	315.	440.	580.
		740.	925.		
	1150.	1410.	1710.	2090.	2650.
		3500.			
0.0	120.	280.	420.	590.	780.
		1000.	1220.		
	1470.	1730.	2040.	2400.	2880.
		3600.			
0.0	130.	320.	500.	720.	950.
		1190.	1450.		
	1720.	2020.	2330.	2700.	3130.
		3780.			
0.0	140.	400.	640.	880.	1150.
		1450.	1740.		
	2030.	2370.	2680.	3040.	3470.
		4000.			
0.0	150.	420.	700.	960.	1300.
		1650.	2000.		
	2320.	2660.	3000.	3350.	3700.
		4150.			
0.0	160.	425.	740.	1080.	1480.
		1850.	2210.		
	2580.	2970.	3350.	3730.	4120.
		4530.			
0.0	170.	430.	770.	1160.	1550.
		1950.	2350.		
	2800.	3230.	3600.	3980.	4400.
		4800.			
0.0	180.	480.	880.	1300.	1680.
		2100.	2550.		
	3020.	3480.	3950.	4400.	4800.
		5000.			
0.0	190.	500.	920.	1350.	1820.
		2250.	2700.		
	3200.	3680.	4150.	4600.	5000.
		5300.			
0.0	190.	520.	950.	1420.	1930.
		2390.	2850.		
	3350.	3850.	4320.	4800.	5200.
		5600.			
0.0	190.	540.	980.	1460.	1960.
		2460.	2960.		
	3460.	3960.	4460.	4960.	5460.
		5960.			

8.5.6 CONTINUED.

0.0	0.5	1.0	1.5	2.0	2.7	3.5	4.4	5.4	6.0
7.0	8.0	9.0	10.5	12.3	14.5	17.0	20.3	23.8	27.5
31.0	35.0	38.2	42.0	45.5	50.0	54.0	58.0	62.0	65.0
0.0	0.7	1.2	2.0	2.7	3.5	4.4	5.3	6.2	7.4
8.4	9.8	11.2	12.6	14.4	16.7	19.4	22.0	25.0	28.0
31.0	35.0	38.2	42.0	45.5	50.0	54.0	58.0	62.0	65.0
0.0	1.4	2.7	3.8	5.2	6.6	7.9	9.2	10.5	11.7
12.9	14.0	15.5	17.0	18.8	20.8	23.0	25.0	27.8	30.4
33.3	36.5	39.8	43.3	47.0	51.0	54.5	58.4	62.3	66.0
0.0	2.9	5.7	8.5	10.5	11.8	13.0	14.0	15.2	16.4
17.7	18.8	20.0	21.5	23.0	24.8	26.5	28.4	30.6	33.4
36.0	39.0	42.5	45.0	48.8	52.0	55.5	59.2	63.0	67.0
0.0	9.0	12.0	14.0	15.1	16.2	17.2	18.4	19.5	20.8
22.0	23.2	24.5	25.6	26.9	28.3	30.0	32.0	34.3	36.5
39.2	42.0	45.0	47.7	50.7	54.0	57.5	60.7	64.2	68.0
0.0	16.0	17.5	18.4	19.6	20.5	21.3	22.1	23.0	24.0
25.4	26.6	28.0	29.2	30.6	32.3	33.5	35.6	37.6	40.0
42.2	45.0	48.0	50.7	53.7	56.7	60.0	63.0	66.0	70.0
0.0	18.0	20.7	22.0	23.0	24.0	25.0	25.9	26.9	27.8
29.0	30.0	31.3	32.7	34.2	35.6	37.0	38.5	40.0	43.0
45.0	48.0	50.8	53.9	56.7	59.6	62.4	65.3	68.0	72.0
0.0	20.0	22.4	24.1	25.6	26.8	28.0	29.0	30.0	31.4
32.5	33.6	34.9	36.0	37.5	39.0	40.5	42.6	44.0	45.6
48.2	50.7	53.5	56.4	59.4	62.5	65.6	68.0	71.0	75.0
0.0	22.5	24.2	25.6	27.0	28.5	30.0	31.1	32.5	34.0
35.5	36.6	38.0	39.5	41.1	42.5	43.9	45.5	46.9	48.5
50.6	53.0	55.6	58.5	61.3	64.4	67.3	70.0	73.0	78.0
1.80	0.69	0.53	0.50	0.49	0.49	0.49	0.49	0.50	0.52
0.54	0.57	0.59	0.62	0.64	0.66	0.69	0.73	0.75	0.78
0.81	0.85	0.88	0.91	0.94	0.97	0.99	1.02	1.05	1.08

9.0. References.

- 1) Adkins, B. : "The General Theory of Electrical
Machines",
(Chapman & Hall, 1957).
- 2) Ellison, A. J. : "Electromechanical Energy Conversion",
(Harrap, 1965).
- 3) White, D. C. &
Woodson, H. : "Electromechanical Energy Conversion",
(Wiley, 1959).
- 4) Fitzgerald, A. E.
& Kingsley, C. : "Electric Machinery",
(McGraw-Hill, 1961).
- 5) Tustin, A. : "Direct Current Machines for Control
Systems",
(Spon, 1952).
- 6) Bentall, A. A. L.
& Hill, E. P. : "Control of d. c. machines",
(Metropolitan-Vickers Special Publication,
No. 7415/1, 1950).
- 7) Lebenbaum, P. : "The design of d. c. motors for use
in Automatic Control Systems".
(Trans. American Inst. Electrical
Engineers, Vol. 68, 1949, p. 1089).
- 8) Opel, L. G. : "Limitations in Design of D. C.
Adjustable Speed Motors",
(Trans. American Inst. Elect. Engineers,
Vol. 68, 1949, p. 1095).
- 9) Alger, J. R. M. &
Bewley, D. T. : "An Analysis of d. c. Machine Commutatio
(Trans. American Inst. Elect. Engrs.,
Vol. 76, Pt. 3, 1957, p. 399.)

- 10) Tustin, A. & Ward, H. : "The e. m. f. 's induced in the armature coils of d. c. machines during commutation", (Proc. I. E. E., 1962, Vol. 109C, p. 456).
- 11) Morris, D. G. O. : "Influence of parasitic brush currents on the performance of d. c. motors", (Proc. I. E. E., Vol. 112, No. 8, 1965, p. 1535).
- 12) Hammond, P. H. : "Feedback Theory and its Applications", (E. U. P., 1958) p. 238.
- 13) Macfarlane, A. G. J. : "Engineering Systems Analysis" (Harrap, 1964), p. 65.
- 14) Moullin, E. B. : "Electromagnetic principles of the Dynamo" (O. U. P., 1955).
- 15) Liwschitz-Garik, M. & Whipple, C. C. : "Electric Machinery, D. C. Machines", (Van Nostrand, 1956, 2nd edn.), p. 139
- 16) Linville, T. M. : "Current & Torque of d. c. Machines on Short Circuit", (Trans. American Inst. Electrical Engrs Vol. 65, p. 956).
- 17) Tarkanyi, M. : "The influence of the commutating coils on the main flux of a d. c. machine", in "Commutation in rotating machines". (I. E. E. Conf. Publ. 11, 1964, p. 28).

- 18) Pohl, R. : "Rise of flux due to impact excitation: retardation by eddy currents in solid parts". Proc. I. E. E., Vol. 96, pt. II, 1949, p. 57.
- 19) West, J. C. : "Servomechanisms", (E. U. P., 1954) p. 169.
- 20) Steel, G. K. : "Programming of digital computers for transient studies in control systems" Int. Journ. Elect. Engrg. Educ., Vol. 3, p. 261.
- 21) Ralson, A. : "Numerical integration methods for the solution of ordinary differential equations" in "Mathematical Methods for digital computers", Ralston & Wilf, (Wiley, 1960).
- 22) McCracken, D. D. "A guide to Fortran IV programming" (Wiley, 1965).
- 23) McCracken, D. D.: "Numerical methods and Fortran Programming" & Dorn, W. S. (Wiley, 1964).
- 24) Wilde, D. J. : "Optimum seeking methods" (Prentice-Hall, 1964).
- 25) Bellman, R. : "Dynamic Programming" (Princeton Univ. Press, 1957).
- 26) Rosenbrock, H. H. & Storey, C. : "Computational techniques for chemical engineers" (Pergamon Press, 1966) Chapter 9.
- 27) Wilde, D. J. & Beightler, C. S. : "Foundations of optimisation" (Prentice-Hall, 1967).
- 28) Eveleigh, V. W. : "Adaptive control and optimisation techniques" (McGraw-Hill, 1967), p. 116.
- 29) Riaz, M. : "Dynamics of d. c. machine systems", Trans. American Inst. Elec. Engrs. pt. II, Vol. 74, 1955, p. 365.

- 30) Ahamed, S. V. : "Flux distribution in saturated d. c. machines on no-load", I. E. E. E. Transactions Vol. 84 Power Apparatus & Systems, 1965, p. 375.
& Erdelyi, E. A.
- 31) Ahamed, S. V. : "Flux distribution in d. c. machines on load and overloads", I. E. E. E. Transactions Vol. 85, Power Apparatus & Systems, 1966, p. 960.
& Erdelyi, E. A.
- 32) Hamilton, H. B. : "Magnetic saturation and eddy current effect in d. c. machine voltage build-up", I. E. E. E. Transactions, Vol. 83, Power Apparatus & Systems, 1964, p. 606.
- 33) Todd, J. (Ed.) : "A survey of numerical analysis", (McGraw-Hill, 1962) Chapter 7, p. 255.